Wireless Communication Techniques for Indoor Positioning and Tracking Applications

Dissertation
zur Erlangung des akademischen Grades

Doktoringenieur
(Dr.-Ing.)

von **M.E. Tariq Jamil Saifullah Khanzada**
geb. am 13. August 1973 in TandoAllahYar, Pakistan

genehmigt durch die Fakultät für Elektrotechnik und Informationstechnik
der Otto-von-Guericke-Universität Magdeburg

Gutachter:

Prof. Dr.-Ing. Abbas Omar
Prof. Dr.-Ing. Christian Diedrich
Dr.-Ing. Lutz Rauchhaupt

Vorsitzender:

Prof. Dr.-Ing. habil. Frank Palis

Mitglied:

Prof. Dr.-Ing. Andreas Lindemann

eingereicht am: 28 Oct 2009
verteidigt am: 30 August 2010

Dedications

First and above all I am thankful to my God (Allah Subhana Taala) who gave me strength to produce this work and then I dedicate this work to my parents, wife and children who supported me a lot to complete this dissertation

T. J. S. Khanzada

Acknowledgement

Zusammenfassung

Diese Arbeit leistet einen Beitrag auf dem Gebiet der Ortung in Gebäuden mit konkreten Anwendungen unter Nutzung des Signaldesigns für zukünftige drahtlose Kommunikationssysteme. Die Arbeit konzentriert sich auf den Vergleich von zwei alternativen Strukturen der OFDM und SCT signale bezüglich ihres strukturellen Designs, der Kodierungseffekte und des Transceiverdesigns. Die TDOA-Methode wurde insbesondere deswegen betrachtet, da sie bei der Einschätzung realer Abstände in realen geschlossenen Innenräumen anderen konkurrierenden Methoden überlegen ist. Ein weiteres wichtiges Ziel ist es, die hochauflösenden Algorithmen zu vergleichen und dabei den optimalen zur Erhöhung der Genauigkeit in NLOS Umgebungen vorzuschlagen. Zur Realisierung dieser Ziele wird ein gemeinsamer OFDM und SCT Transceiver zur Innenraum-Positionierung entwickelt. Ein modifiziertes Kriterium für DFE und SCT wird eingeführt, welches exponentiell abfällt und die Qualität der Entscheidung während der Entzerrstufe verbessert. Zwei verschiedene Varianten von CP sind für die OFDM und die SCT Signalstrukturen implementiert worden. Die Verbesserung der Kanalperformance für die DFE-Implementierungen wird durch variable Lengen erreicht. Ein Codeabschnitt ist auf dem kombinierten OFDM/SCT Transceiver implementiert, was sich positiv auf die Effizienz des Systems auswirkte.

Die ESPRIT, Root-MUSIC und MP Algorithmen werden auf Messdaten ausgeführt, um die DME auf weniger als 1 Meter zu reduzieren. Die Schätz- Algorithmen werden auf zwei verschiedene Arten (WP1 und WP2) auf die erfassten Daten der CMWCE der Uni Magdeburg angewendet. In WP1 besteht das System aus zwei Antennen und wird in WP2 auf bis zu sieben Antennen erweitert. MDL und AIC werden zur Bestimmung der Modellreihenfolge in WP1 genutzt. In WP2 werden die drei Varianten verallgemeinerte Pencil-Function, Vorwärts- und Rückwärts-Mittelwertbildung und die Hankel-Matrix-Methode als MP1, MP2 und MP3 eingeführt. Darüber hinaus werde drei weitere Reihenfolgekriterien vorgestellt: EIG, modifiziertes MDL und die automatische Auswahl.

Ein neues Schema wird eingeführt, das auf zwei verschiedenen Antennen basiert, welche OFDM/SCT-Symbole auf verschiedene Träger im WLAN verteilen. Das Schema verringert den Messfehler der Abstandsschätzung und der DME auf nahezu Null. Eine Analyse der Auswirkungen der unterschiedlichen SNR, bezüglich variabler

Bandbreite und Variation der Anzahl der Träger auf der DME-Schätzung wurde auch erstellt. Die Algorithmen MP1-MDL und MP3-MDL erreichen die höchste Genauigkeit bei der Bestimmung der Abstände und sind in der Lage, die Objekte effizient und mit hoher Genauigkeit zu verfolgen. Daher sind sie prinzipiell für die Einbettung in ein mobiles Gerät zur Positionierung geeignet.

Abstract

This dissertation makes a contribution in the field of indoor positioning applications using concrete signal design for the forthcoming wireless communication systems. It focuses on the comparison of two alternative signal structures of OFDM and SCT, their structure designs, coding effects, and the transceiver design are considered for the indoor positioning applications. Furthermore, the TDOA method is considered specifically to estimate the distance in a real indoor environment due to its accuracy amongst all counterpart methods. Another major goal is to compare the super resolution algorithms and to propose the optimal one for increasing the accuracy in NLOS conditions. In order to accomplish these goals a joint OFDM and SCT transceiver is developed for the indoor positioning application. A modified criterion is also introduced for the DFE of the SCT, which decays exponentially and improves the decision performance at the equalization stage. Two different variants of CP are implemented for both the OFDM and the SCT signal structures. A variable length improved channel performance for the DFE implementations is achieved. A coding block is implemented on the combined OFDM/SCT transceiver, which brought an efficiency drift in the system.

The ESPRIT, Root-MUSIC and MP algorithms are implemented on the real data sets to reduce the DME to be less than 1 meter. The estimation algorithms are applied at the CMWCE, University of Magdeburg for the captured data in two stages, known as WP1 and WP2. In WP1, the system consists of two antennas and is extended upto seven antennas in WP2. MDL and AIC are utilized as model order in WP1. In WP2, three variants of the MP algorithm using generalized pencil function, forward-backward averaging method and Hankel matrix method are introduced as MP1, MP2 and MP3 respectively. Furthermore three more model order criteria of EIG, Modified MDL and automatic model order selection are introduced.

A new scheme based on two different antennas, transmitting OFDM/SCT symbols mapped to multiple carriers using WLAN system is introduced. The scheme increases the accuracy of the distance estimations and DME approaching to zero is achieved. An analysis for the effects of the varying SNR, variable bandwidth and varying the number of carriers on the DME estimation is also performed.

The algorithms MP1-MDL and MP3-MDL achieve the most accurate estimation

and are capable of tracking the position of the moving objects with efficiency and accuracy. Hence they can be embedded in any wireless positioning device.

Table of Contents

List of Figures

List of Tables

List of Abbreviations

Table 1: Abbreviations - used in the dissertation

Legends	Desciption
3GPP	3rd Generation Partnership Project
4G	Fourth Generation
AIC	Akaike's Information Criterion
AOA	Angle of Arrival
AP	All Pass
AWGN	Additive White Gaussian Noise
BRAN	Broadband Radio Access Networks
BS	Base Station
CDMA	Code Division Multiple Access
CE-FDE	Channel Estimate based FDE
CFIR	Complex FIR
CIBS	Chip Interleaved Block Spread
CIR	Channel Impulse Response
CLOQ	Cooperative Localization with Quality of estimation
cm	centimeters
CMFB	Complex Modulated FB
CMWCE	Chair of Microwave and Communication Engineering
CP	Cyclic Prefixes
CTF	Channel Transfer Function
DAB	Digital Audio Broadcasting
DDC	Decision-Directed Correction
DDFSE	Delayed Decision Feedback Sequence Estimation
DDP	Dominant Direct Path
DEM	Distance Estimation Methods
DFE	Decision Feedback Equalizer
DFT	Discrete Fourier Transform
DLOS	Direct LOS
DME	Distance Measurement Error
DOA	Direction Of Arrival
DORIS	Doppler Orbitography and Radio-positioning Integrated by Satellite
DRM	Digital Radio Mondiale
DS-CDMA	Direct Sequence Code Division Multiple Access

Abbreviations continued from the previous page

Legends	Desciption
DSSS	Direct Sequence Spread Spectrum
DVB	Digital Video Broadcasting
E-911	Enhanced 911
EIG	Eigenvalue criteria
ELT	Extended Lapped Transform
EMFB	Exponentially-Modulated Filter Bank
EVs	Eigen Values
FB	Filter Bank
FDE	Frequency Domain Equalizer
FDP	First Detection Peak
FF	Feed Forward
FFT	Fast FT
FHSS	Frequency Hoping Spread Spectrum
FIR	Finite Impulse Response
FT	Fourier Transform
G-CRLB	Generalized Cramer Rao Lower Bound
GI	Guard Interval
GLONASS	GLObal'naya NAvigatsionnaya Sputnikovaya Sistema
GMC	Generalized Multi-Carrier
GPS	Global Positioning System
HIPERLAN/2	HIgh PErformance Radio Local Area Network 2
IB-DFE	Iterative Block DFE
IBI	Inter Block Interference
ICA	Independent Component Analysis
ICI	Inter-Carrier Interference
IDFT	Inverse DFT
IFDE	Iterative FDE
IFFT	Inverse Fast Fourier Transform
IFT	Inverse Fourier Transform
IRNSS	Indian Regional Navigational Satellite System
ISI	Inter-Symbol Interference
KSP	Known Symbol Padding
LBS	Location Based Services
LE	Linear Equalizer
LMS	Least Mean Squares
LOS	Line-of-Sight
LP	Linear Predictor
LP-FIR	Linear Phase FIR FIR)
LS	Least Squares
LST	Layered Space Time
LTE	Long Term Evolution
MC	Multi-Carrier

Legends	Desciption
MCS	Multi Carrier Signal
MDL	Minimum Descriptive Length
MDX	MDX a modified form of MDL
MFB	MF Bound
MIMO	Multiple Input Multiple Output
ML	Maximum Likelihood
MLL	Maximum log-Likelihood
MMAC	Multimedia Mobile Access Communications
MMSE	Minimum Mean Square Error
MP	Matrix Pencil
MS	Mobile Station
MUSIC	MUltiple SIgnal Classification
NBI	Narrow Band Interference
NDDP	Non-Dominant Direct Path
NLOS	Non Line of sight
OFDM	Orthogonal Frequency Division Multiplexing
OFDM-CP	OFDM-Cyclic Prefix
OFDM-ZP	OFDM-Zero Padding
PAPR	Peak-to-Average-Power Ratio
PDP	Power Delay Profile
PN	Pseudo Noise
POA	Phase of Arrival
PSK	Phase Shift Keying
QAM	Quadrature Amplitude Modulation
QoS	Quality of Service
QZSS	Quasi-Zenith Satellite System
RLS	Recursive Least Squares
RMS	Root Mean Square
Root-MUSIC	Root Multiple Signal Classification
RPs	Reference Points
RSS	Received Signal Strength
RT	Ray Tracing
S/CMFB	Sine/Cosine-Modulated Filter Bank
SCBS	SC Block Spread
SCBT	SC Block Transmission
SCT	Single Carrier Transmission
SCT-FDE	Single-Carrier Transmission with Frequency Domain Equalization
SCT-TDE	Single-Carrier Transmission with Time Domain Equalization
SFBC	Space Frequency Block Coded
SNR	Signal-to-Noise Ratio
STBC	Space Time Block Coding
STFBC	Space Time Frequency Block Code

Abbreviations continued from the previous page

Legends	Desciption
TD	Time Domain
TDMA	Time Division Multiple Access
TDOA	Time Difference Of Arrival
TOA	Time of Arrival
TOF	Time of Flight
TR	Time Reversal
UDP	Undetected Direct Path
UMB	Ultra Mobile Broadband
UWB	Ultra Wide Band
VOFDM	Vector OFDM
WIMAX	Worldwide Interoperability for Microwave Access
WLAN	Wireless Local Area Networks
WLS	Weighted LS
WP1	Working Package 1
WP2	Working Package 2
WSN	Wireless Sensor Networks
WSSUS	Wide Sense Stationary Uncorrelated Scattering
ZF	Zero Forcing
ZP	Zero Padding

Chapter 1

Introduction

1.1 Wireless Communication Systems

Modern Broadband Wireless Communication Systems, which utilize bit rates of tens to hundreds of megabits per second, have variety of applications like Digital Audio Broadcasting (DAB), Digital Video Broadcasting (DVB), Digital Radio Mondiale (DRM), Worldwide Interoperability for Microwave Access (WIMAX), Wireless Local Area Networks (WLAN) [1,2], 3rd Generation Partnership Project (3GPP) Long Term Evolution (LTE), 3GPP2-Ultra Mobile Broadband (UMB) and IEEE 802.16 standard [3]. The transfer of information originating from one or several sources is required to be received by one or more destinations in various forms, applications and complying several limitations. Efficient transmission speed, lower cost, higher throughput, larger capacity, better Quality of Service (QoS), minimal hardware implementation and numerous applications motivate enhancing new wireless technologies. Controlling and monitoring remote objects using specific sensors is a new aspect being researched, introduced in the literature by the name of Wireless Sensor Networks (WSN) [4]. Another similar use of these technologies involves estimating how far one terminal is from the other one and finding the location of the specific object. This is termed as positioning applications used in indoor and outdoor environments. Wireless location applications are often referred to the Location Based Services (LBS), particularly when provided by the cellular networks for adding value to their basic services of mobile telephony [5]. LBS are an integrated part of the positioning applications.

1.1.1 Application Areas

The number of positioning applications are huge and rapidly growing. Personal safety, industrial monitoring and control, military and commercial usage are the major areas of these applications [6, 7]. Various methods are utilized to find the location information which require distance estimation [8,9]. Distance estimation systems are governed by the complexity, accuracy, and the environment [7]. Determination of distance in the presence of noise and interference is the issue which remains a challenge

for these applications. The best epitome of wireless location finding system is the Global Positioning System (GPS) [10], however, its performance deteriorates in urban environments and indoor applications where noise and interference are generated through various sources. Another issue, in the indoor environments, is the inaccuracy of the distance estimations due to the multi-path effects.

1.1.2 Contemporary Positioning and Navigational Systems

GPS and wireless Enhanced 911 (E-911) services [11] initially address the issue of location finding and are still globally utilized positioning systems, although a number of navigational systems have been proposed throughout the world. GLObal'naya NAvigatsionnaya Sputnikovaya Sistema (GLONASS), was a fully functional navigation constellation [12] but it is partially available to date and the full global functionality is expected by 2010. The Quasi-Zenith Satellite System (QZSS), is an enhancement for GPS [13] covering Japan, scheduled to be launched in 2009. The Indian Regional Navigational Satellite System (IRNSS) is an autonomous regional satellite navigation system [14] being developed by Indian space research organization, expected to be functional till 2012. Beidou or Big Dipper is a Chinese regional navigation system intended to be expanded into a global navigation system; under the program named as Compass [15]. Doppler Orbitography and Radio-positioning Integrated by Satellite (DORIS) is a French precision navigation system [16] being worked out. Galileo Positioning System is an alternative to GPS [17] introduced jointly by the European Union and the European Space Agency scheduled to be working from 2012.

The positioning applications are numerous and are mostly implemented within the cellular networks [5]. Another use in the network application is to the plan system loading and the channel allocation as well as the deployment of additional cells [18]. Location based advertising has an application in a scenario in which the cell phone of a visitor to a mall can be located and can be made to display an advertisement of a shop very near to where its holder is located [5]. Person and asset tracking applications involve hospitals, hospital equipment, vehicle theft, RFID tags, inventory and tracking wildlife. GPS receivers which are included in the transmitter can detect the animal's position and send coordinate data to a satellite or to a receiving terminal in the vicinity [19]. Criminals can be monitored using the LBS. Tracking inmates in prisons, navigating policemen, fire fighters and soldiers to complete their missions are the usage in public safety domain. Location Services for Vehicles and Traffic (LSVT) involve traffic intersection, collision avoidance, electronic parking payments, kilometer monitoring of vehicles on highways, location relative mobile marketing and location based tourist information service. The term for describing traffic-related services is traffic telematics [5]. Localizing and tracking inventory items in warehouses, materials and equipment in manufacturing floors is a general use of LBS. Banking

and restaurant search for a particular spot is also included in telematics [4].

Challenges

The challenge for a researcher in the area of positioning systems is to develop the efficient applications with minimal hardware requirements, producing accurate positioning and location information. This can only be accomplished when the transmitted signal is capable of annihilating the distortion and degradation introduced by the noise and the the multi-path wireless channel. Hence selecting the nature of the signal and it's transmission format is a challenging task which must adapt itself according to the varying channel conditions. This will be a major step to increase the accuracy of the positioning applications because all location finding and positioning applications are governed by the nature of the transmitted signal and the wireless channel environment [18]. Another major challenge for the indoor positioning application is Non Line of Sight (NLOS) conditions which often severely dwindle the estimation of the distance. Several researchers attempted different aspects of NLOS. The probability of NLOS and blockage of the direct path is very high [20, 21]. Therefore, the NLOS propagation (unavailability of the direct path), the multi-path fading and degradation due to heavy noise are the main challenges in indoor positioning systems.

Combating Techniques

To improve the ranging accuracy and to combat the multi-path effects, several techniques have been proposed for the low bandwidth systems [8, 22]. In recent years research focus has been diverted to resolve the errors in the NLOS situation [23, 24]. To achieve the acceptable levels of accuracy in indoor environments a large number of Reference Points (RPs) are needed [25] which is the cost of improving accuracy in all these techniques. In the sequel, we present the recent approaches adopted to overcome the main challenges faced by the positioning applications.

Ultra Wide Band (UWB)

UWB is a charming alternative to reduce the multi-path and the noise effects at low power for the positioning application. Due to available excess system bandwidth UWB signals produce accurate Time of Arrival (TOA) based ranging [26, 27]. Although in NLOS the accuracy of the estimation is not much precise [25]. Some UWB contributions involve algorithms presenting precision accuracy in [26], multi-path and multi-user environments in [27], distance error modeling in [28], UWB for WSN in [29] and that for the ad-hoc networks in [30]. Furthermore, algorithm for Undetected Direct Path (UDP) is presented in [31], for Line-of-Sight (LOS) in [32] and for LOS mitigation using linear programming in [33]. In the same sequel indoor sensor networks localization algorithm is presented in [34], TOA estimation algorithm in [35] while the channel modeling using TOA and Received Signal Strength (RSS) is presented in [36]. The drawback of UWB radio is that it can not cover very high range

due to the short pulses.

Ray Tracing

Ray Tracing (RT) algorithms save the efforts and time consumed in managing on site measurements for the positioning applications. The algorithms using reference radio map for the pattern recognition based on RT [37, 38] provided an alternative to the on site measurement. When direct path is not available the RSS and the TOA methods have the limited accuracy. With the change of bandwidth this accuracy can be improved. Some solutions regarding this idea have been provided in [39, 40] An intelligent RT trained neural network algorithm is used for the hybrid TOA-RSS based localization in [40].

WSN

Multi-hop WSN is another dimension of research for the positioning applications. WSNs have been studied in [41, 42]. The cooperative localization bounds for the WSN are presented in [43]. Characterization of ranging error in LOS, NLOS and DP blocked NLOS conditions are analyzed in [4, 44, 45]. Generalized Cramer Rao Lower Bound (G-CRLB) in dense cluttered indoor environments for the WSN is derived in [46] which also focuses impacts of node density, anchor density, building dimension and probability of NLOS and probability of the NLOS and the DP blockage on the cooperative localization performance. The impact of the channel condition on estimation error has been presented in [47, 48] to analyze the position error bounds for the dense cluttered environments. Cooperative Localization with Quality of estimation (CLOQ) to provide accurate location information is presented in [49, 50].

Motivations

All the techniques discussed above contribute a great worth in the considered domain. However, every technique has some drawbacks and limitations. Therefore, it is necessary to improve the performance of the existing techniques in order to get accurate estimation performance specially in heavy noise propagating environments with multi-path effects. Signal design issues are normally not considered while implementing the positioning algorithms, this causes to design the transmitted signal in a way that it should have the potential to combat the progressing noise and the multi-path effects. Orthogonal Frequency Division Multiplexing (OFDM) and Single Carrier Transmission (SCT) signals have these properties by their pedestrianism code structures and multi-carrier signal design respectively. Although some research using these signals has already been carried out but it is only at the initial level. Furthermore, tracking and positioning multiple objects is another issue which has not been explored to the satisfactory level in the present research to the best of our knowledge. Therefore, there is a need for the novel localization algorithms that are specifically designed for the harsh indoor environment.

Objectives

The principal goal of this research work is to develop an analytical framework for assessing the impact of the indoor propagation channel on the performance of Time Difference Of Arrival (TDOA) based localization. Super resolution algorithms enhanced the accuracy of TDOA estimation.

This dissertation makes a contribution in the field of indoor positioning applications using concrete signal design for the forthcoming wireless communication systems. It focuses on the comparison of two alternative signal structures of OFDM and SCT, their structure designs, coding effects, and the transceiver design to be used for the indoor positioning applications. Furthermore, the TDOA method is considered specifically to estimate the distance in a real indoor environment due to its accuracy amongst all counterpart methods. Another major goal is to compare the super resolution algorithms and to propose the optimal one for increasing the accuracy in NLOS conditions which often hampers the positioning applications. The following three sections lay the building blocks for understanding the central ideas of this dissertation. These building blocks provide a skeleton on which further development of the issues is carried out.

1.2   Wireless Channel Environment

Typically, the signal is received through more than one transmission paths between the transmitter and the receiver in a wireless environment known as multi-path. Multi-path fading occurs when the signal arrives at the receiver through mechanisms of line of sight transmission, reflection, diffraction, and scattering as shown in Fig. 1.1. As a consequence, the transmitted signal reaches the receiver through different propagation paths [51, 52] and the received signal is the sum of many versions of the transmitted signal with varying delays (τ's) and attenuations. This is the main source of distortion in the wireless channels. It produces frequency selective fading and Inter-Symbol Interference (ISI). These factors lead to performance degradation of the communication systems. In order to combat the deterioration caused by the multi-path effects, it is necessary to design a signal which is capable of annihilating these effects. Therefore, appropriate characterization of the channel is essential before the signal design. There are several methods and techniques, which have been used and investigated to study such effects [53, 54]. In indoor environments, wireless channel parametric models can be used to describe the complex transfer function or the Channel Impulse Response (CIR).

In the next section we discuss the design of the signal to be used in multi-path environment.
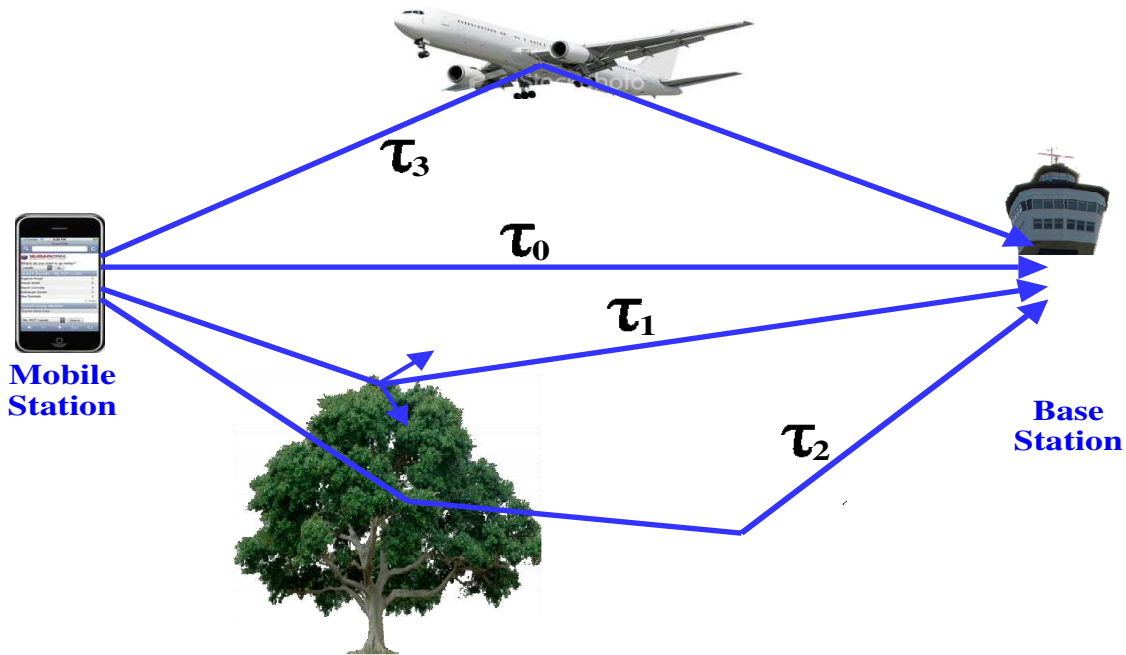
Figure 1.1: Multi-path propagation channel

1.3 Wireless Signal Structures

Multi-carrier signals combat the noise effects efficiently and hence are utilized in the most wireless communication systems. OFDM achieves the lowest bit rate, highest spectral efficiency and is robust against the multi-path effects [55]. It was found to be an optimal candidate technique for the future broadband systems, because of its high spectral efficiency, achieved by orthogonal carriers and ability to resist the multi-path fading channels [56, 57].

1.3.1 OFDM Signal Structure

In OFDM systems the information bit stream of a high data rate r is subdivided into M-bit-blocks that are mapped onto symbols of a lower transmission rates $r_s = r/M$. These symbols have duration of T_s each and are separated by the guard intervals of a duration T_g. A symbol is created by subdividing the available transmission bandwidth B into N sub-bands (sub-channels) whose mid-frequencies are those of corresponding sub-carriers. Choosing $BT_s = N$ guarantees the orthogonality of the sub-carriers over T_s. The M bits of a data block are then grouped into N sub-blocks whose bit constellations are used to modulate the N sub-carriers according to a Quadrature Amplitude Modulation (QAM) or a Phase Shift Keying (PSK) modulation scheme. Choosing T_g longer than the maximum channel-delay-spread τ_c eliminates the ISI in both time-invariant (constant τ_c) and time-varying (variable τ_c) channels, as shown

in Fig. 1.2. Moreover, the sub-carrier orthogonality shown in Fig. 1.3, eliminates the
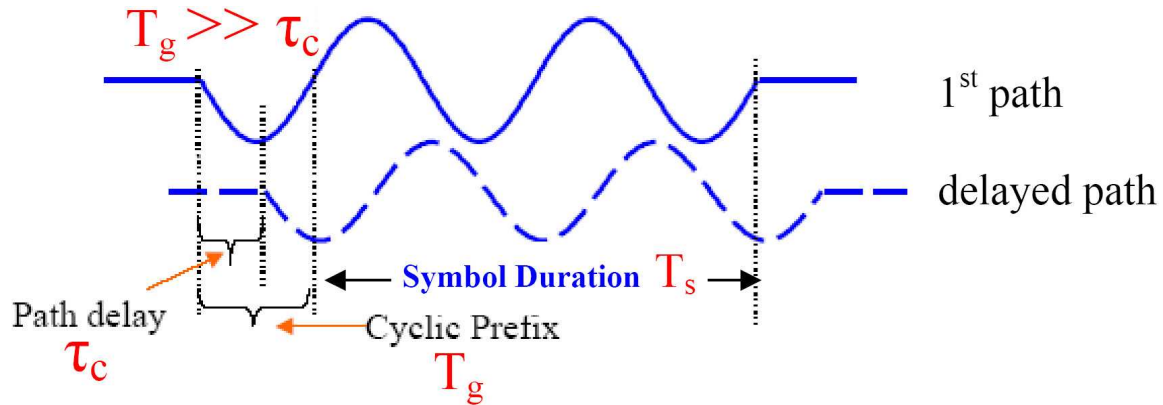
Figure 1.2: OFDM symbol design CP greater than delay spread

Inter-Carrier Interference (ICI) in time-invariant channels irrespective of their delay characteristics. On the other hand, eliminating ICI in time-varying channels needs additional signal processing at the receiver side, which necessitates a continuous monitoring of the channel. The latter is achieved by initially characterizing the channel using training signals followed by regularly transmitting pilot signals that are used to update the receiver information about the channel characteristics [58, 59].

Applications
Cimini [60] was the pioneer to introduce OFDM for wireless communications. Currently, OFDM has become the standard of some WLANs such as HIgh PErformance Radio Local Area Network 2 (HIPERLAN/2), IEEE 802.11a and IEEE 802.11g, DAB, DVB, and Multimedia Mobile Access Communications (MMAC).

Advantages
An OFDM system possesses a number of advantageous features. One of these is its high spectral efficiency due to minimum spectral spacing between the sub-carriers, which is caused by their orthogonality. A second feature is the system adaptability to frequency-selective fading. This is done by adapting the information capacity of the sub-channels (number of bits in the corresponding data sub-blocks) to the corresponding Signal-to-Noise Ratio (SNR). Moreover, an OFDM system shows high immunity against the impulsive noise. This is due to the fact that the transmitted information in an OFDM system is distributed in the frequency domain, where impulsive noise is more or less uniformly distributed. This means that the effect of impulsive noise occurring within a symbol duration is distributed over all bits of the corresponding data block.
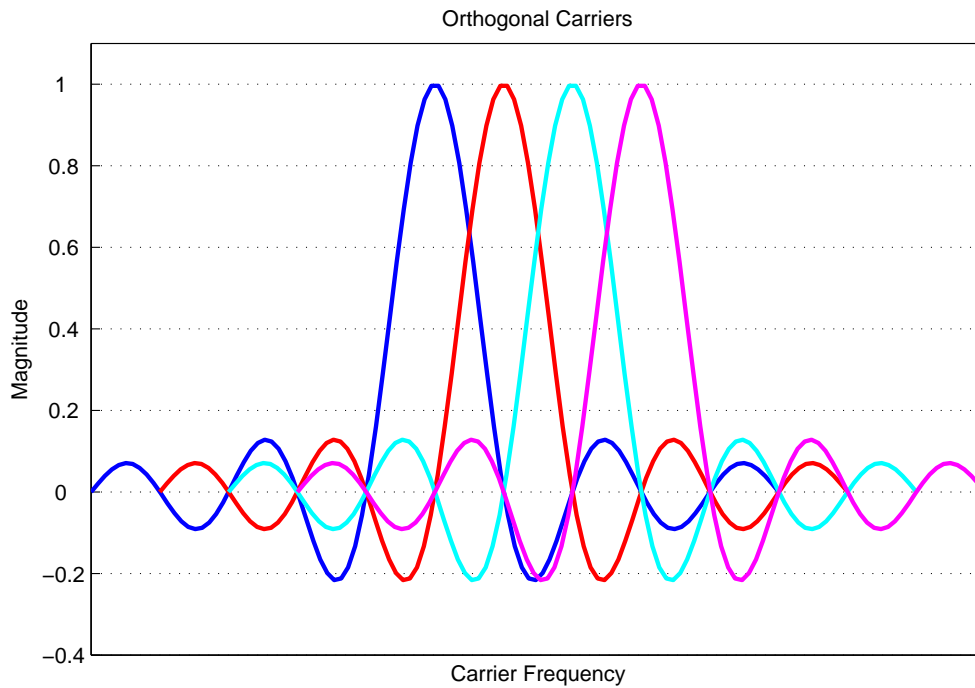
Figure 1.3: Orthogonal carriers used in OFDM signal structure

Drawbacks

OFDM systems suffer, however, from a number of drawbacks. The most significant one is the high Peak-to-Average-Power Ratio (PAPR) [55, 61]. This is caused by constructive interference between many sub-carriers, which may occur at few time instants within the symbol duration. One of the obvious difficulties related to high PAPR is the necessity of having very wide linearity dynamic-range for the power amplifiers at the transmitter RF stage. The ICI in time-varying channels represents another difficulty for the OFDM systems [62,63]. Channel estimation techniques [62,64] are usually applied to overcome this problem. The estimated channel transfer function, which is regularly updated by transmitting the pilot signals, is used to recover an ICI-free signal at the receiver. Such techniques fail, however, when the channel characteristics change considerably within a symbol duration.

Alternatives

In broadband systems multi-path effect can cause severe destruction. To provide low cost solutions, several variations of the OFDM have been proposed as effective anti-multi-path techniques [65]. Anti-multi-path approaches can be categorized as [66];

1. OFDM

2. Single-Carrier Transmission with Time Domain Equalization (SCT-TDE)

3. Single-Carrier Transmission with Frequency Domain Equalization (SCT-FDE)

OFDM provides in fact noticeable benefits in performance over SCT-TDE and combats the multi-path fading and long multi-path spread [60,67]. Conventionally, Time Domain (TD) equalizer processing in SCT (or SC) alleviates the power back-off and phase noise sensitivity problems. Hence SCT-FDE is a competing technique for OFDM. An equalized SCT system offers the same anti-multi-path and anti-noise capability as an adaptive OFDM [68] system does.

1.3.2   Signal Structure of Single Carrier Transmission (SCT)

SCT maintains the major advantages of OFDM and gives better solutions to both PAPR and ICI problems. It keeps the global OFDM signal structure (transmitting symbols of duration T_s separated by the guard intervals of duration T_g, with T_g being longer than the maximum channel-delay-spread τ_c) in order to eliminate the ISI which is known as Inter Block Interference (IBI) when we consider the block transmission using SCT.

In order to reduce (or even eliminate) the effect of frequency-selective fading, the envelop-waveform of the sub-symbols is designed such that the corresponding spectrum has minima or even nulls at the fading frequencies. To minimize the effect of impulsive noise, the bits of the M-bit-blocks are firstly scrambled and then subdivided into N equal sub-blocks that are mapped onto N symbols. If a symbol is corrupted (or even destroyed) by the impulsive noise, the corresponding effect will be distributed over all bits of the M-bit-block due to the initial scrambling. The mapping of a sub-block onto the corresponding symbol is done using a QAM or a PSK scheme. This SCT signal structure is shown in Fig. 1.4 and the symbol mapping to a unique carrier in contrast to the OFDM is shown in Fig. 1.5.

Benefits over OFDM
The SCT offers better solutions to the main problems of OFDM (namely, PAPR and ICI in time-varying channels). The periodic shape of the symbol envelop in an SCT (attributed to the fact that all its symbols have the same envelop-waveform) can lead to a very moderate PAPR if the symbol envelop waveform is properly designed. On the other hand, ICI in OFDM is equivalent to IBI in SCT. Both can be minimized (or even entirely eliminated) in the time varying channels using digital signal processing if updating the receiver information about the channel characteristics is fast enough. In order to extract information about the channel characteristics from the pilot carrying sub-carriers, an integration over the entire symbol duration T_s is required, which makes the updating process in OFDM systems more suitable for the slowly varying channels.
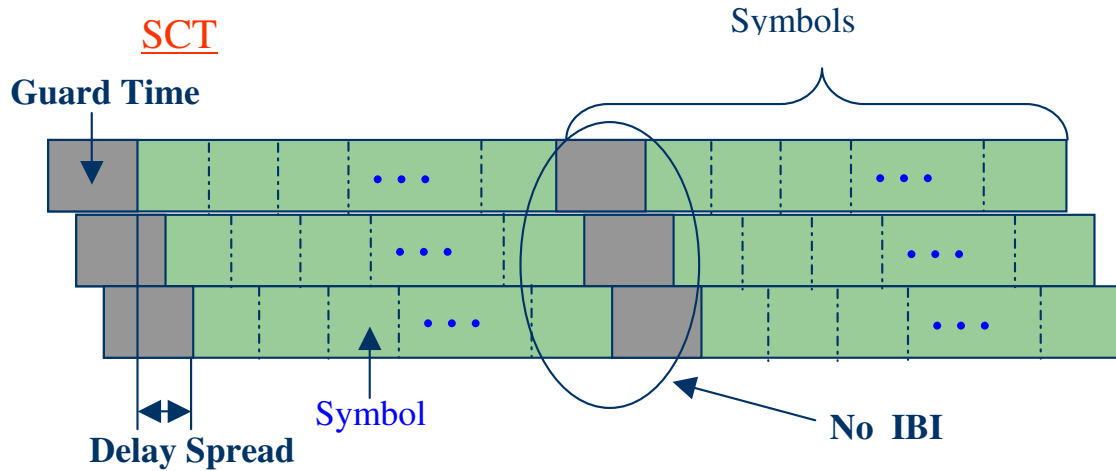
Figure 1.4: SCT signal structure
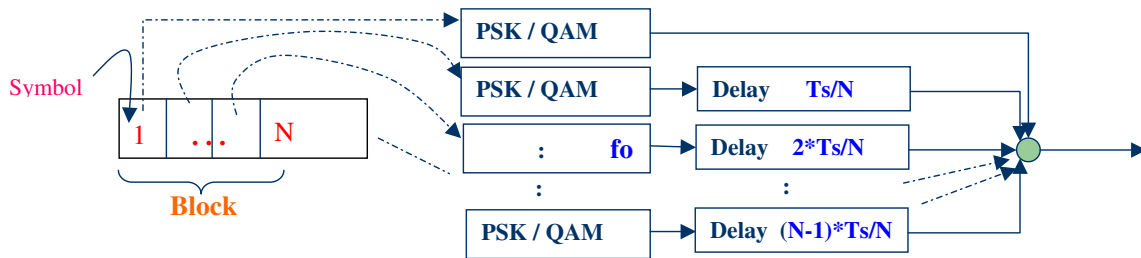
Figure 1.5: Mapping of the symbol block to a single carrier

Frequency Domain Equalizer (FDE)

A Decision Feedback Equalizer (DFE) yields better performance than a Linear Equalizer (LE) for the radio channels. SCT encompasses low PAPR which enables SCT technique to use a cheaper power amplifier than that which is used in the OFDM systems [69]. Recent developments in FDE using DFE have greatly improved the system based on the SCT technique. However, in contrast with OFDM which uses hundreds or thousands of sub-carriers, SCT uses a single carrier which encompasses the PAPR to be small enough to have less peak power backoff [66, 70].

Falconer [66] summarizes the attractive features of SCT with the FDE as under;

- Reduced PAPR thereby causing cheaper power amplifiers

- Performance similarity with that of OFDM

- Complexity reduction similar to that of OFDM

- Coding is not necessary to combat frequency selectivity

We can find a large number of literature explaining the benefits of the OFDM over the traditional SCT systems [55, 57]. A survey of the chronological development for the OFDM and SCT and their comparison has already been published in our work [71]. Since early 90's [65, 72] SC-FDE emerged as a competing technique for the OFDM, specially in the severe multi-path dispersive channels [68].

1.3.3 OFDM/SC Transceiver in Indoor Positioning Application

Multi-carrier distance measuring techniques using Frequency Hoping Spread Spectrum (FHSS) and OFDM are applied for the indoor positioning applications in order to get higher resolutions of the signal through greater clock rates and signal bandwidth [73]. In order to estimate the distance accurately we have designed a combined OFDM-SCT transceiver which has been published in [74]. Two different variants of Cyclic Prefixes (CP) are implemented to compare the performance. The CP variants are implemented for both OFDM and SCT signal structures, namely OFDM-Cyclic Prefix (OFDM-CP), OFDM-Zero Padding (OFDM-ZP), SC-CP and SC-ZP. This work has been published in [75]. A new SC-DFE model is presented which compares both OFDM and SC-DFE techniques in variable length channel environments. The effects of coding on OFDM and SCT have been analyzed in [76]. The next section discusses the basic features of the distance estimation methods used for positioning applications.

1.4 Distance Estimation Methods (DEM)

The major factor, which governs the accuracy and efficiency of the positioning applications, is estimation of the distance between transmitter and receiver. There are various methods for estimation of the distance [20] and can be classified in the following categories;

- Time of flight

- Angle of arrival

- Received signal strength

- Proximity

- Fingerprinting

Time of Flight (TOF)

TOF is the time interval between the transmission time of an epoch[1] to its reception at a distant receiver. The distance between them is the TOF times the speed of propagation which is speed of light in free space. TOF can be further sub-categorized in TOA, TDOA and Phase of Arrival (POA) where;

- **TOA** is the time of arrival of a signal at a receiver when the transmission time is known,

- **TDOA** is the difference of reception times at different locations and

- **POA** is the phase of the received signal which is related to time and distance through the signal wavelength and the speed of light [73].

Angle of arrival (AOA)

AOA or Direction Of Arrival (DOA) is the angle between wavefront (perpendicular to the direction of propagation) and the point in pattern rotation where the signal strength is maximum. For AOA measurement, the knowledge of transmitted power is not required. Distance cannot be found directly using an AOA measurement. At least two AOA measurements or an AOA and a TOF or RSS measurements are required to determine the position of a wireless terminal [21].

Received Signal Strength (RSS)

RSS is the power density strength of the received signal which is proportional to the transmitted power and inversely proportional to the square of the distance to the source. [36] The combination of waves that reach a receiver over different paths are the basis for estimating distance and location from the signal strength measurements.

Proximity

Proximity refers to the detection of a mobile terminal as being within radio range of a fixed location so that the mobile is known to be within an area around that location [18].

Fingerprinting

Fingerprinting locates a terminal by comparing various characteristics of a signal or signals received at or from that terminal with a database of the same type of characteristics that has been compiled in advance over a given area or volume [4].

---

[1]Epoch is a particular instant on the baseband waveform, for instance the start of a particular frame or the first bit after a synchronizing preamble.

1.4.1 Comparison of DEM

Proximity and fingerprinting are subcategories of RSS and sometimes of TOF [77]. The location sensing elements measure the RSS, AOA, and TOA as the location metrics. The TOA and TDOA methods use geometric relationships based on distances or distance differences between a mobile station and a number of fixed terminals to determine the position coordinates of the mobile target. The data for the distance estimations are derived from the arrival times of radio signal epochs at one or more receivers. TOA based systems are sensitive to available bandwidth and also to the occurrence of UDP channel conditions, while RSS based systems are less sensitive to the bandwidth and more resilient to UDP conditions [36]. On the other hand the measurements of RSS and AOA provide less accurate metrics than the TOA does [4, 7] because indoor radio channel suffers from severe multi-path propagation and heavy shadow fading, therefore, we focus only on the TOA and the TDOA methods in the sequel.

1.4.2 TOA/TDOA Methodology

In TOA location, estimates are computed by determining the points of intersection of circles or spheres whose centers are located at the fixed stations and the radii are estimated distances to the target where TDOA locates the target at intersections of hyperbolas or hyperboloids that are generated with foci at each fixed station of a pair. TDOA measurements are also foreseen for the positioning applications in the future Fourth Generation (4G) mobile communication systems, as it is proposed, e.g., within the WINNER project [78, 79]. The TOA and TDOA based location systems may be divided in two categories [73] which are;

Unilateral Systems in which the target communicates with or receives fixed terminal transmissions to measure time durations, and

Multilateral Systems where location calculations are performed independently of the target, either at one of the base stations or at a separate network infrastructure computing function.

All of the independent values in a set are based on at least one measurement of time of arrival between a base station and the target that is not used in any other measurement in the set. It is often considered sufficient to include only the independent TDOA in the location estimation process [80]. However, in a noisy environment additional pairs of measurements that are not independent according to the above criterion may be added for redundancy, since the noise that is not correlated between those pairs gives them a degree of independence [81]. In the presence of noise, the resulting multiple hyperbolas or hyperboloids, will not intersect at a single point and

a criterion must be established for determining the location that provides the best fit to the system of equations. Several methods of estimating location from over determined TDOA measurements are compared in [80, 81].

The geometric principles of the TOA and TDOA location methods are same for unilateral and multilateral systems.

1.5 Super Resolution Algorithms

Multi-path highly faded channels disperse the actual CIR by noise effects causing an inaccurate estimate of the TOA and hence the TDOA. The basic problem in the TOA/TDOA based techniques is that they accurately estimate the propagation delay of the radio signal arriving from the Direct LOS (DLOS) propagation path. However, in the indoor and urban areas, due to severe multi-path conditions and the complexity of radio propagation, the DLOS cannot always be accurately detected [20, 21]. In this situation the conventional IFFT and correlation based TOA/TDOA estimation normally result in inaccurate results [82]. Hence super resolution algorithms like Estimation of Signal Parameters via Rotational Invariance Technique (ESPRIT) [83], Root-Multiple Signal Classification (Root-MUSIC) [22] and Matrix Pencil (MP) [84] are to be applied. These algorithms use the Eigen Values (EVs) of the decomposed noise and signal subspaces. This opts to eliminate the effects of noise in the received corrupted signal and to generate an accurate estimate of the TOA and DOA for indoor portioning systems. Super resolution algorithms got noticeable attention in recent years for the time domain analysis [20, 82] and the spectral estimation of the time dispersion parameters [21]. The other applications include electronic devices parameter measurement [85, 86] and multi-path radio propagation studies [87]. In [87] a super-resolution algorithm is employed in the frequency domain to estimate multi-path time dispersion parameters such as the mean excess delay and the root-mean-square delay spread. A similar method is used in [54] to model the indoor radio propagation channels with the parametric harmonic signal models.

1.5.1 Super Resolution Algorithms with TOA/TDOA

Recently a lot of research work has been carried out for some of these algorithms. In [8], ESPRIT has been used to estimate accurate TOA for the indoor geolocation with diversity combining schemes. The performance of ESPRIT and Root-MUSIC algorithms for the TOA estimation have been studied through computer simulations based on measurements of indoor radio propagation channels in [8] and [21]. The idea of establishing empirical performance bounds for the real implementation of the super resolution indoor geolocation systems has been promoted. In [37] the generation of reference radio maps has been examined using radio propagation models to

replace the on-site measurements for calibration of the indoor geolocation systems. In addition the performance of the nearest neighbor and the maximum likelihood location estimation techniques have been compared. In [34] empirical models for the behavior of the Distance Measurement Error (DME) for the development of more precise indoor geolocation systems have been devised. The performance comparison for DME models derived from the UWB measurements with reference points has been presented in [6]. The effects of dielectric properties of the building materials on indoor position estimates have been presented in [88]. Indoor positioning using multiple pseudolites signals, has been studied in [89] to figure out an optimal geometric design for the indoor positioning.

We have utilized OFDM/SC-DFE signal structure presented in our previous work [74] and [75] to examine the performance of the super resolution algorithms. We have presented the comparisons of IFFT, correlation, ESPRIT, Root-MUSIC and MP algorithms in [90] by our computer simulations applied on the indoor positioning system. The data sets for the transmitted and the received signals are captured at a typical indoor area. The super resolution algorithms for estimations are applied at the Chair of Microwave and Communication Engineering (CMWCE), University of Magdeburg.

1.5.2   Model Order Criterion

The information theoretic criteria for the model selection is normally applied [91] in order to detect the number of sources involved in transmission from multiple sources. The detection of the number of sources is counted by multiplicity of the smallest EVs of the correlation matrix. There exist many model selection criteria for this purpose, enlisted as following;

MDL
Minimum Descriptive Length (MDL) criterion is the criterion to calculate the minimum effective length of the channel by eliminating the noise component from the dispersive CIR [92]. MDL [86] is regarded as the classical estimation algorithm which is still effective. There is no need to find the autocorrelation matrix or its EVs in MDL. This significantly reduces the computation complexity. MDL [93] is defined as

$$MDL(k) = L(\theta) + f(k, N_p) \tag{1.1}$$

where $f(k, Np)$ and $L(\theta)$ are the penalty function and the log-Likelihood function, given the by following equations;

$$f(k, N) = \frac{1}{2}k(2N - k)\log(M_B) \tag{1.2}$$

$$L(\theta) = -N\log(\det(R_{HH})) - tr(R_{HH})^{-1}R_{HH} \tag{1.3}$$

where tr represents the trace of the matrix and R_{HH} is the diagonal matrix of correlation of the CTF. The close expression of the Maximum log-Likelihood (MLL) function can be obtained as

$$L(\theta^{(k)}) = -(N-k)M_B \log(\frac{G(\lambda_{K+1}, \ldots, \lambda_N)}{A(\lambda_{K+1}, \ldots, \lambda_N)})$$ (1.4)

where the functions G and A are the geometric and the arithmetic means of their arguments, respectively. The value of M_B needs to be selected such that it provides a balance between the resolution and stability of the criteria. The CIR length L is taken to be the value of $k \in 0, 1, \ldots, N-1$ for which $MDL(k)$ is minimum.

EIG
EV criteria (EIG) finds the EVs of the correlational matrix, normalizes the EVs, and chooses the number of paths as all the EVs greater than a particular threshold [91]. This threshold is related to the noise variance.

AIC
Akaike's Information Criterion (AIC), developed by Hirotsugu Akaike under the name of "An Information Criterion" in 1971, is proposed in Akaike (1974) [94]. It is a measure of the goodness of fit for an estimated statistical model. Given a data set, several competing models may be ranked according to their AIC, with the one having the lowest AIC being the best. AIC is actually calculated as

$$AIC(K) = 2k - 2ln(L)$$ (1.5)

where k is the number of parameters in the statistical model, and L is the maximized value of the likelihood function for the estimated model.

Modified MDL (MDX)
MDX is the modified form of MDL. It is formed by using the new penalty function shown as following

$$P_f(k, N) = \frac{1}{2}k(2N - K)\log(M_B)$$ (1.6)

The AIC and MDL criteria use EVs to detect the number of arrival signals. EVs corresponding to noise subspace are equal to the noise power and those noise EVs have roots in Gaussian distribution. Both methods assume the cost function based on Gaussian distribution using information theory. This cost function estimates the threshold which divides EVs into the signal and the noise EVs.

A new scheme is proposed in this thesis. It is based on two different antennas used to transmit the OFDM symbols, mapped to multiple carriers, for the WLAN system. Two multi-path faded signals, corrupted by the Additive White Gaussian Noise

(AWGN) are received through the OFDM receiver where signals are added. Super resolution algorithms like ESPRIT, Root-MUSIC and MP are used to estimate the TDOA and consequently the actual distance between the transmitter and the receiver. The DME are compared for the conventional and the super resolution algorithms. An analysis of DME estimation, presented for varying the SNR, the time resolutions and the number of carriers, is published in [90].

1.6 Thesis Contributions

We sum up the contributions of the thesis in this section, which have already been mentioned in the above text;

1. A joint OFDM and SCT transceiver is designed and implemented which has been published in [74].

2. A detailed chronological survey has been carried out for the development of the OFDM and SCT, published in [71].

3. A modified criteria for the DFE of the SCT is implemented which decays exponentially and improves the decision performance at the equalization stage. The work has been published in [75].

4. Two different variants of CPs are implemented for both the OFDM and the SCT signal structures namely OFDM-CP, OFDM-ZP, SC-CP and SC-ZP. It has been published in [75]. These variants are compared for the variable length channel environments and improved performance is achieved for the DFE implementations.

5. A coding block is implemented in order to testify the effects of coding on OFDM and SCT, which has been published in [76]. The coding performance has been analyzed which brought an efficiency drift in the current system.

6. A comparison of traditional and super resolution algorithms is performed using the real data sets to distinguish and verify the performance of super resolution algorithms. The best performance is achieved by the MP algorithm, which reduces the DME to less than 1 meter. The data sets for the transmitted and the received signals are captured at the typical outdoor and indoor areas. The estimation algorithms are applied at the CMWCE, University of Magdeburg. This has been presented in [95].

7. A new scheme is proposed which is based on two different antennas used to transmit the OFDM symbols mapped to multiple carriers using WLAN system. Two multi-path faded signals, corrupted by AWGN are received through

the OFDM receiver where both signals are added. The scheme increases the accuracy of the distance estimations, published in [90].

8. An analysis of the DME estimation is presented for the varying SNR, variable time resolutions and multiple number of carriers, published in [90].

9. Variants of the MP algorithm are introduced and tested to compare the results in different situations. Four model order criteria of MDL, AIC, EIG and MDX and an automatic criterion are utilized. All possible combinations of MP variants and model criteria are used to rectify different combinations for the particular situation, presented in [96].

1.7 Thesis Organization

The rest of the thesis is organized in the following order;

Chapter 2 reviews the characterization of wireless communication channels. It presents the parameters of the channel models used for the indoor positioning system. Time invariant and variant considerations are discussed along with their statistical properties.

Chapter 3 presents the transceiver design of the combined OFDM and SCT signal structure. A survey of the comparisons in this domain is also presented. The transceiver implementation has also been modified and tested by the coding block, which improves the performance of the system.

Chapter 4 focuses on the estimation methods used for indoor positioning system. It compares and rectifies the best amongst these methods with a real time implementation scenario.

Chapter 5 demonstrates the super resolution algorithms and their usage for improving the accuracy in the noisy environments. It focuses specifically on the MP algorithm variations. Furthermore, the model order criteria variants are also elaborated. The combinations of all possible MP and model order criteria variants have been implemented to investigate the best possible solution for the positioning and tracking objects.

Chapter 6 summarizes the thesis and concludes the findings to propose the future possible dimensions of research.

Chapter 2

Channel Characterization for Indoor Positioning Applications

The channel is a vital and integrated component of the wireless communication system. Its design governs the variety of performance and value of any system under consideration. Therefore, accurate knowledge of the channel is either required or to be estimated while the design of the wireless communication system is initiated. This is termed as channel characterization. For the indoor positioning used in this thesis, we have focused on estimating the wireless channel which is always very unpredictable with the harsh and challenging propagation situations. Multi-path reception is a characteristic of the wireless channel. With multi-path channel various vital impairments are associated which are propagation path loss, shadow fading, Doppler spread, time dispersion, delay spread and the other parameters. In the following section we introduce the multi-path channel model and then some of its important impairments.

2.1 Wireless Communication Channel Model

We can simply model the wireless channel by taking the ratio of the received and the transmitted frequency domain signal which is known as the Channel Transfer Function (CTF). Applying the Inverse Fast Fourier Transform (IFFT) produces the CIR in time domain. If a signal is transmitted in the wireless communication environment, the incident field $E(\omega, r, t)$ caused by the received signal is a function of the angular frequency ω, the distance $\mathbf{r}$ and the time t. Assuming that the signal is propagated in free space, the received electromagnetic wave can be written as

$$E(\omega, r, t) = E_o e^{j\omega t - j\beta r} \tag{2.1}$$

where E_o is the initial electric field and β is called phase factor and represented by

$$\beta = \frac{\omega}{c} \tag{2.2}$$

where c is the speed of light in free space. The received signal will have a time delay τ depending on the distance r between the transmitter and the receiver. The relation

between time delay and the distance can be written as follows

$$\tau = \frac{r}{c} \tag{2.3}$$

The electric field now can be written as

$$E(\omega, r, t) = E_o e^{j\omega t - j\omega \tau} \tag{2.4}$$

The signal is received through multiple number of paths in a typical wireless communication system. These paths, shown in Fig. 2.1, are caused by the numerous reflections, diffractions and scattering by the different objects lying between the transmitter and the receiver.

A typical wireless channel generally comprises these paths and its CIR can be represented by a tapped delay module, shown in Fig. 2.2. Multi-path interference
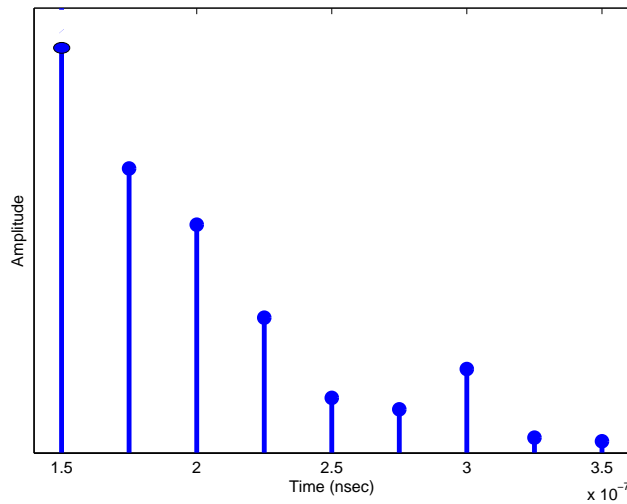
Figure 2.1: CIR comprising multi-paths

introduces the path delay and fading in the received signals. The fading is modeled as a number of sinusoids [97, 98] each of which corresponds to different scattered and reflected rays. The CIR for this model can be written as

$$h(\tau) = \sum_{l=1}^{L} a_l \delta(\tau - \tau_l) \tag{2.5}$$

where a_l and τ_l are the propagation path amplitudes and the delays respectively. Each multi-path component will have different phase resulting in constructive or destructive
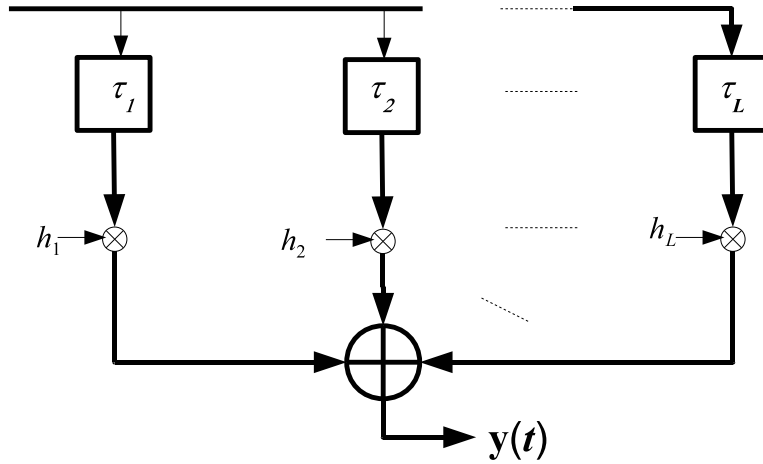
Figure 2.2: Tapped delay line channel model

interference due to the delay. The CTF is obtained by applying Fourier Transform (FT) to the CIR with respect to the delay τ as follows

$$H(f) = \int\limits_{-\infty}^{\infty} h(\tau)e^{-j2\pi f \tau}d\tau \tag{2.6}$$

Eq. 2.6 shows the frequency-selectivity, which is a transfer function characteristic property of a multi-path radio channel. This means that due to the multi-path interference the channel is frequency selective fading. Fig. 2.3 mimics this effect. The multi-path parameters can be calculated by CIR. If a high data rate stream is transmitted over the frequency selective channel, multiple data symbols interfere with each other, making the data detection difficult. Therefore, some design technique is needed to overcome this situation.

2.1.1 Time Varying Wireless Channels

If there is a relative movement with random speed and direction between the transmitter and the receiver, there is a frequency shift due to the Doppler's effect [99]. When the receiver is moving, the Doppler shift f_d is given by [97]

$$f_d = \frac{\nu}{\lambda}\cos\alpha \tag{2.7}$$

where ν is the velocity of the moving receiver and λ & α are the wavelength and the angle of arrival of the direction of incoming horizontal signal at frequency f, respectively. Thus the Doppler shift associated with the received signal frequency f
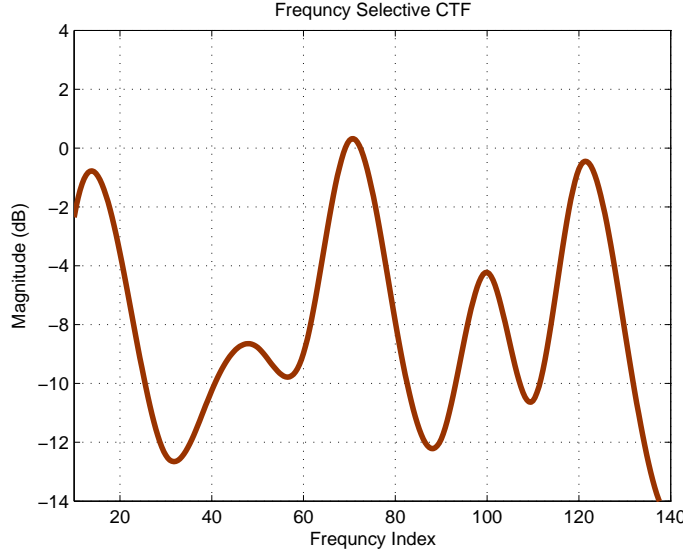
Figure 2.3: Frequency selective CTF

by the factor f_d changes f as $f = f \pm f_d$. Assuming that L multi-path components reach the receiver, then the time variant CIR $h(\tau, t)$ can be expressed as

$$h(\tau, t) = \sum_{l=1}^{L} a_l(t)\delta(\tau - \tau_l(t)) \tag{2.8}$$

where $a_l(t)$ and $\tau_l(t)$ are the time varying amplitudes and the delays of the path l respectively. The corresponding time variant CTF with respect to τ is given by

$$H(f, t) = \int_{-\infty}^{+\infty} h(\tau, t)e^{-j2\pi\tau f}d\tau \tag{2.9}$$

The Doppler dependant CIR can be calculated by taking the FT of eq. 2.8 with respect to t as

$$S(\tau, f_d) = \int_{-\infty}^{+\infty} h(\tau, t)e^{-j2\pi\tau f_d}dt \tag{2.10}$$

and the Doppler dependant CTF can be calculated by taking the double FT of eq. 2.8 with respect to τ and t respectively as

$$T(f, f_d) = \int_{-\infty}^{+\infty}\int_{-\infty}^{+\infty} h(\tau, t)e^{-j2\pi\tau f}e^{-j2\pi t f_d}d\tau dt \tag{2.11}$$

This multi-path channel can be modeled as a linear filter with the AWGN.

2.1.2   Channel Behavior for Indoor Positioning

If d is the distance between the transmitter or the Base Station (BS) and the receiver or the Mobile Station (MS), we can rewrite eq. 2.5 of the CIR as

$$h(t) = \sum_{i=1}^{L} a_l \delta[\tau - \tau_l] \tag{2.12}$$

where L is the number of multi-path components, $a_l = |a_l|e^{j\phi_l}$ and τ_l represents the random complex amplitude and random propagation delay of the lth path, respectively. Having finite bandwidth ω; the transmitted signal $x(t)$ and the received signal $r(t)$ can be modeled as

$$r(t) = \int_{-\infty}^{+\infty} x(t)h(\tau - t)d\tau \tag{2.13}$$

2.1.3   TOA Estimation from the Channel Profile

The TOA of the direct LOS path between the transmitter and the receiver indicates the distance between the transmitter and the receiver. The TOA of the First Detection Peak (FDP) of the channel profile above a detection threshold is used as an estimate TOA of the direct LOS path denoted by $\hat{\tau}_1$. The estimated distance between the MS and the BS is calculated as $\hat{d} = c \times \hat{\tau}_1$, where c is the speed of light.

The actual expected and the estimated direct path are the same in an ideal situation, whereas the multi-path channel causes an estimation error because the peak of the channel profile shifts from the expected TOA. This estimation error is known as DME. The DME can be calculated as

$$\varepsilon = |\hat{d} - d| \tag{2.14}$$

Categories of Channel Profiles

Channel profiles can be categorized in three types depending upon the availability of the direct path, given below [20]

- **Dominant Direct Path (DDP)** The strongest path in the profile is the direct path detected by the receiver.

- **Non-Dominant Direct Path (NDDP)** The direct path is not detected as the strongest path by the receiver. It requires the complex signal processing to be detected, and

- **UDP** The other paths are detected and the direct path is below certain threshold level. The FDP is assumed to be a direct path by the receiver which causes the huge DME.

The system bandwidth affects the channel profile. With its increment the channel profile tends to be ideal and TOA estimation becomes more accurate and hence DME is reduced [36]. This reduction of DME with the bandwidth increment is only applicable to DDP and NDDP conditions, however, for UDP conditions the DME is not necessarily reduced [100].

2.1.4 IEEE Channel Models for Positioning

The IEEE 802.11 recommended channel models have been adopted as a standard for WLAN systems. Average path loss estimation is provided by these channel models [101]. There are five different models ranging from A to E, depending upon the various RMS delays to form the different environment group [102]. These IEEE 802.11 path loss models, shown in table 2.1, are defined using the following legends;

- d is the distance in meters,

- L is the path loss in dB,

- L_{FS} is the free space loss,

- d_{BP} is the break point distance and is defined as;

    The distance to which the path loss is considered to be α_1 and above which it is considered to be α_2,

- X is the shadow fading component; modeled with a zero mean Gaussian probability distribution and

- α_x is the standard deviation of the shadow fading.

The free space path loss is defined as

$$L_{FS}(d) = L_0 + 10 \cdot \alpha_1 \log_{10}(d) + X \tag{2.15}$$

The overall path loss for any distance model is

$$L(d) = \begin{cases} L_{FS}(d) + X & d \leq d_{BP} \\ L_{FS}(d) + 10 \cdot \alpha_2 \log_{10}(\frac{d}{d_{BP}}) + X & d \geq d_{BP} \end{cases} \tag{2.16}$$

Model A is the flat fading model with $0\,ns$ rms delay spread. It has one tap at $0\,ns$. It is an optional channel model and should not be used for the system performance comparisons, however, it can be used for stressing system performance for the indoor channel simulation. Models B to E are suitable for indoor positioning and present different channel environments.

2.2 Spectral Methods for Multi-Path Estimation

The spectral estimation algorithms can be used to evaluate the channel parameters (complex exponents) depending on the model of Eq.(2.8) from the given measurements. The most common conventional method of spectral estimation is based on the FT technique because it is easy to implement and computationally attractive. The ability of FT technique, to distinguish the spectral response of two or more signals that are close in time delays, is limited. In real systems the CTF is available only for the bandwidth of **B** Hz. The measured CTF can be written as follows

$$H_m(f) = H(f)rect(B) \tag{2.17}$$

where

$$\mathbf{rect(B)} = \begin{cases} 1 & \textbf{if} \quad |f| \quad \leq \frac{\mathbf{B}}{2}, \\ \\ 0 & \textbf{if} \quad |f| \quad > \frac{\mathbf{B}}{2}. \end{cases} \tag{2.18}$$

The Inverse Fourier Transform (IFT) of Eq.(2.17) can be written as the CIR convolved with the Sinc function Q as follows

$$h(\tau) = \sum_{l=1}^{L} h_l Q(t - \tau_l) \tag{2.19}$$

where

$$Q = \frac{\sin(2\pi\mathbf{B})}{2\pi\mathbf{B}} \tag{2.20}$$

The plot of the CIR versus t will show L Sinc functions, each Sinc function will appear at $t = \tau_l, l = 1, \cdots, L$. In order to separate two components of τ_1 and τ_2 with $\tau_2 > \tau_1$ in frequency domain, it is necessary to have a frequency response with a bandwidth of [103]

$$\mathbf{B} = \frac{1}{\tau_2 - \tau_1} \tag{2.21}$$

This shows that the spectral resolution of the FT based approach is limited by the frequency bandwidth of the given system. However, there are several performance limitations of FT such as spectral leakage and low resolution, which reduce its ability to estimate rays with short delay. Therefore, an alternative approach is required.

2.3 High Resolution Spectral Estimation Techniques

Other advance spectral estimation methods offer better resolution in estimation and have less variance [104]. The spectral estimation techniques can be classified into three different types, the conventional techniques, the subspace based techniques (super resolution algorithms) and the parametric techniques. The super resolution algorithms

exploit the Eigen structure of the input data matrix. Generally we can say that the IFT and correlation based method, known as (Xcorr) use the peak detection method, because their accuracy is directly limited by the sampling rate. These methods give strict estimation for the distances by rounding the estimated distances and an error of 1.5 meter is normally expected. On the other hand super resolution algorithms are also affected by the sampling rate (signal bandwidth in general), but the estimation accuracy is better than the IFT and correlation based algorithms [8].

The use of super resolution algorithms can provide high resolution estimation of the signal parameters with good performance. The super resolution algorithms rely on the decomposition of the observation space into signal subspace and noise subspace [104]. The number of sources is determined by the number of significant eigenvalues. Generally modern high resolution subspace estimation methods are classified into three types [105]. First, spectral searching techniques like MUltiple SIgnal Classification (MUSIC) [106], next the polynomial rooting such as root-MUSIC [107] and finally matrix shifting method such as ESPRIT [108] and MP [64, 109].

The disadvantage of MUSIC algorithm [106] is its computational complexity. It needs multidimensional search to find the peaks of the cost function. Root-MUSIC is preferred because it posses less loss of the resolution effect [110]. The algorithms which use the maximum likelihood technique to estimate the parameters have good performance but are often computationally very intensive. Another approach for spectral estimation also based on Prony technique has been recently introduced [111]. The suitability of the super resolution algorithms for a certain application is an important issue. MP have been used in the field of spectral analysis. We leave the further details of super resolution algorithms for the chapter 4, where we explain how these algorithms work with their application to the real indoor positioning applications.

Table 2.1: IEEE 802.11 Path Loss Models for the Indoor Channels

Model	RMS Delay Spread (ns)	d_{BP} (m)	α_1	α_2	Standard Deviation α_x of shadow fading (dB)		**Description**
					Before d_{BP}	After d_{BP}	
A	0	5	2	3.5	3	4	Flat Fading Model (optional)
B	15	5	2	3.5	3	4	Residential Small Office
C	30	5	2	3.5	3	5	Typical Office
D	50	10	2	3.5	3	5	Large Office
E	100	20	2	3.5	3	6	
F	150	30	2	3.5	3	6	Hall or Large Space

Chapter 3

Multi-Carrier Signals and Transceiver Design

3.1 Multi-Carrier Signals

Multi-carrier signals are widely used in the communication systems [1]. They are modulated using QAM techniques based on M-ary QAM like BPSK, QPSK, 16QAM or 64QAM, in which constellations are used to map the bits onto the symbols. Extracting timing measurements from the communication signals directly results in a synchronization problem where normally the arrival time of the transmitted signal from the BS has to be measured at the MS. Several algorithms are widely used for positioning applications implicating CDMA signal structure [77]. Generalized Multi-Carrier (GMC) signals [112] based systems, like OFDM, are much relevant to improve the performance of these algorithms due to their specific modulation scheme. As specified in chapter 1, the OFDM and SCT signals are the two parallel alternatives for the 4G communication systems specially in the indoor positioning applications.

We have already compared the basic structures of OFDM and SCT in chapter 1, in this chapter we initially present a survey of the evolutions in recent years for the OFDM and SCT design in section 3.2. This survey has been published in our work [71]. In section 3.3 we present our newly designed equalizer [75] which is used for the current positioning application studies in chapter 4 of this thesis. As stated earlier that recent developments in FDE using DFE have greatly improved the efficiency of the systems based on the SCT. We present the comparison of two different variants of both OFDM and SCT, namely OFDM-CP, OFDM-ZP, SC-CP and SC-ZP in the subsequent section. SC variants are simulated with LE and DFE. The block DFE structure iteratively improves itself and performs better as we increase the number of iterations. The effect of coding on both OFDM and SCT equalizer have been published in [76]. Implementation of the joint OFDM/SCT transceiver and comparison results for BER simulations of both variants of OFDM and SC with LE and DFE

are presented in section 3.4. These results verify the supremacy of CP versions of the SC-LE and SC-DFE over the OFDM-CP and OFDM-ZP.

3.2 Recent Developments for OFDM and SCT Transceiver

As we have already mentioned in chapter 1 that the SCT technique has been used conventionally for decades with the TDE [113, 114]. In this section we attempt to review maximum literature produced in order to obtain the latest optimized DFE. It is Hikmet Sari at el [65] of SAT, Division Telecommunications, France who initially described the FDE for SCT and then proposed it for terrestrial broadcast channels [68, 115] in 1994. In the next year the same authors discovered that TDE can not handle ISI on channels with very long impulse responses and may fall on single frequency network. He found a strong analogy between the OFDM and SC systems with FDE and proposed it for the digital terrestrial TV broadcasting systems to handle same type of channel impulse responses as of the OFDM systems [72]. This opened a new perspective for research on a technique equivalent to OFDM in the modern communication systems. In [65, 72] the same authors indicated that the SC-FDE have essentially the same low complexity as of OFDM systems, when combined with Fast FT (FFT) processing and the use of a CP.

Berberidis, 1995 [116] described a version of a FD-DFE, which feeds decisions back after a certain delay for better performance. In 1996, Ariyavisitakul [117], developed a reduced-complexity TD adaptive DFE for the long impulse responses. He investigated two basic techniques DFE and Delayed Decision Feedback Sequence Estimation (DDFSE) for highly dispersive channels to minimize the complexity. In the same year, Hara et al, 1995 [118] discussed the co-existence problem of Direct Sequence Code Division Multiple Access (DS-CDMA) and Time Division Multiple Access (TDMA) systems, where they simulated both systems sharing the same frequency band to improve spectral efficiency.

Karstten, 1997 [119] elaborated the duality of Multi-Carrier (MC) spread spectrum and SCT in 1997. Czylwik, 1997 [120] compared the MC-OFDM and SCT schemes by simulating different time variant transfer functions and found that the SCT performance was significantly better than that of OFDM with the fixed modulation schemes.

Clark, 1998 [121], introduced a kind of adaptive equalizer that operates in the spatial frequency domain and uses either Least Mean Squares (LMS) or Recursive Least Squares (RLS) adaptive processing to get the performance gains and complexity savings. The equalizer was capable of alleviating nonlinear distortion and carrier synchronization problems of OFDM. Aue, 1998 [70] compared the performance of linearly equalized SCT and coded OFDM and shown that for low SNRs and low code rates,

the cutoff rates of both systems are approximately the same and for the un-coded systems, SCT outperforms OFDM.

Gusmao, 2000 [122] has emphasized on the impact of channel coding and amplification for the MC and SC transmission using FDE and found the equivalent effect. In the same year, Wang, 2000 [112] described the MC transmitting with CP and ZP techniques, with slightly increased complexity, to eliminate Multi-User Interference (MUI) and ISI. CP technique has the feature of simple equalization while ZP technique guarantees successful symbol recovery at the receiver end. He also described the block equalization types that are Pre, Post and Balanced equalizations, to be used for the complexity reduction and efficiency improvement of MC systems. In the same article he introduced the concept of GMC CDMA for an efficient MU transmission.

Al-Dhahir, 2001 [123] proposed a low-complexity scheme for combining Space Time Block Coding (STBC) with SC-FDE to achieve the significant diversity gains. Tubbax, 2001 [124] studied front-end nonidealities of OFDM and SC-CP WLAN modems and shown by his simulations that for the same data rate, bandwidth and transmit power constraints SC-CP allows the design of a more power efficient modem than OFDM and is therefore a better candidate for the portable wireless terminals. Ayanoglu, 2001 [125] described and compared Vector OFDM (VOFDM) as a coding, modulation and spatial processing technique (for Fixed Broadband Wireless Internet Access Applications) with SCT and analyzed its performance to show that it provides substantial improvements over SCT, but VOFDM had worse limitations of power amplifier back-off and phase noise on that of SCT. Alhava, 2001 [126] defined an adaptive Sine/Cosine-Modulated Filter Bank (S/CMFB) equalizer for transmultiplexers to improve the performance of the equalizers.

Falconer, 2002 [66] presented a convertible SC-OFDM receiver, which could alter the receiver processing depending upon the received signals between OFDM and SCT [66]. He also proposed employing OFDM in the downlink and SC-FDE in the uplink for reducing the subscriber unit cost and complexity. In Falconer, 2002 [127] the compatibilities of the SCT with the OFDM and its extensions via the DFE & overlap-save processing of both techniques were discussed by the same authors. The same authors, a year later, introduced a simpler hybrid time-frequency domain DFE approach [66] to avoid the feedback delay problem. It was performed using the FD filtering only for the forward filter part and the conventional transversal filtering for the feedback part of the DFE . It was also concluded in [66] that the PAPR for SCT signals is smaller than that of OFDM. Hence it required a smaller linear range to support a given average power, or equivalently required less peak power backoff, therefore, it enabled the use of cheaper power amplifier than a comparable OFDM system. In the same year Benvenuto, 2002 [128] presented a similar FD-DFE for SCT

which was simulated for the HIPERLAN/2 scenario and achieved similar conclusions as of [66]. Furthermore, a reduced complexity technique for the FD-DFE was developed which had similar computational complexity as that of OFDM. Benvenuto also proposed an Iterative Block DFE (IB-DFE) for the SCT, which was used to cancel the precursors and postcursors of the ISI to get better performance [129]. SC Block Transmission (SCBT) in DS-CDMA is also known as Chip Interleaved Block Spread (CIBS) CDMA. Petre, 2002 [130] worked on downlink SCBT with Known Symbol Padding (KSP) instead of the ZP, as a postfix that can be used for training purposes at the receiver. He proposed three different methods for direct equalizer estimation using KSP. He analyzed outstanding performance with the semi-blind joint CDMP/KSP-trained method which was one of his proposed methods in (SCBT) DS-CDMA.

In Zhou, 2003 [131], Zhou studied STBC for SCBT and proposed a novel transmission scheme that achieved a maximum diversity of order $N_t N_r (L+1)^1$ in rich scattering environments. He developed transmission enabling ML optimal decoding based on Viterbi algorithm, as well as turbo decoding for achieving high capacity. It was proposed that the single receive and two transmit antennas should be used to have no capacity loss. It was also concluded that the joint exploitation of the space multi-path diversity leads to significantly improved performance in the presence of the frequency selective fading channels. Petre, 2003 [132], in the same year, designed the transceiver by combining SC Block Spread (SCBS) CDMA and Time Reversal (TR) STBC techniques, to resolve MUI problem in the downlink. It allowed deterministic ML user separation through low complexity code matched filtering as well as deterministic transmit stream separation through linear processing to guarantee maximum diversity gains. Alhava, 2003 [133] defined Exponentially-Modulated Filter Bank (EMFB) based on the Extended Lapped Transform (ELT) and alterative realization structures for the S/CMFB to increase the efficiency. Gusmao, 2003 [134, 135] also verified the performance advantage of the SC-FDE in space diversity within the block transmission schemes when compared with the MC modulation schemes. Schniter, 2003 [136] presented a low complexity two stage receiver for the SC-CP to truncate the effective Doppler response optimally and to perform soft interference cancelation in these stages, respectively.

In Wang, 2004 [137] comparisons of the OFDM with SC-ZP block transmissions in aspects of the PAPR, BER performance, system throughput, un-coded system performance & complexity and coded system performance & complexity were performed. It was confirmed by the simulations that SC-ZP has considerable edge in terms of the PAPR, robustness to carrier frequency offset and un-coded performance, at the

---

[1]$N_t (N_r)$ is the number of transmit (receive) antennas, and is the order of the Finite Impulse Response (FIR) channels.

cost of slightly increased complexity. Tran, 2004 [138] proposed the SC systems for STBC coded and concatenation of a FEC code with a STBC over ISI fading channels based on successive interference cancelation technique. He has shown that the STBC system outperforms the OFDM receiver under the power constraint scenario and also when multiple receiver antenna diversity is applied. Oltean, 2004 [139] verified the performance supremacy of the SC-FDE over OFDM. Tomeba, 2004 [140,141] studied the FD pre-equalization at a transmitter as an effective technique to improve the transmission performance. Zhang, 2004 [142] proposed the Channel Estimate based FDE (CE-FDE) scheme using the LMS or RLS algorithms. It was proposed that the diversity combining for the channels with high Doppler frequency and tap selection strategy for the channels with sparse multi-path propagation, improve system performance and reduce the complexity simultaneously. Dinis, 2004 [143] presented an iterative Layered Space Time (LST) receiver structure for SCT which combined LST principles with IB-DFE techniques to get the performance closer to the MF Bound (MFB) in few iterations. Schniter, 2004 [144] presented Iterative FDE (IFDE) scheme based on Doppler channel shortening, soft iterative interference cancelation and block decision feedback which outperformed the FIR-MMSE-DFE in both the performance and the complexity. Hidalgo, 2004 [145] developed a Filter Bank (FB) based Narrow Band Interference (NBI) detection and suppression method with the excision algorithm, which had an efficient implementation than the conventional FB.

Yang, 2005 [146] used the Complex Modulated FB (CMFB) for SC instead of conventional FFT-based FDE and found that with modest number of sub-bands this technique provides better performance without use of the CP. A multi-antenna FD pre-equalization (pre-FDE) was presented in Adachi, 2005 [147] for the Spread Spectrum SC systems to improve the BER performance. It was perforemd by implementing the pre-FDE transmission for the downlink and FDE reception for the uplink at the base station. Coon, 2005 [148] presented an adaptive FDE algorithm for implementation in the SC Multiple Input Multiple Output (MIMO) systems and a reduced complexity method to train the equalizer. Agathe, 2005 [149] improved the iterative FD-DFE with reduced complexity and fast convergence with respect to the linear MMSE and ZF equalizers.

At the start of 2006 Jang [150] proposed a Space Frequency Block Coded (SFBC) SC-FDE system, to have the transmit sequence that supported spatial and frequency diversities combining receiver, which was derived under a MMSE criterion. SFBC SC-FDE system significantly outperformed the STBC SC-FDE system while it provided lower computational complexity than the system combined of OFDM with SFBC. Gusmao, 2006 [151] worked on CP assistance methods in SC transmission and presented an algorithm for a Decision-Directed Correction (DDC) of the FDE inputs for

insufficient CP and CP-free conditions to improve the performance with slightly increased complexity. Yune, 2006 [152] presented the similar work as [150] and further proposed another diversity scheme. It combined STBC and SFBC, to become Space Time Frequency Block Code (STFBC) SC-FDE system which had better immunity to the distortion compared to the SC-FDE system with STBC or SFBC scheme and had the lower computational complexity. In [153, 154] Viholainen, 2006 used EMFB to study various implementation structures for the EMFBs with ELT algorithm to resolve a simpler structure for ICI and ISI mitigation in the MC modulation. Yang, 2006 [155] tuned the FBE amplitude response to enhance the NBI suppression. In the same year, Martin, 2006 [156] proposed a channel shortening equalizer that directly minimized the BER of the wireless multi-carrier systems. In Agathe, 2006 [157], Agathe updated the iterative FD-DFE to improve the BER performance by assuming the perfect equalization at the first iteration and with minimize sum of noise and decision error power at the threshold detector input. Sarperi, 2006 [158] proposed a semi-blind equalizer based on Independent Component Analysis (ICA) for the SC-CP MIMO systems to obtain the BER performance close to the ideal channel with perfect CSI at the receiver. The semi-blind SC-CP method outperformed the OFDM with perfect CSI at moderate to high SNRs.

In our previous work, Khanzada, 2006 [74], we have also verified the supremacy of the SCT over OFDM for the fast varying channels. Tomeba and Takeda, 2006 in [159, 160] and [161] further analyzed the performance of the SC-FDE with spaced time delays and using Tomlinson-Harashima pre-coding.

Recently in 2007, a Complex FIR (CFIR) filter structure and a cascade of a Linear Phase FIR (LP-FIR) filter and an All Pass (AP) filter structures were presented by Yang, 2007 [162]. He improved his previous work Yang, 2005 [146] on CMFB for FDE in the SC systems. It was observed that the fractionally spaced processing provides significant performance benefit, with a similar complexity to the symbol rate system, when the baseband filtering was included. NBI was also claimed to be significantly suppressed. Tang, 2007 [163] proposed an extended data model for a low complexity FDE, which was incorporated using a receiver window to enforce the banded channel matrix and inter-block interference reduction. Martin, 2007 [164, 165] presented the receiver design for SCT and the channel shortening technique to improve its performance in the time varying channels for CP systems.

In Khanzada, 2008 [75] which is the continuation of our work of Khanzada, 2006 [74], we have designed the block iterative SC-DFE combined with the CP and ZP techniques and compared it with the SC-LE and similar variants of the OFDM. The coefficients of our block DFE converge more quickly than that of Agathe, 2006 [157] by decaying exponentially at each iteration. Comparison results verified the supremacy

of the CP versions of SC-LE and SC-DFE over OFDM-CP and OFDM-ZP. The effects of coding on the model presented in [75] were analyzed in our recent work Khanzada, 2008 [76], where it was noticed that more coding gain was comparatively achieved by the CP versions of SC-DFE when ISI is encountered and by the OFDM when ISI is not encountered.

3.3 OFDM/SC Transceiver Model

In this section we describe the system model for our newly designed SC-FDE transceiver. FDE is computationally simpler than the corresponding TDE. It has been pointed out in [65] that when combined with the FFT processing and CP is used, a SC system with FDE (SC-FDE) has essentially the same performance and low complexity than that of OFDM. In Fig. 3.1 transceiver block diagrams of combined OFDM and SC-FDE are shown which we will use for the indoor positioning application in chapter 4. The coding, interleaving, S/P, P/S blocks are skipped in the figure for simplicity. Fig. 3.2 shows the LE for SCT. A DFE model is shown in Fig. 3.3.

In SCT an IFFT operation is located between the equalization and the decision. This IFFT operation spreads the noise contributions of all the individual sub-carriers on all the samples in time domain [120, 149]. Fig. 3.1 is updated implementing the coding block to yield the coded transceiver block diagram of the combined OFDM and SC-FDE, shown in Fig. 3.4. Both OFDM and SC systems involve one Discrete Fourier Transform (DFT) and one Inverse DFT (IDFT) block. The only difference is that SC-FDE utilizes both blocks at the receiver [149]. In the next subsection we elaborate the mathematical model for this combined OFDM/SCT transceiver.
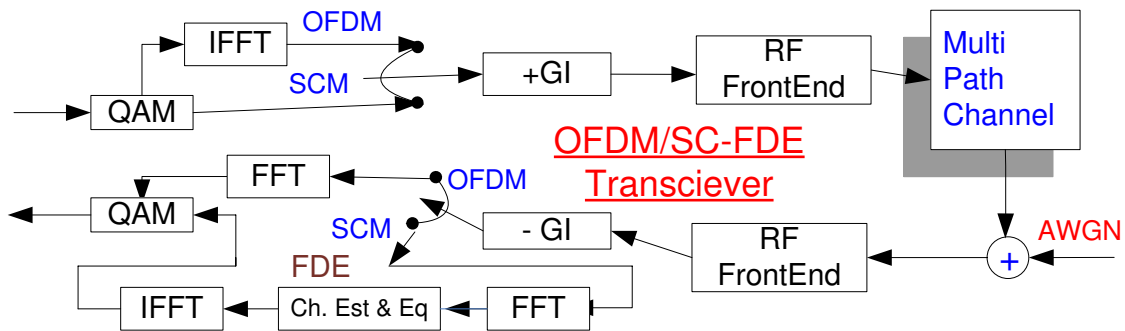
Figure 3.1: Transmit and receive block diagrams of OFDM and SCT

3.3.1 OFDM Conventional Model

In order to describe the SC-DFE mathematical model, we start with the OFDM conventional model. We recall from the chapter 1 that in an OFDM scheme, the
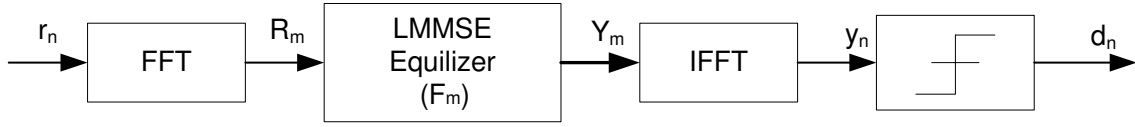
Figure 3.2: FD-LE for SCT block diagram
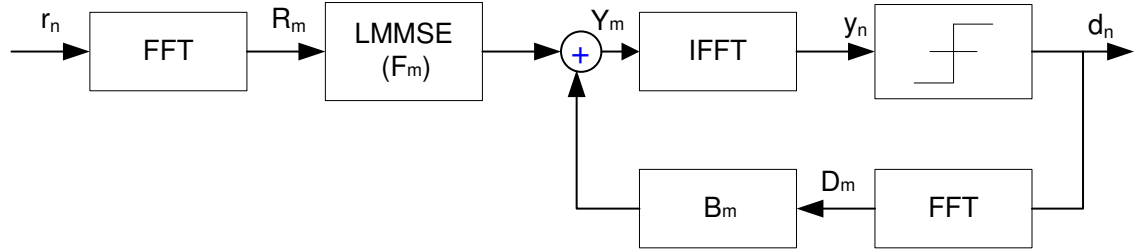
Figure 3.3: FD-DFE for SCT block diagram

information is coded in symbols of duration T_s. The available channel bandwidth B is uniformly subdivided into a number N of sub-bands (sub-channels), whose mid-frequencies characterize orthogonal sub-carriers. The data block mapped onto a symbol is subdivided into the same number N of sub-blocks, each corresponds to one of these sub-bands and then N-point IDFT is taken for the resulting blocks. The output is serialized and a Guard Interval (GI) is added at the transmitter, after that further RF modulation operations are applied. At the receiver the GI is removed and a N-point DFT is taken for the resulting signal. If m is the carrier frequency index, k is the OFDM symbol index, the data symbols are denoted by $a_m(k)$, the corresponding additive noise by $\omega_m(k)$ and the channel transfer function by $H_m(k)$ then the N signal samples at the DFT output during the kth OFDM symbol can be written as [166]

$$R_m(k) = H_m(k)a_m(k) + \omega_m(k), \qquad m = 1, 2, \ldots, N \qquad (3.1)$$

From eq. 3.1, it is clear that OFDM needs only a complex multiplier bank at the DFT output to completely eliminate the channel distortion. Denoting the set of multiplier bank coefficients by $(C_1, C_2, \ldots, C_M)$, their values, which invert the CTF, are given by eq. 3.2. These values describe the optimum solution regardless of the noise level and known as Zero Forcing (ZF) equalizer criterion.

$$C_m = \frac{1}{H_m}, \qquad m = 1, 2, \ldots, N \qquad (3.2)$$

Since the noise contributions of highly attenuated subcarrier can be rather large, a ZF equalizer shows the poor noise performance, therefore, a Minimum Mean Square Error (MMSE) equalizer is used for the SC systems. The MMSE criterion [56] can
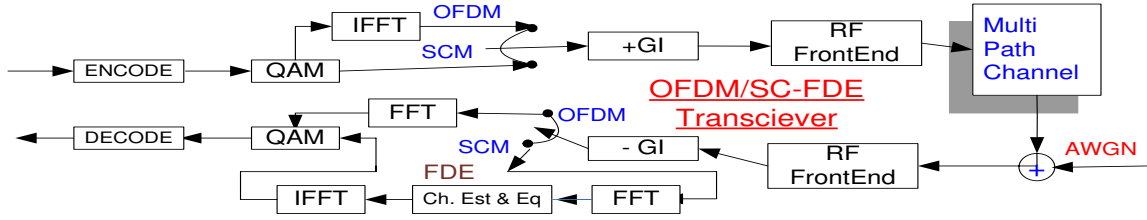
Figure 3.4: Transmit and receive block diagrams of OFDM and SCT with coding

be calculated by (3.3)

$$C_m = \frac{H_m^*}{|H_m|^2 + \sigma_\omega^2} \tag{3.3}$$

where σ_ω^2 is the variance of the additive noise.

3.3.2 SC-DFE Model

To define our DFE for SCT, we use the existing SCT model proposed by [68] and further improved by the subsequent authors. In order to improve the performance of SC-FDE, it was proposed in [66] to use a DFE with time domain feedback. Another DFE scheme was proposed in [129] for SCT, where both the Feed Forward (FF) and the feedback parts were implemented in FD. Furthermore, the DFE was made iterative by using the decision block of previous iteration to compute better equalizer output. We can define the generic SC-DFE structure used and updated by [157] as under;

If a symbol block is denoted by $(a_1, a_2, \ldots, a_N)$ and the corresponding received signal block by $(r_1, r_2, \ldots, r_N)$ then $(R_1, R_2, \ldots, R_M)$ would be the DFT output block. This output block is multiplied by FF coefficients $(F_1, F_2, \ldots, F_M)$ [2] the equalizer and the resulting signal block enters an inverse DFT, which yields the output block $(y_1, y_2, \ldots, y_N)$ on which the threshold detector bases its first decision set for the transmitted signal block. Once the receiver makes a first set of decisions, the decision block is fed to a feedback filter with coefficients $(B_1, B_2, \ldots, B_M)$, and an iterative DFE is implemented. The iterative DFE of [129] is optimized under the MMSE criterion. At the ith iteration, we can calculate the output of DFE by (3.4)

$$Y_m(i) = F_m(i)R_m + B_m(i)D_m(i-1), m = 1, 2, \ldots, N \tag{3.4}$$

where $F_m(i)$ and $B_m(i)$ are the coefficient sets of the FF and feedback filters, respectively, at the ith iteration, and $D_m(i-1)$ are the FD decisions at the previous iteration. The initial equalizer decisions are made using the control parameter $\alpha_0 = 1$

---

[2] F_m is the DFE version of C_m; i.e. $F_m = C_m$

that makes it a MMSE equalizer having

$$F_m(0) = \frac{H_m^*}{\sigma_\omega{}^2 + (|H_m|)^2}, \quad m = 1, 2, \ldots, N$$

where H_m is the channel frequency response and

$$B_m(0) = 0$$

then the parameter α is decreased exponentially by using $\alpha_i = 1 - \frac{\sqrt{i}}{\sqrt[10]{I}}$ where I is the total number of iterations. The FF and feedback coefficients for the rest of iterations are calculated by (3.5) and (3.6) respectively.

$$F_m(i) = \frac{H_m^*}{\sigma_\omega{}^2 + (1 - \alpha_{i-1}^2)|H_m|^2} \tag{3.5}$$

$$B_m(i) = \alpha_{i-1}[H_m(i)F_m(i) - \frac{1}{M}\sum_{m=1}^{M} H_m F_m(i)], \tag{3.6}$$

$$for \ m = 1, 2, \ldots, N$$

This equalizer structure performs better than OFDM and improves its performance when the number of iterations increase. We have designed the equalizer to provide two types of GI, the CP based GI and the ZP based GI as discussed in [137] and [112]. The next section discusses the simulation results for implementing this model.

3.4 Implementation

In this section we present the results of our simulations for the model presented in the previous section. We have compared the OFDM technique with SC-DFE by simulating a WLAN system. The performance of the presented FD iterative DFE was investigated using QPSK modulation with different flat and frequency selective fading channel models. Simulations were carried out for both OFDM-CP and OFDM-ZP, with SC-LE and SC-DFE (CP and ZP). SC-DFE was simulated and compared with different number of iterations (L=2, 4 and 6). Initially the simulations were carried out for the un-coded system with variable channel lengths then the similar simulations were carried out for the coded system in order to verify the effects of coding on the designed transceiver.

3.4.1 Un-Coded System Simulations

Fig. 3.5 and Fig. 3.6 show the comparisons of the simulation results for BER of SC-CP-LE and SC-ZP-DFE respectively, both with OFDM-CP and OFDM-ZP for flat fading channel (channel length=1). OFDM variants perform better than SC ones. Fig. 3.7 and Fig. 3.8 show similar results for frequency selective fading channel when

there is no ISI (channel length=5). The performance for SC-LE-CP and SC-DFE-CP got noticeable improvements as compared to both OFDM variants. However, the OFDM variants perform better than that of both SC-LE-ZP and SC-DFE-ZP ones, only in high signal to noise ratio values. Fig. 3.9 and Fig. 3.10 show the similar comparisons for frequency selective fading channel when ISI is encountered (channel length=20).
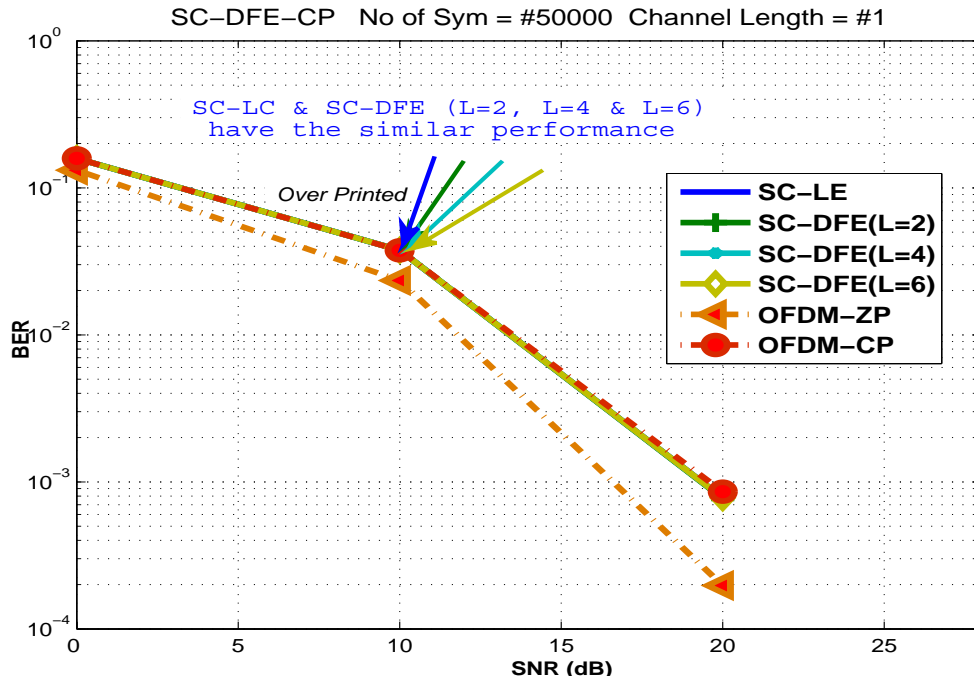
Figure 3.5: BER comparisons of SC-CP-LE, SC-CP-DFE with OFDM-CP and OFDM-ZP (channel length=1)

Both of the SC-CP variants perform quite better than those of the OFDM ones, even in this case. It is clearly shown by all figures that the OFDM-CP performs better than the OFDM-ZP and SC-LE-CP and gives more performance gain over the OFDM-CP. SC-DFE-CP improves the performance further as we increase the number of iterations up to a maximum of 6.

3.4.2 Coded System Simulations

Conventional coding with the coding rate $\frac{1}{2}$ was used with Viterbi decoding to implement the coding part of the system. Simulations were carried out for the coded and un-coded versions of the OFDM, SC-LE and SC-DFE.

Fig. 3.11 shows the coded and un-coded versions of OFDM-CP, OFDM-ZP, SC-LE and SC-DFE for the frequency selective fading channel. Fig. 3.12 shows the similar results when ISI is encountered. It is obvious from both figures that more coding gain
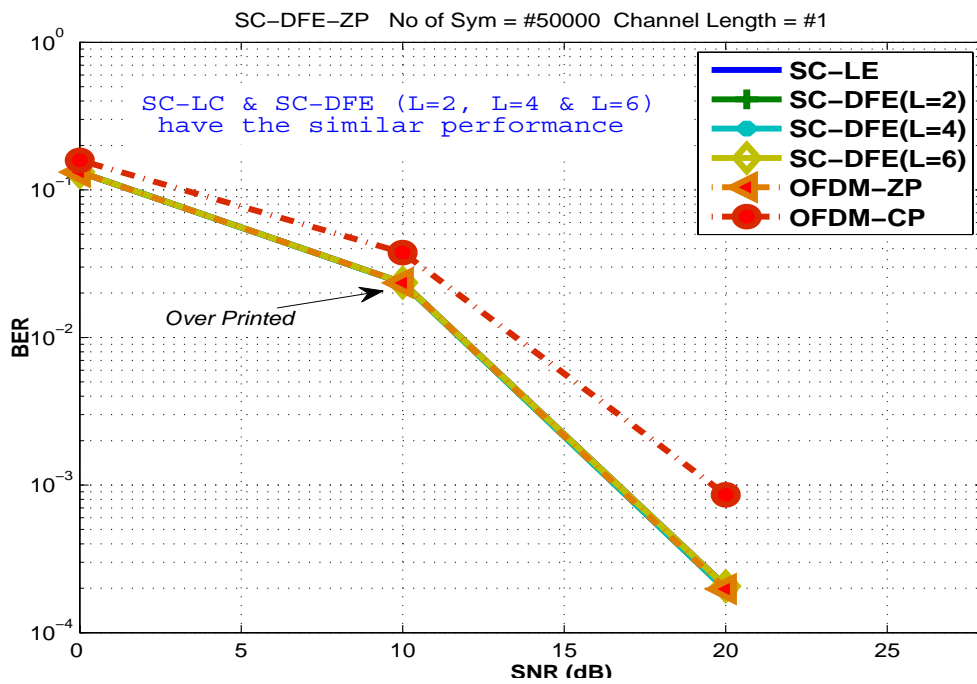
Figure 3.6: BER comparisons of SC-ZP-LE, SC-ZP-DFE with OFDM-CP and OFDM-ZP (channel length=1)
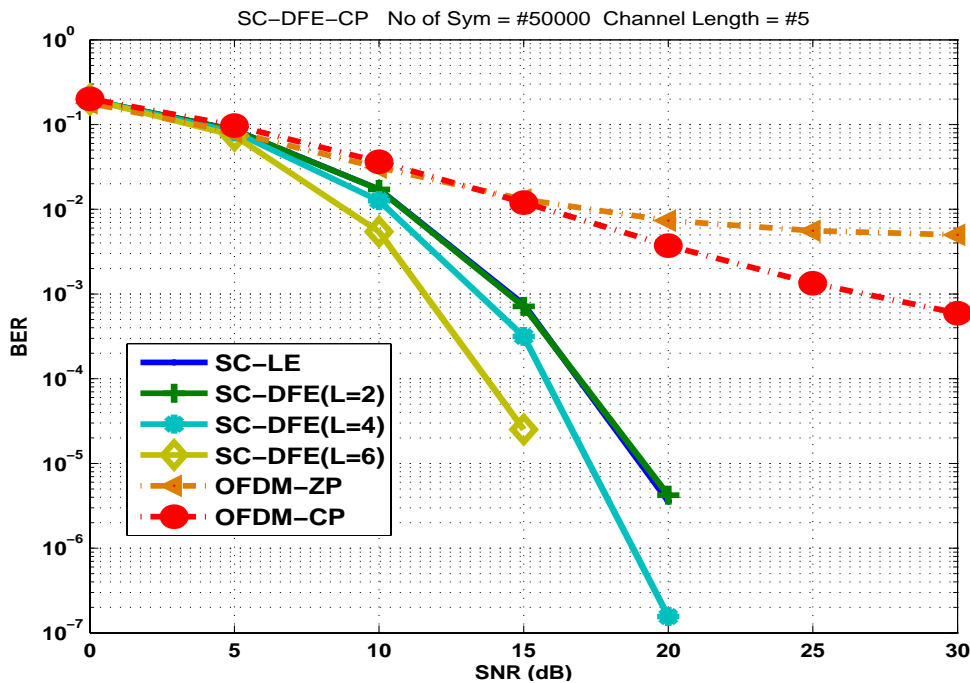
Figure 3.7: BER comparisons of SC-CP (channel length=5)
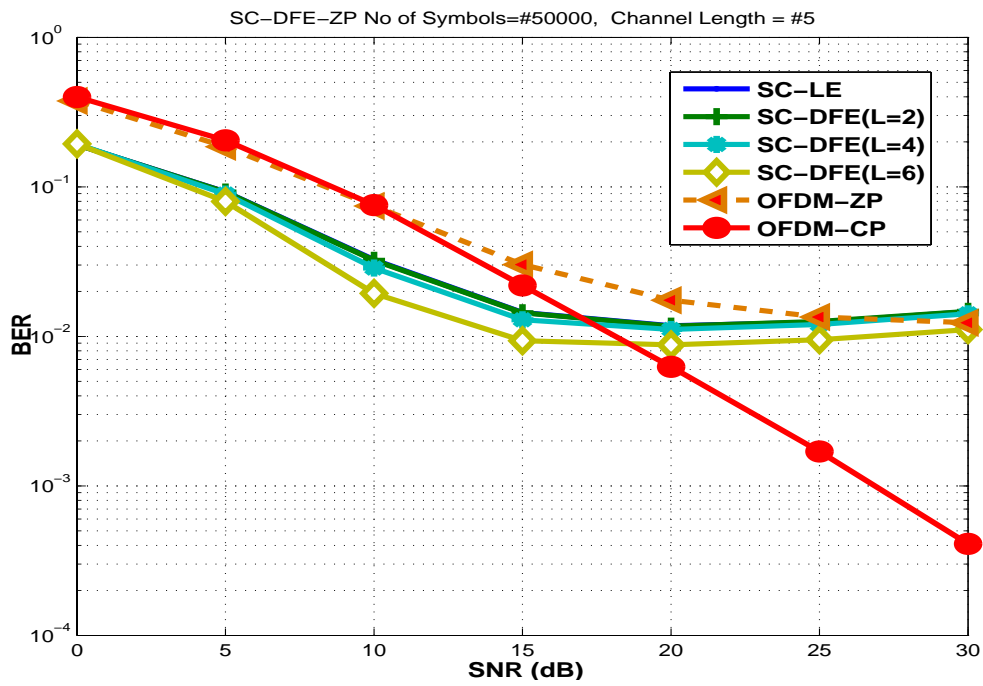
Figure 3.8: BER comparisons of SC-ZP (channel length=5)
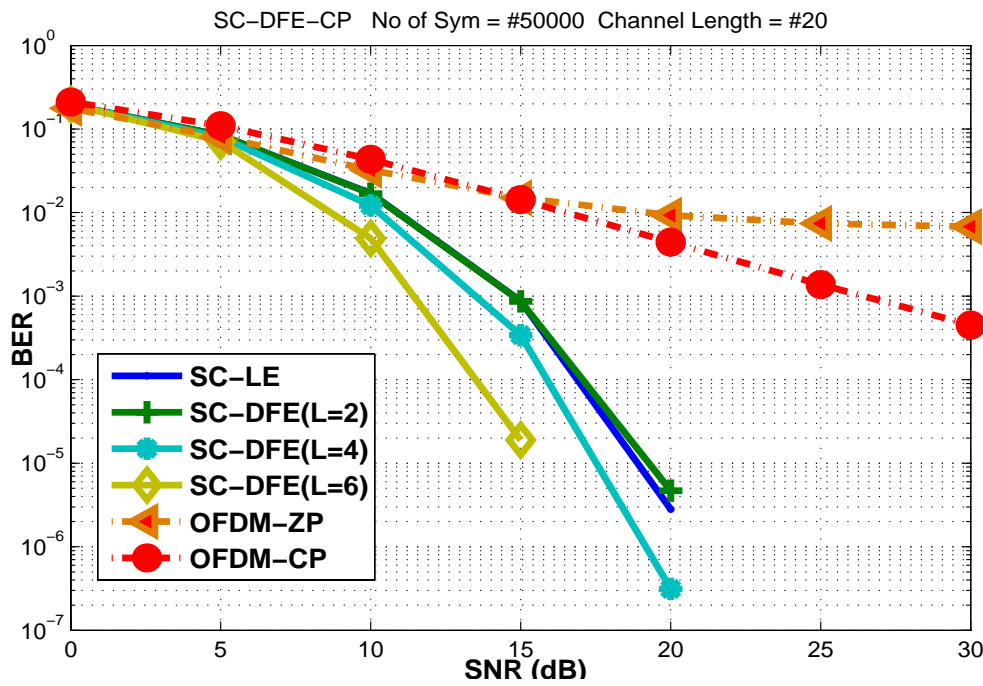
Figure 3.9: BER comparisons of SC-CP (channel length=20)
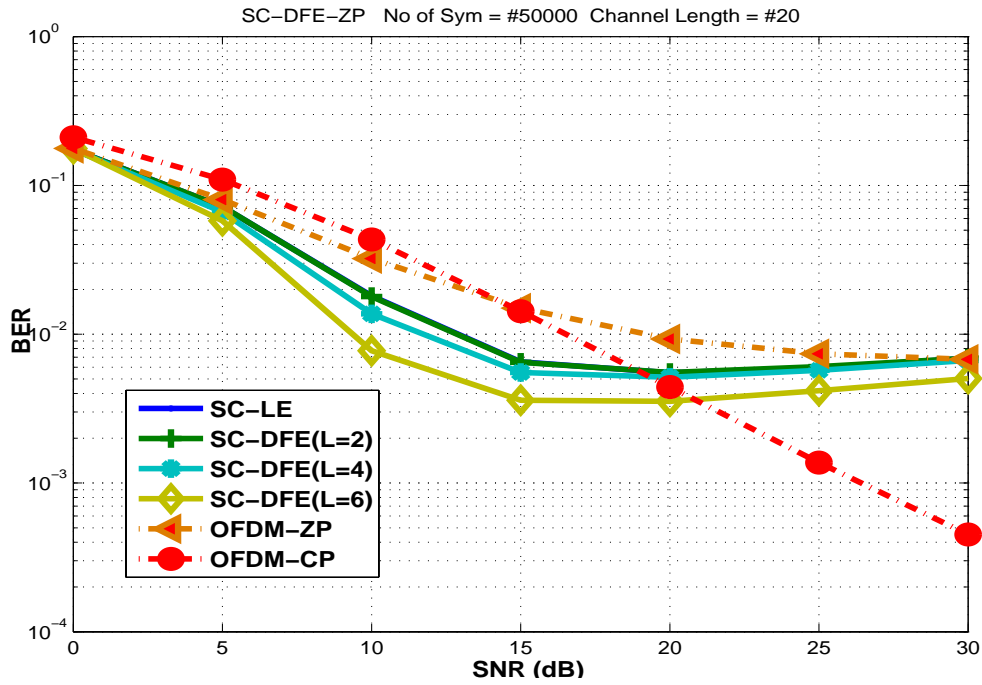
Figure 3.10: BER comparisons of SC-ZP (channel length=20)
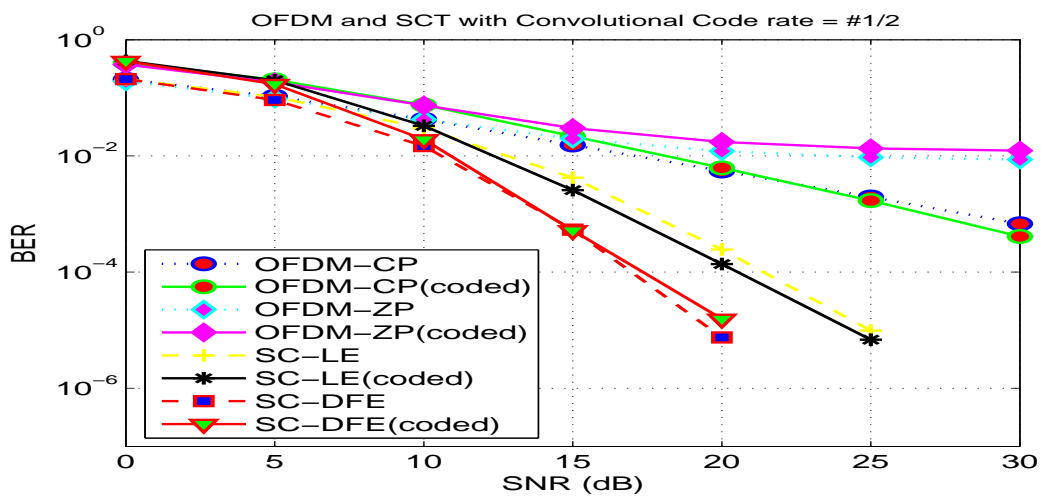
Figure 3.11: Coded and un-coded OFDM vs SCT for FSF channel
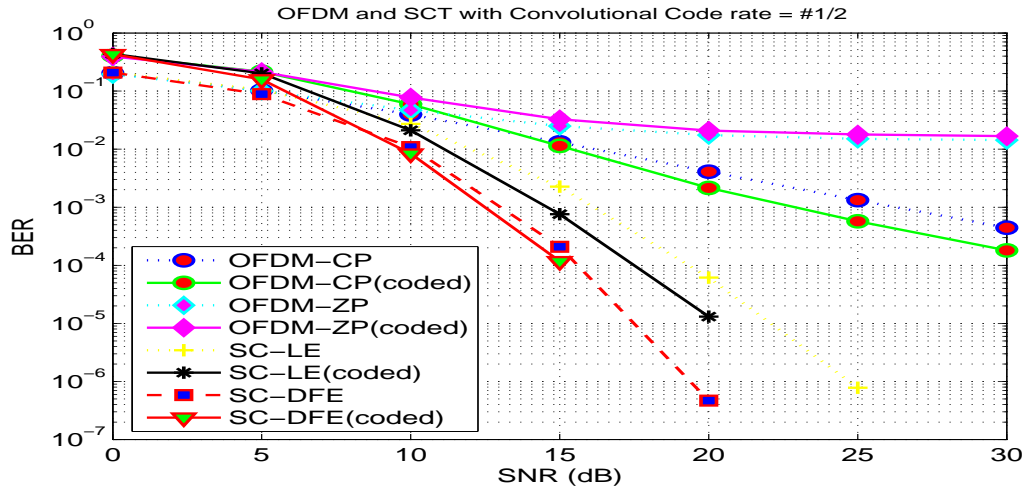
Figure 3.12: Coded and un-coded OFDM vs SCT for FSF channel with ISI

is comparatively achieved by the SC-DFE when ISI is encountered and by the OFDM when ISI is not encountered. The CP and ZP versions of our LE & DFE model [76] are also compared with OFDM variants. Fig. 3.13 compares the CP and ZP versions of OFDM with CP versions of SC-LE and SC-DFE while Fig. 3.14 compares them with ZP versions of the later.   It can be noted from Fig. 3.13 that the un-coded
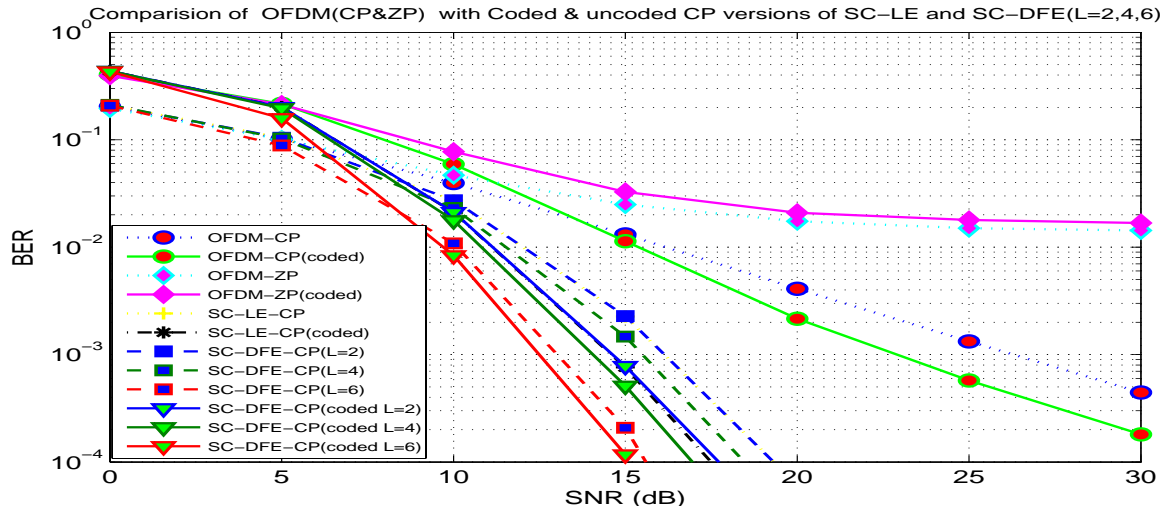
Figure 3.13: OFDM vs SC-DFE-CP variants with different iterations

and coded versions of the OFDM-CP achieve approximately 2 to 3 dB gain as we get higher SNR from 10^{-3} to 10^{-4}, however, SC-LE gets 1 dB gain in the same range and SC-DFE gets lower than that of SC-LE. Furthermore, as we increase the number of iterations, the coding gain for SC-DFE becomes more insignificant. Coding gain for the ZP versions of the OFDM, SC-LE and SC-DFE are equivalent for the low SNR, as expected and OFDM gets more coding gain for the high SNR values compared to the SC-DFE variants.
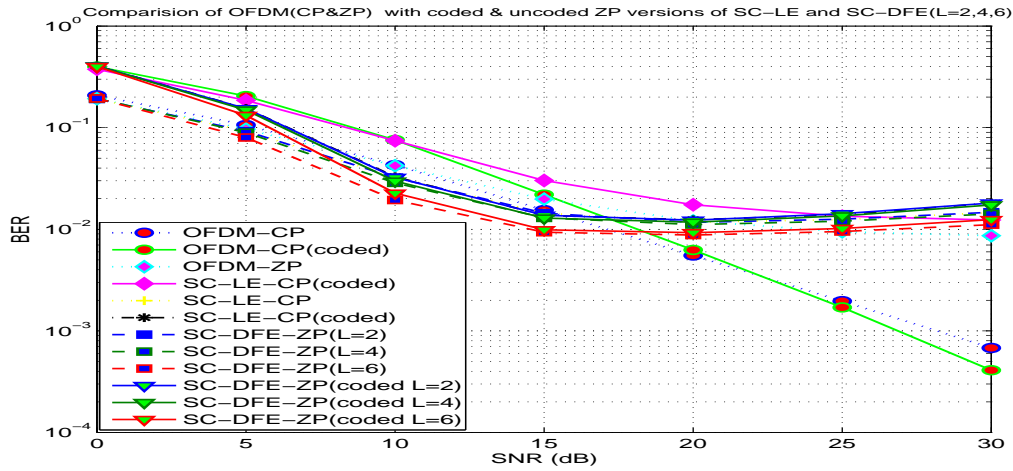
Figure 3.14: OFDM vs SC-DFE-ZP variants with different iterations

In this chapter we have presented a design for the block iterative SC-DFE combined with CP and ZP techniques and compared it to SC-LE and similar variants of OFDM. The new block DFE structure iteratively improves itself and performs better as the number of iterations is increased up to a maximum of 6. Comparison results of BER simulations for both variants of the OFDM and the SCT with LE and DFE verify the supremacy of the CP versions of SC-LE and SC-DFE over OFDM-CP and OFDM-ZP. However, ZP versions of SC-LE and SC-DFE perform better for the low signal to noise ratio values while OFDM variants perform better in the high signal to noise ratio values in this case.

Chapter 4

Positioning System and TOA/TDOA Estimation Techniques

4.1 Wireless Positioning System

A wireless positioning system can be defined as a communication system used to determine the coordinates of a MS; with respect to some known reference locations which are known as reference points. The location of a MS is determined by measuring some signal parameters communicated between the MS and multiple BS's. The final estimates are determined by the localization algorithm. Fig. 4.1 shows the block diagram of a typical positioning system. In literature the terms geolocation [21] and location sensing [167] are used in parallel to the positioning [36] interchangeably.

Location metric finding system is used to determine the desired metric from the

Indoor Positioning and Distance Measurement Error System
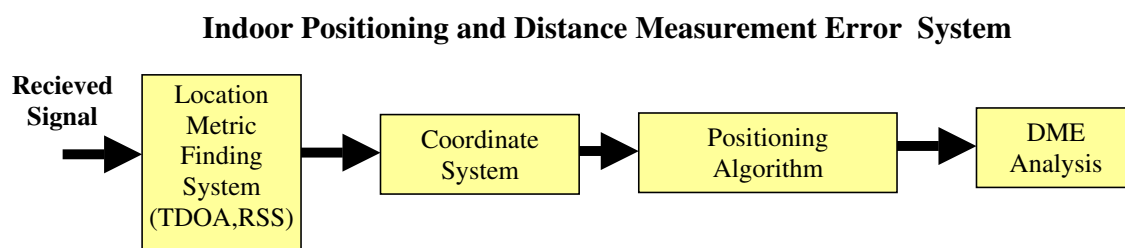
Figure 4.1: Indoor positioning and distance measurement system

received signal. We have already summarized these metrics under the section DME of chapter 1. For our application we use TDOA from these metrics because of its accuracy and performance. Normally some coordinate system is used to locate the position of the target. A positioning algorithm matches the best coordinate of the target using distance measurement techniques like least square or weighted least square.

Finally, the estimated positions and distances are compared from the measured one to analyze and reduce the error in the estimation.

The desired accuracy of a positioning system is dictated by the application requirements and the environment. For many outdoor applications accuracies of 30-50 m are acceptable [168], while for indoor environment a number of applications demand accuracies of 1-10 m [169]. This accuracy level is demanded to be increased as there are many applications in this area. Various techniques have been implemented to increase the accuracy further [4,31,170]. The main challenges to the positioning system are the performance, cost, security and the limited bandwidth [38,39].

4.1.1 Bandwidth Considerations

Bandwidth is an important parameter affecting the accuracy and performance of the positioning system. The techniques employed in positioning application can be divided in three categories with respect to the transmitted signal and the bandwidth it occupies [7]. The techniques are narrow-band signal ranging techniques, wide-band signal ranging techniques also known as super resolution algorithms and the UWB signal ranging techniques. In the narrow-band ranging techniques, the distance between two points is measured by the phase difference between the received and the transmitted carrier signals. The phase of a received carrier signal, f, and the TOA of the signal, t, are related by $t = f/\omega_c$, where ω_c is the carrier frequency in radian.

In multi-path environment the phase of narrow-band signal changes with the multiple paths, therefore, it is unable to provide accurate estimate of the distance [25]. Pseudo Noise (PN) sequence is transmitted to code a wide-band signal like Direct Sequence Spread Spectrum (DSSS). DSSS is also used in the positioning applications [10]. The PN sequence is generated at the receiver, which is correlated with the received signal. The arrival time of the first correlation peak is used to determine the distance when it is multiplied with the speed of light. The problem with this method is that some times the first correlation peak doesn't provide the actual peak when replete with noise and multi-path components [77]. UWB signal ranging techniques are recently being utilized for the indoor positioning applications [6]. Higher bandwidth provides more attenuation to the signal therefore if the lower segment of UWB up to 3 Ghz is utilized then it would not be much effected by the multi-path fading [171].

4.1.2 Estimation Error

The target to be positioned receives the signals from more than one transmitters or BSs. Range measurements are extracted from the received signal. RSS is not utilized where the accuracy is the major concern, however, it is easier to implement than the TOA or TDOA techniques which are more accurate because the arrival

time corresponds to the direct path distance. Triangulation techniques are applied to estimate the distance of the target from multiple transmitters. Before going in details of the positioning system we emphasize the issue of unavailability of the direct path in the signal transmission. The performance of TOA-based techniques depend on the availability of the DP signal [20, 21] which is very strongly present in the LOS environments. In NLOS environments the accuracy severely degrades due to the following reasons [172];

- Multi-path components corrupt TOA estimates,

- Propagation delay adds a positive bias to the TOA estimates and

- The UDP conditions arrive due to multiple objects present in indoor environments.

The estimation error is increased dramatically in UDP conditions. However, the challenge is the accuracy of estimate in the NLOS conditions, which can be characterized as site-specific and dense multi-path environments [20, 172]. To reduce this area of error various positioning algorithms are employed. The Least Squares (LS) and Maximum Likelihood (ML) algorithms are utilized to find the distance. Iterative algorithms are used in the geometrical techniques which estimate the target position by formulating and solving a set of non-linear equations [49, 10]. If the statistics of the error are not available in advance the LS algorithms provides the optimal estimations, otherwise, the Weighted LS (WLS) algorithm is used. It uses the variance of the error distribution to weigh the measurements. The LS and its alternative algorithms are described in appendix C.

4.2 Two Dimensional TOA/TDOA Positioning System

4.2.1 Simplest Model Geometry

In order to have a positioning system the minimum requirement is to detect the position of a target MS by sending the signal from at least two BS. The geometric relationship of such a system with one MS and two BSs; BS_1 and BS_2 (all three located in the same plane) is shown in Fig. 4.2.

The distances d_1 and d_2 are found by multiplying the measured signal propagation time between each base station and the target by the speed of light, while the coordinates of BS_1 and BS_2 are known in advance. The equations of the two intersecting circles and their solutions for finding x, y co-ordinates for the MS are shown in appendix A. It summarizes that the TOA method gives the correct location of the target
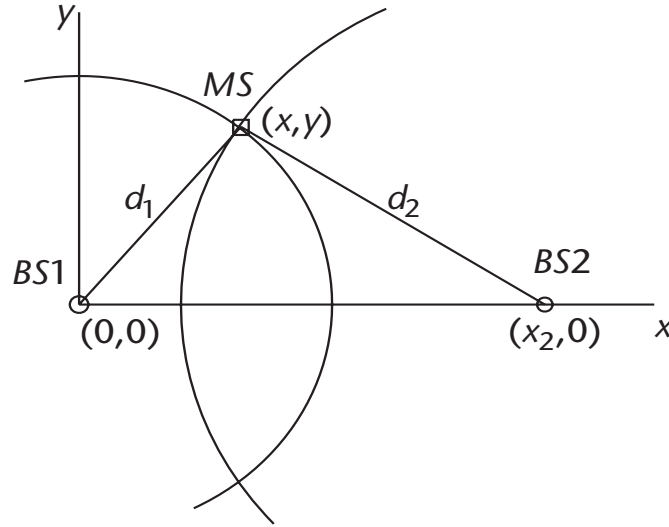
Figure 4.2: Geometry of MS and BS in 2D-TDOA

in two dimensions without ambiguity if at least three fixed BSs are used in the measurement. This shows that the positioning accuracy can be improved by incorporating a larger number of fixed BSs in the location setup layout.

4.2.2 Unambiguous Estimation Model Geometry

In order to remove the ambiguity in target position estimation, the signal should be transmitted using at least three BSs to a MS, as discussed in the previous section. Such a two dimensional positioning system is shown in Fig. 4.3. The accuracy depends upon the measurement, geometry of the transmitters and their numbers.

The estimation error shown by the yellow area in Fig. 4.3 is caused by many factors which include the physical inaccuracy of the transmission & reception hardware, bandwidth unavailability and the complexity of the multi-path indoor channel. If we consider the first BS at origin the Fig. 4.3 can be transformed to the geometric relationship which is shown in Fig. 4.4. The equation of the third circle centered on BS_3 and passing through the target MS can be written as [73]

$$d_3^2 = (x - x_3)^2 + (y - y_3)^2 \tag{4.1}$$

Considering eqs. A.1, A.2 and eq. 4.1 from appendix A and solving them we get

$$x = \frac{x_2^2 + d_1^2 - d_2^2}{2 \cdot x_2} \tag{4.2}$$

and

$$y = \frac{x_3^2 + y_3^2 + d_1^2 - d_3^2 - 2 \cdot x \cdot x_3}{2 \cdot y_3} \tag{4.3}$$
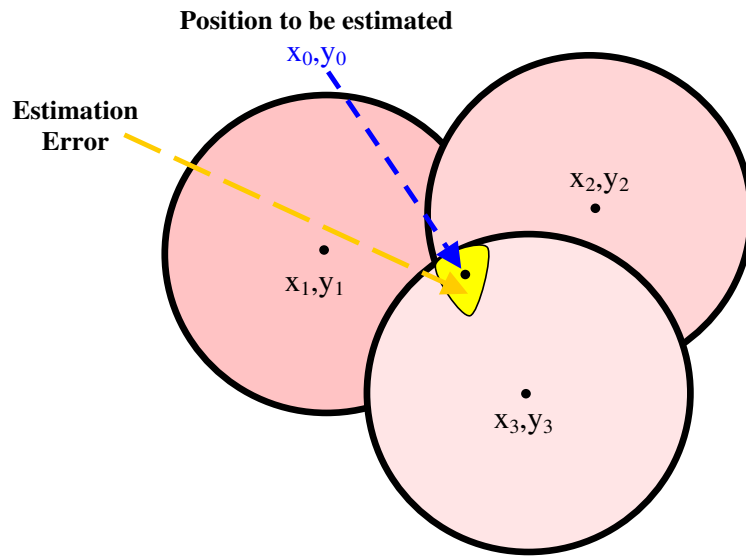
Figure 4.3: 2D receiver position estimation using three transmitters

Notice that the position calculated by the three circles intersection is unique and
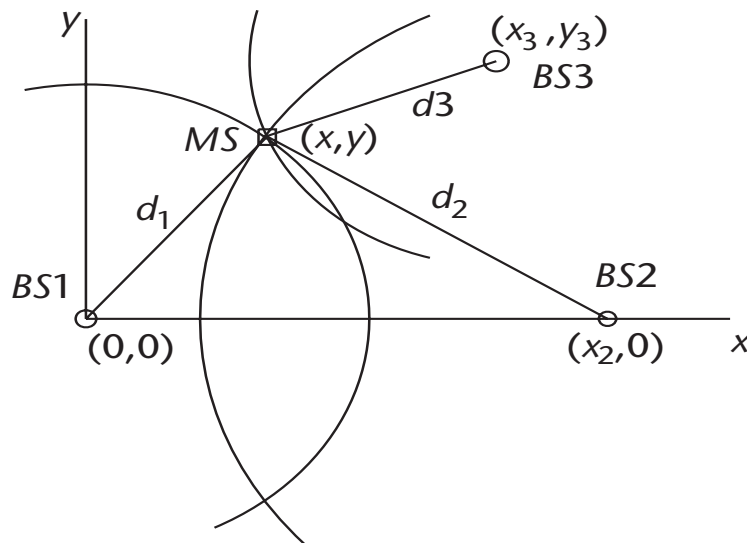
Figure 4.4: 2D receiver position estimation using three transmitters

has no ambiguity. Positioning accuracy can be further improved by increasing the number of fixed stations in the location setup layout. A two-dimensional layout of four fixed terminals with known coordinates, and a target terminal, whose location to be determined, is derived in appendix B.

4.2.3 TDOA Geometry

Instead of measuring the TOF of a transmission between two terminals, TDOA measures the difference in the times of flight between a target terminal and a pair of fixed reference terminals. Clock synchronization is required only on one side of the communication link, which is the fixed terminals side [18]. A classical example of TDOA unilateral system is Loran-C [173]. The fact that the TDOA location method can operate with transmitters using their normal communication protocol and with no modification of hardware or software, gives it more applications than TOA [73], except for GPS. While TDOA transmissions do not need to include a special message for the purpose of the location function, they must have a modulated identity that includes a specific epoch that can be recognized by the receivers [81]. TDOA cannot be used where transmitters emit unmodulated carriers.

The geometric model for estimating the position coordinates using TDOA is the intersection of hyperbolas in 2D and the intersection of hyperboloid in 3D as described by [73]. If a BS is located at one focus of a hyperbola and another BS at the other focus, then a target is positioned on the hyperbola. The hyperbola is characterized
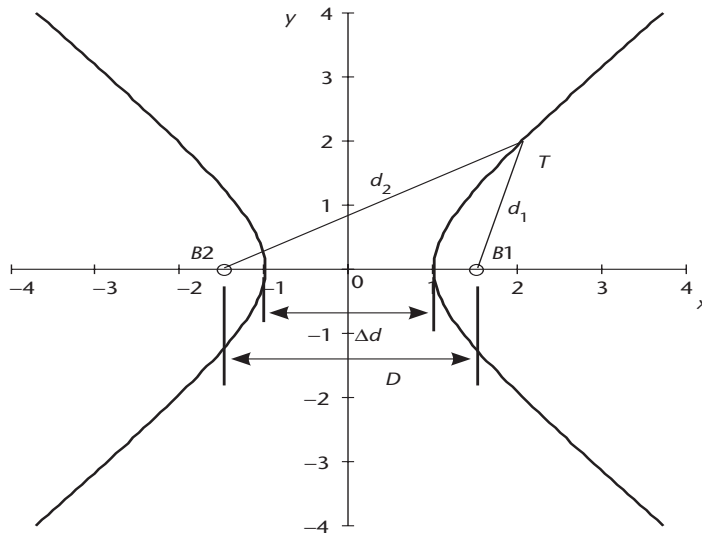
Figure 4.5: Improved TDOA estimation system using 4 terminals

by the fact that the difference in distance, $d_2 - d_1$, between any point on it and the two foci is constant, as shown in Fig. 4.5. The difference value is positive if the point is located on the right branch of the hyperbola and negative if it is located on the left branch. The distances are expressed as follows:

$$d_2 = \sqrt{y^2 + (x + \frac{D}{2})^2} \qquad (4.4)$$

$$d_1 = \sqrt{y^2 + (x - \frac{D}{2})^2} \tag{4.5}$$

The equation of the hyperbola that defines the locus of the target is then

$$\Delta d = d_2 - d1 = \sqrt{y^2 + (x + \frac{D}{2})^2} - \sqrt{y^2 + (x - \frac{D}{2})^2} \tag{4.6}$$

where (x, y) are the coordinates of the target, D is the distance between BSs located at equal distances from the origin on the x-axis and Δd is the constant difference of distances from target to BSs. The Δd is calculated as the time difference of arrival times the speed of light as $\Delta d = \Delta t \cdot c$, where c is the speed of light.

The location of a target terminal is at the intersection of two or more hyperbolas that are defined from TDOA measurement data. The total number of TDOA values, K, obtainable from M BSs is

$$K = \frac{M!}{2(M - 2)!} \tag{4.7}$$

4.3 Measurement Equipment and Initial Tests

4.3.1 The Real Channel Measurements

In order to have a real measurement channel we have taken the measurement of the indoor positioning system. The super resolution estimation algorithms are implemented at Chair of Microwave and Communication Engineering (CMWCE), University of Magdeburg. The test measurements were carried out for the indoor environments at initial phase. The indoor test area is used for several tests. The snapshots of the top view of the building 2 and 3, used for measurements is shown in Fig. 4.6.

The initial measurements are taken in a frequency band between 50-2650 MHz and are recorded with an omnidirectional broadband antenna. Accurate coordinates for the transmitter positions as well as the nominal receiver positions have to be determined. Agilent Signal Generator $N5182AMXG - VSG$ [174], Agilent Vector Signal Analyzer $N9010A - VSA$ [175] and Anritsu Signal Generator & Analyzer $MS2692A - SA\&SG$ [176] are used in the measurement. These equipment function in the frequency range of $50Hz - 26.5Ghz$ and have powerful features to develop and mimic the real wireless test environments. Snapshots of these measurement equipments are shown in Fig. 4.7.

In order to choose the optimal antenna various measurements have been initially taken using four different types of antennas whose parametric properties are enlisted in table 4.1 and their snapshots are shown in Fig. 4.8. The best coordinate solutions
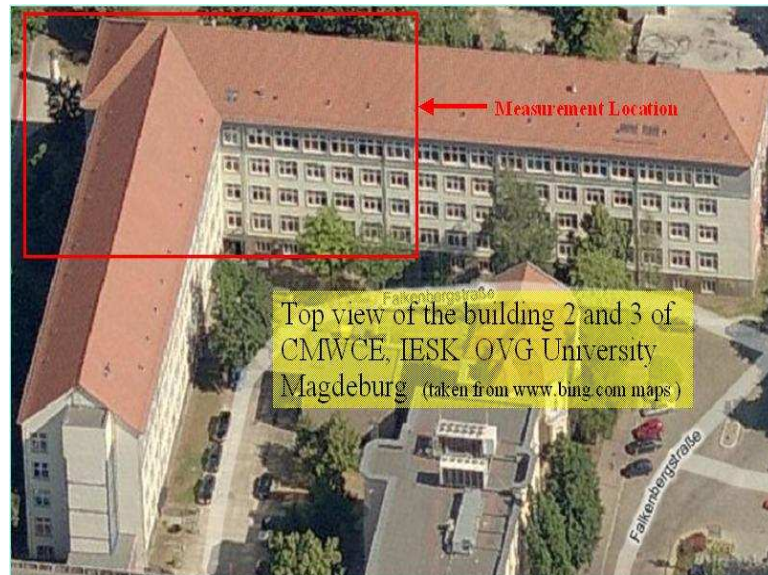
Figure 4.6: Top view of the building 2 and 3 at OVGU Magdeburg

Figure 4.7: Measurement equipments a.) Agilent Signal Generator $N5182AMXG - VSG$ (top-left), b.) Anritsu Signal Generator & Analyzer $MS2692A - SA\&SG$ (top-right) and c.) Agilent Vector Signal Analyzer $N9010A - VSA$ (bottom)

are obtained for the signal using IESK-Spiral and Hyperlog antennas. The results
for the signals using DWL-M60AT and IESK antennas are only a little worse. All
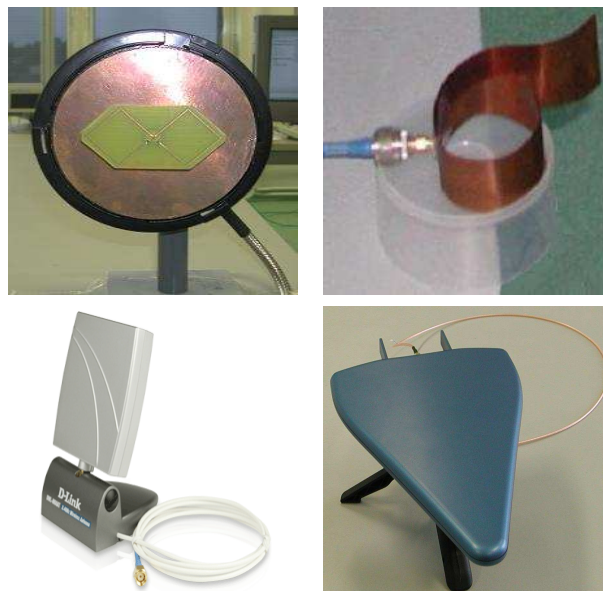
Figure 4.8: Indoor antennas used for measurements a.) IESK 9dBi (top-left) b.)
IESK-Spiral 8dBi (top-right), c.) D-Link DWL M60AT 6dBi (bottom-left) d.) Hyperlog 4dBi (bottom-right)

antennas are used during further measurements in order to have variability of results.
Initial setup stage concluded that the ranging performance depends on the transmitter
and the receiver positions, distances, environment, obstacles and interferences.

Table 4.1: Indoor antennas used and their properties

S.No	Name of Antenna	Frequency Range	Antenna Gain	Make
1	IESK	2.4Ghz-2.6Ghz	9dBi	designed at IESK-OVGU
2	IESK-Spiral	800Mhz-18Ghz	8dBi	designed at IESK-OVGU
3	DWL M60AT	2.4Ghz-2.5Ghz	6dBi	D-Link
4	Hyperlog	700Mhz-64Ghz	4dBi	Aronia AG

4.3.2   Multi-Carrier Signal Selection and Data Recording Parameters

Initially four different types of OFDM/SC signals are used, named as OFDM/SC-1,
OFDM/SC-2, OFDM/SC-3 and OFDM/SC-4. Each type of signal is transmitted
multiple times varying different WLAN parameters detailed in table 4.2. The SC

versions of the signal are transmitted in blocks in order to equate the multi-carrier transmission. These signals use the OFDM/SC transceiver model described in chapter 3. The standard WLAN transmission is maintained having 64 carriers, 48 for data, 4 for pilots and 16 for GI[1]. Variable number of symbols are used in each transmission in order to have optimal error reduction by taking average of multiple sets. Furthermore, variable data rates are maintained in order to guarantee the reliability of the results. Table 4.2[2] also summarizes these transmission parameters of the signals.

Table 4.2: Multi-Carrier Signals–OFDM & SC(block)

S.No	Type of OFDM/SC Signal (MCS)	Data Rate (MBits/S)	Modulation Scheme	Coding Rate	Bandwidth (MHz)	Transmission Frequency (GHz)	# of Carriers	# of Symbols transmitted
1	OFDM/SC-1	6	BPSK	$\frac{1}{2}$			64 Total 48 Data	Variable
2	OFDM/SC-2	12	QPSK	$\frac{1}{2}$	20	2.4	04 Pilots 16 GI	Starting from 10 ...
3	OFDM/SC-3	36	16QAM	$\frac{3}{4}$			in accordance to OFDM	to 100000
4	OFDM/SC-4	54	64QAM	$\frac{1}{2}$			WLAN standard	

The best performances are obtained for the OFDM/SC-3 signals, which are $16QAM$ OFDM/SC transmission signals. The directional transmission antennas improved the performance but the distance estimation is erroneous upto few meters. It is concluded that this amount of the error can be reduced significantly using better signal design and complex signal processing techniques like super resolution algorithms.

After the initial tests, the selected multi-carrier signals, OFDM/SC-3, are generated and transmitted through both the reference and the data channels. Measurement data sets are observed for each measuring point at different locations. These data sets consist of 30 files for the reference channel and 30 files for the antenna line channel. Initially each file contains 200000 samples and this figure is changed in later tests. The details of these data file parameters are shown in table 4.3. The files are processed using a MatLab script to estimate the absolute range between the transmitter and the receiver. The length of the data files are $2e6$ samples with a sampling rate of $200MS/s$. The signal data vector has the same length of $2e6$ samples. The signal is constantly transmitted and received.

---

[1]The SC is used as a block transmission scheme.

[2]Number of carriers are # of blocks in case of SC transmission in the table.

4.4   Measurements Setup

In order to deploy the positioning system and to find the optimal estimation algorithm, the measurements of the recorded signals are carried out in two stages. The first stage, referred as, the Working Package 1 (WP1), is confined to the measurements upto four transmission antennas. The aim of WP1 is to choose the best super resolution algorithm capable of reducing the error amongst the conventional algorithms as well as amongst all of its counterpart algorithms. The second stage, referred as, Working Package 2 (WP2), consists of the measurements upto 7 antennas and the 8th antenna is used as a reference. The aim of WP2 is to find out the optimal algorithm in different situations having various combinations of the MP algorithm with different model order criteria. The following two subsections detail about the WP1 and WP2 setups. The estimation procedure and results for these stages are left to the chapter 5.

4.4.1   Working Package 1 (WP1)

To begin the measurements for WP1, initially two channels of the measurement system are used. The first channel is used for the reference data, which is directly connected (LOS) to the system (Channel 1). The second channel is used for the NLOS data which is connected over an antenna connection. The initial target is to estimate the direct path delay in the reference data file (Channel 1), then the estimate of the direct path delay in the NLOS data files (Channel 2) is calculated. The system delays are subtracted from the NLOS data files and then the NLOS delay is subtracted from the reference delay. The result is conventional TOA delay of the 1D range between the transmit and the receive antennas. The data samples in the reference files are not corrupted because the signal line is directly connected via cable from signal generator to the analyzer. The NLOS data files are corrupted with multi-path, NLOS conditions, attenuation and dispersion. Fig. 4.9 shows the block diagram of the system setup for WP1 used to obtain the data values for the transmitted and the received signals. For the later measurements reference channel is removed and the delay is calculated by transmitting two different signals separately and then by comparing their TDOA. The other antenna branch has additional delay through the cable and the amplifier for all the measurements. The extra delay is subtracted from the estimated delays to get the actual estimates.

Table 4.3: MCS-2 Signal Properties

Property	Value
Number of data files processed per indoor point	30
Length of recording per data file	$2e6$ samples
Sampling rate of recorded signal	$200MS/s$
Number of data samples	200000 samples
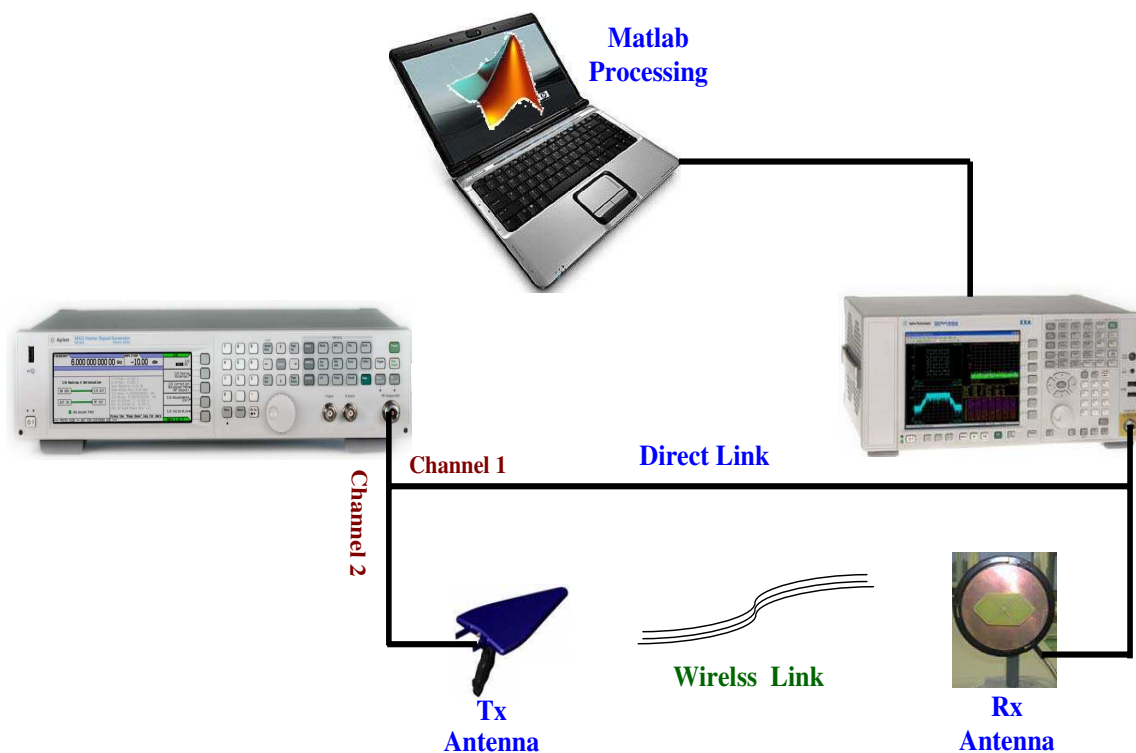
Figure 4.9: Block diagram of the WP1 system

In order to get real measurements, the transmit antennas are placed at fixed points in a way that they surround the receiver antenna object within the building selected for the measurement. The receive antenna object is moved from point to point. The outside views of the building are shown in Fig. 4.10 and the inside views of the measurement locations in Fig. 4.11.

The aim of the indoor tests is to evaluate the position accuracy besides the ranging performance. Therefore, ranges to four different transmitter positions are necessary. The geometry for the four antenna transmission is shown in Fig. 4.12. Two dimensional positions are determined using a very simple least squares algorithm.

4.4.2   Recorded Data Sets for WP1

In WP1, we have two different scenarios for the recorded data sets. For each scenario different data packages are processed. Each data package consists of the transmitted (reference) and the received (data) signals. For each signal 30 different recordings are captured, each in a separate data file. Every data package is recorded from different locations and the distances according to the setup shown in Fig. 4.9.

Figure 4.10: Outside views of building 2 and 3 used for recording the data

Data Sets for Single Antenna TOA-System

We have different data packages of the captured data for the single antenna. As specified earlier that, the data transmitted through the channel 2 of Fig. 4.9 from the antenna, stands on a fixed point. It is received by the antenna inside the building which is moved from point to point. For different points different sets of the data packages are captured. The same signal is transmitted through channel 1 and is used as a reference channel. The circuit delay for the first two data packages is 415 ns and the original distances are 16.75 m and 30.25 m respectively. Using the conventional CIR and correlation algorithms we have large errors in the estimated distances, however, the super resolution techniques algorithms described in section 5.2 efficiently reduce the amount of errors in the delay and distance estimations. It is noticed that 1500 samples of the measured signal are enough to estimate the distance in this case. Another scenario for the WP1 is with the two antennas case. In this scenario the reference channel is removed and two different antennas are used to transmit the signal. The both transmitted signals are received by the single receive antenna i.e this is a TDOA system.

Figure 4.11: Inside views of measurement locations within building 2 and 3
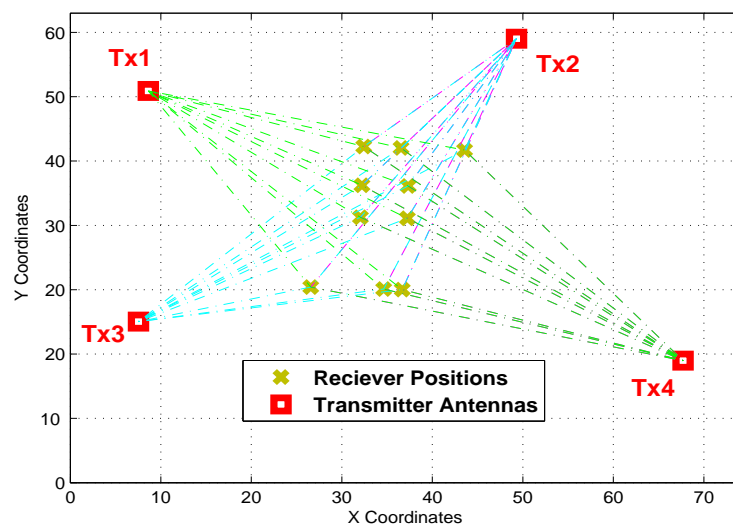
Figure 4.12: Geometry of position estimation through 4 antennas

Data Sets for Two Antenna TDOA-System

The second scenario for recording the data sets is such that we have two transmit and one receive antennas. Both the transmitters send their multi-carrier signals (assuming at the same time). Each transmitter has a GPS timing receiver with a GPS isochronous $10MHz$ signal output. This $10MHz$ reference signal is used for the $10MHz$ reference input from the signal generator. The GPS timing receiver has a $1PPS$ signal, for triggering the baseband output signal one time, for the beginning and starting the first sample. The disadvantage is that, in case of two transmitters, the inaccuracy of the PPS and $10MHz$ output between each GPS receiver can be $+/-10ns$. These $+/-10ns$ are slowly shifted in time and are not predictable. These $10ns$ also cause the additional range estimation failure. Since the channel is static (nothing is moving), the two CIRs are not expected to change between file to file, of a recorded data set. These CIRs are used to estimate the distance between the transmitters. Table 4.4 summarizes all the data sets processed in WP1 with their respective distances and delays for the single and multiple antennas.

Table 4.4: List of Processed Data Sets with Original Distances and Delays

	Single Antenna				**Multiple Antenna**		
S.No	DP Name	Dist (m)	Delay (nSec)	S.No	DP Name	Dist (m)	Delay (nSec)
1	HF-SA1	16.75	415	1	HF-MA1	10.6	0
2	HF-SA2	30.25	415	2	HF-MA2	6.10	0
3	HF-SA3	18.30	350	3	HF-MA3	30.5	0
4	HF-SA4	40.00	350	4	HF-MA4	16.75	0
5	HF-SA5	7.5	350	5	HF-MA5	20.25	0
6	HF-SA6	15.5	225	6	HF-MA6	5.25	0
7	HF-SA7	20.25	225	7	HF-MA7	27.5	0
8	HF-SA8	26.661	225	8	HF-MA8	9.10	0

4.4.3 Proposed Scheme for the DME Analysis

In order to have comparison analysis for the variable SNR, variable time resolutions and different number of carriers we have proposed a scheme for the TDOA estimation [90]. This scheme uses pre-half-zero-carriers and post-half-zero-carriers OFDM symbols transmitted through two transmit antennas of the WLAN system. The symbols transmitted are received by one receiver to be positioned. The block diagram of the proposed TDOA estimation scheme is shown in Fig. 4.13. For simplicity we have skipped the details of OFDM/SC-DFE transceiver, however detailed description can be found in our previous works [74] and [75]. Two different QAM modulated symbol

blocks are generated. In the first block, the first half of the carriers from the total number of N are retained while the rest half of the carriers are replaced by zero padded termed as pre-half-zero-carriers. In the second block reverse way is adopted, i.e., post-half-zero-carriers as shown in Fig. 4.13. Both blocks are separately transmitted through two different antennas using OFDM/SC-DFE transceiver. At the receiver both signal blocks are added. As shown in Fig. 4.14 the CTF and the CIR are calculated using known transmitted signals from both antenna 1 and antenna 2. Conventional algorithms like IFFT & correlation and super resolution algorithms like ESPRIT, Root-MUSIC and MP are applied to estimate the TDOA of the received signal.
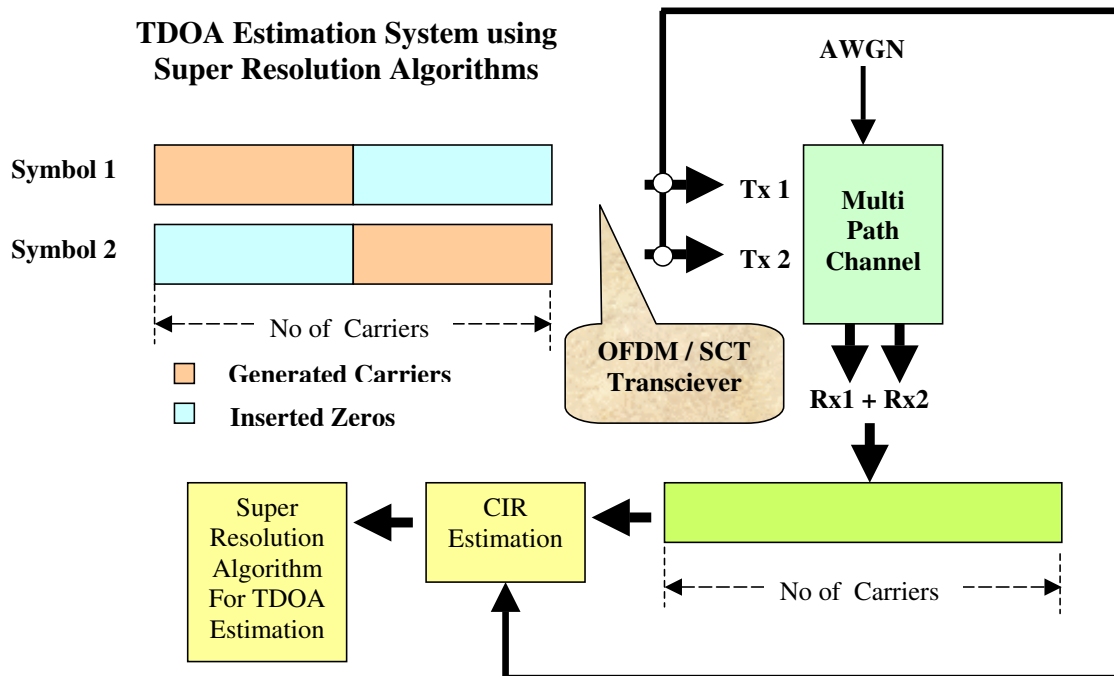
Figure 4.13: TDOA estimation system block diagram and proposed transmitted signal structure

4.4.4 Working Package 2 (WP2)

In WP2 our focus progressed from 4 antennas TDOA to 8 antennas system including one reference antenna implementation and we have tested various recorded data packages using variants of the MP algorithm combined with some old and new model order criteria. The system in WP2 is a unilateral system using the TDOA method because we have used the 8 fixed transmitter antennas to estimate the position of the static and the dynamic receiver by measuring their TDOA. In order to enhance and
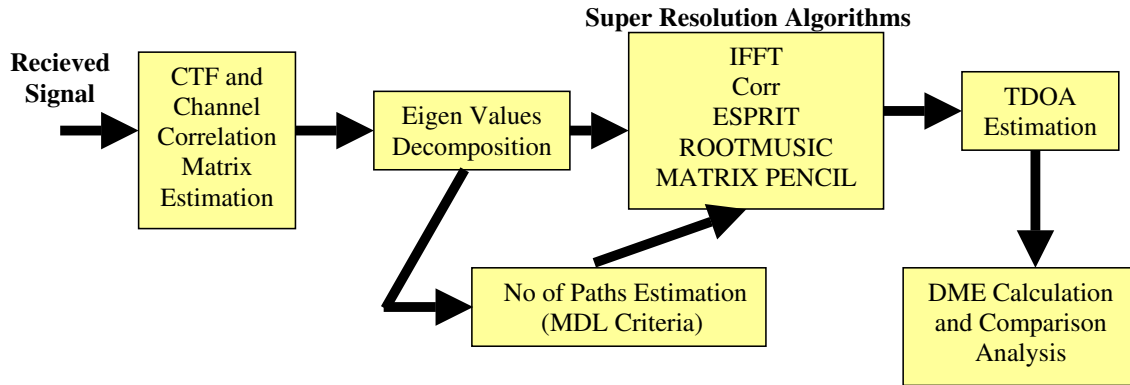
Figure 4.14: Block diagram received signal processing system

validate the system, the measurements are taken in the CMWCE, IESK buildings 2 and 3, already been shown in Fig. 4.10 and Fig. 4.11. The diagram for the enhanced setup with 8 transmitted antennas is shown in Fig. 4.15.

4.4.5 Recorded Data Sets for WP2

Fig. 4.16 shows the plan of the floor considered for the data recordings. The data sets are recorded for different points in the ground floor and the first floor of the building. Some receiver points were on the stairs and on the second floor. The list of receiver measurement points along with their X, Y and Z coordinates is shown in table 4.5. Fig. 4.17 shows the direction of the receiver movement for the dynamic data recordings.

Different data sets are prepared gradually for estimation of the receiver range. Initially static measurement data sets are prepared to validate the basic MP algorithm. Later on the dynamic recordings are performed using a selected direction in the corridors of the building at different floors. The locus of the receiver movement along with 8 transmit antennas positions is shown in Fig. 4.18. The list of all data sets used in WP2 with the number of points in a data set, resolution of recording per point and the number of antennas used for the recording is shown in table 4.6.

Table 4.6 lists the **Package Names** which are given to a particular set of recorded data. A package name is formulated in a way that it mimics nature of the environment and nature of the recordings. Each package name is prefixed by HF to show the data recording related to chair of High Frequency. Further explanation of the package names are as following:

- The **1st letter** of the data package name represents the **Type** of measurement having a value of **S** for the **Static** and **D** for the **Dynamic**.
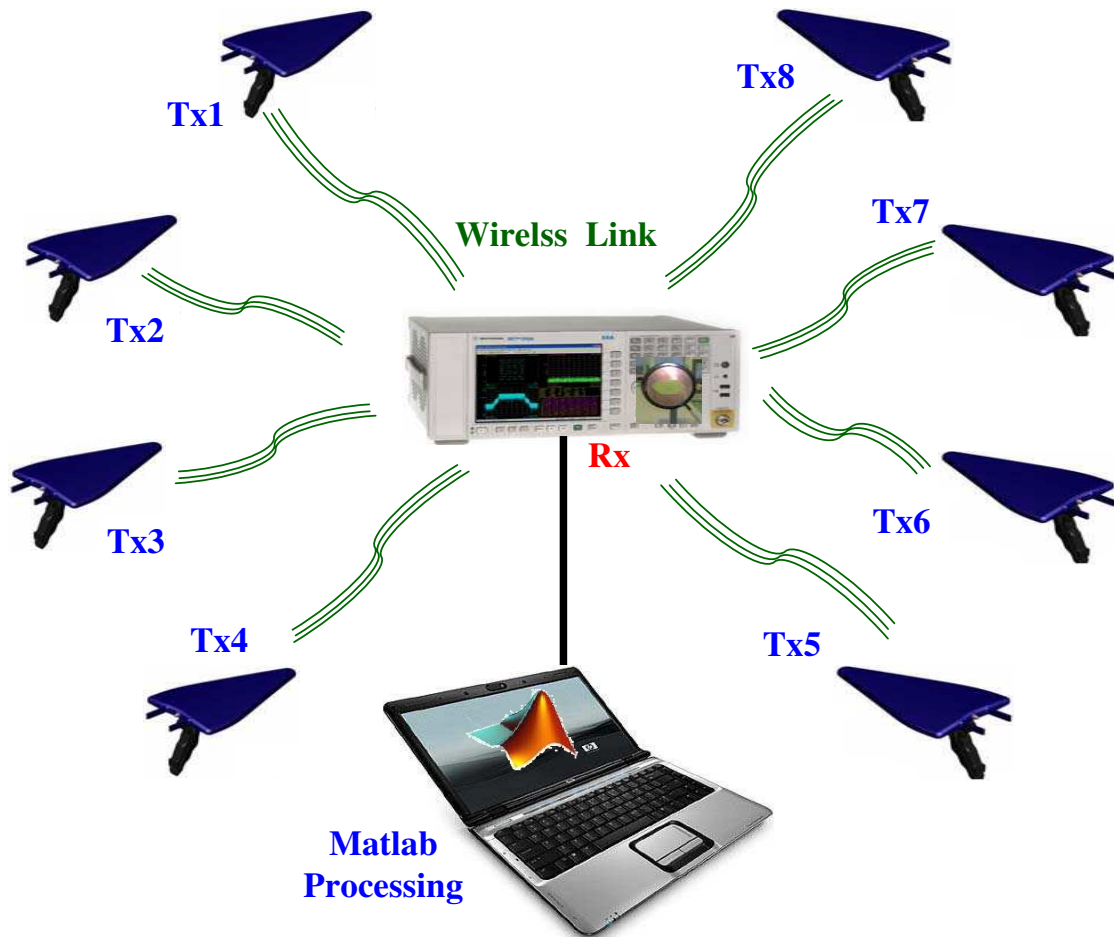
Figure 4.15: Modified setup with 8 antennas
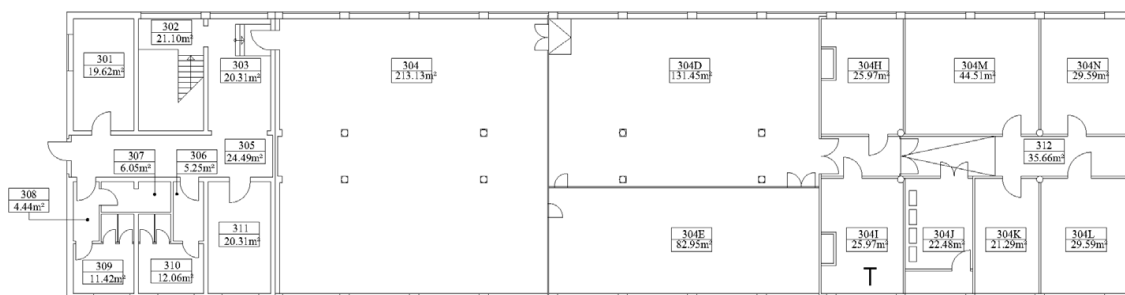
Figure 4.16: The plan of the test area with measurements

Table 4.5: Measurements Coordinates for Different Receiver Positions

Point	X	Y	Z	Point	X	Y	Z
1	145	50	-0.5	16	145	30	7.5
2	151.5	30	-0.5	17	145	20	7.5
3	158.5	30	-0.5	18	145	50	7.5
4	166.5	50	-0.5	19	145	30	7.5
5	145	30	1.25	20	145	20	7.5
6	151.5	20	1.25	21	145	50	7.5
7	158.5	30	1.25	22	145	20	7.5
8	166.3	50	1.25	23	145	30	7.5
9	145	20	4.5	24	145	50	7.5
10	151.5	30	4.5	25	145	20	7.5
11	158.5	50	4.5	26	145	30	7.5
12	166.5	20	4.5	27	145	50	7.5
13	155.5	30	-0.562	28	145	30	7.5
14	165	50	-0.141	29	174.476	30	7.5
15	99.785	64.426	-0.087	30	184.441	30	7.5
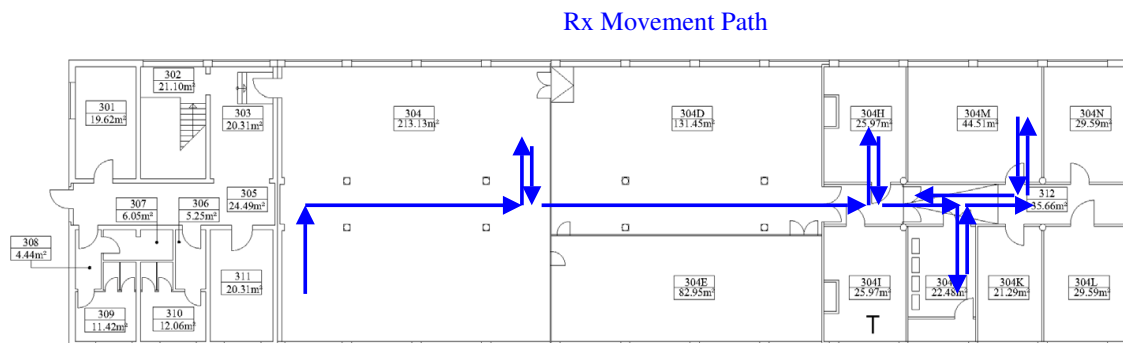
Figure 4.17: The direction of the receiver movement

Table 4.6: The Observed Data Set Packages for the WP2

S.No	Package Name	# of Estimation Points	# of Recordings Per Point	Type of Measurement	# of Antennas Estimation
1	HF-S41	10	20	Static	4
2	HF-S81	15	300	Static	8
3	HF-S82	5	100	Static	8
4	HF-S83	25	100	Static	8
5	HF-D82-GF	Numerous	500	Dynamic	8
6	HF-D82-GF	Numerous	500	Dynamic	8
7	HF-D83-1F	Numerous	1000	Dynamic	8
8	HF-D83-GF2	Numerous	800	Dynamic	8
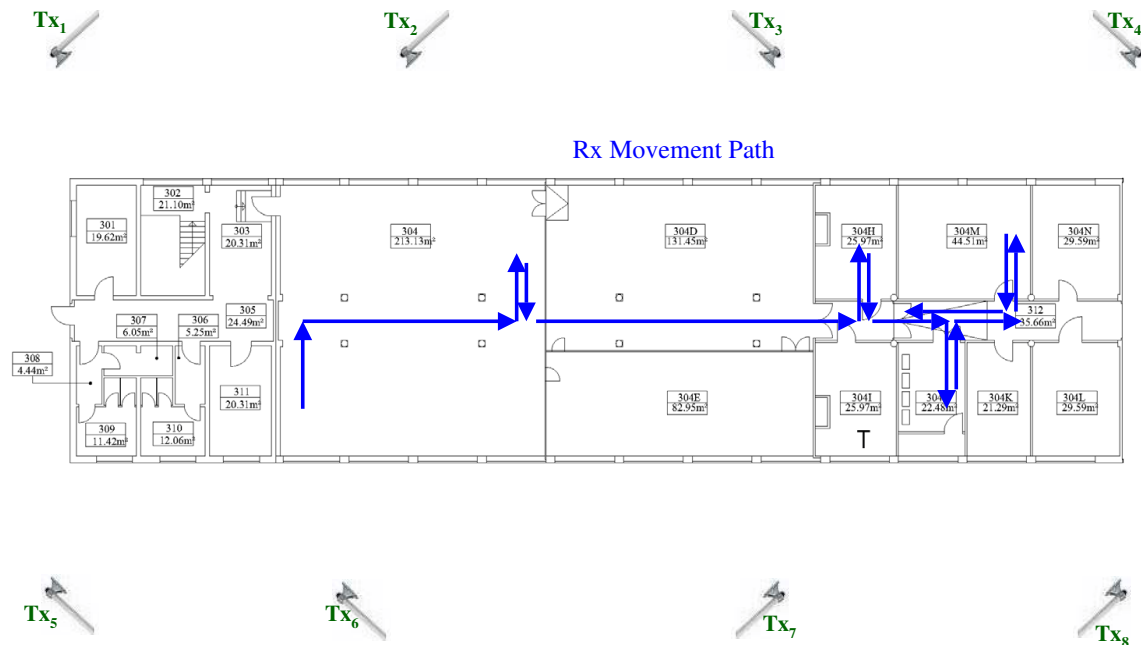
Figure 4.18: The locus of the receiver movement with antenna positions

- The **2nd digit** represents the **Number of antennas** used for the transmission which may have a value of **4** or **8**.

- The **3rd digit** represents the **Number of data package** having values **1,2,...**.

- The **last portion** of the name represents the **Floor** of the building where the data was recorded having a value of **GF** for the **Ground Floor** and of **1F** for the **First Floor**.

For example, if we take the package name **D83-1F**, it means the data set is recorded for the **Dynamic** movement of the receiver, **3rd** recording, using **8** transmit antennas and it is recorded at the **First Floor** of the building. We would use these conventions to refer different data sets in the next chapter of the thesis. The estimation analysis for the WP1 and the WP2 is explained in chapter 5.

Chapter 5

Super Resolution Algorithms and Estimation Results

This chapter presents the estimation of the results for the algorithms implemented to estimate the delays and distances for the indoor positioning system under study. We have already explained the system setup for the two stages WP1 and WP2 in chapter 4.

The first stage, WP1, is regarding the implementations and the comparisons of the conventional and the super resolution algorithms. It is limited to four antennas system only. In the second stage, WP2, emphasis is given to the optimization of the algorithms for efficiency and accuracy. The MP algorithm is assumed to be the most accurate amongst all the algorithms studied in WP1, however ESPRIT gives some efficient implementation results while multiple antennas with numerous points are involved. Furthermore, different variations of the MP algorithm have been implemented in order to analyze the accuracy and efficiency of the estimations in WP2. The focus has been progressed from 4 antennas TDOA system to 8 antennas implementation including a reference antenna. Various recorded data packages have been tested using variants of MP algorithm combined with some old and new model order criteria. An analysis of the results and conclusion for comparison of different variants of the MP algorithm is also presented at the end of this chapter. The chapter also presents the analysis of the results obtained by the simulations of the scheme proposed in chapter 4. The scheme uses the OFDM/SC-DFE signal structure presented in chapter 3.

5.1 The TOA for Mutlipath Indoor Positioning Systems

Recall from the chapter 1 that in order to locate a particular object in indoor positioning systems, accurate estimation of the TOA is required and the multi-path highly faded channels disperse the actual CIR by noise effects causing an inaccurate

estimate of the TOA and thereby TDOA. Therefore, the IFFT and correlation based conventional algorithms result in an inaccurate estimation [82]. Due to this reason the super resolution algorithms got noticeable attention in recent years for the time domain analysis [20, 82] and the spectral estimation of the time dispersion parameters [21].

The TDOA is calculated by considering the time delay of the first arrived signal using all the super resolution algorithms separately. These TDOAs are then used to estimate the distance between the transmitter and the receiver and thereby to estimate the DME in case of each algorithm. The ultimate goal of the super resolution algorithms is to minimize the DME which is high enough for the conventional algorithms. In our analysis we have used the systems detailed under the packages WP1 and WP2. However, the comparison analysis for the variable SNR, time resolutions and number of carriers have been carried out using newly proposed scheme, described under section 4.4.3 of chapter 4.

In the next section, we investigate the conventional and the super resolution algorithms. The modified steps, performed to improve the estimation, are also presented.

5.2 Conventional and Super Resolution Algorithms

The IFFT and Xcorr based conventional algorithms use the peak detection methods, because their accuracy is directly limited by the sampling rate. These methods give strict estimation of the distances by rounding the estimated distances and an error of 1.5 meter is normally expected. On the other hand super resolution algorithms which are also affected by the sampling rate (signal bandwidth in general), have better estimation accuracy than that of the conventional algorithms [8]. In sequel we briefly describe these algorithms. The details of the algorithms can be found in [64, 108, 177, 178].

5.2.1 CIR

We can model the CIR based technique in multi-carrier signal by expressing k as the carrier frequency index, the transmitted signal as $X(k)$ and the corresponding additive noise as $W(k)$, all in frequency domain. Consequently eq. 3.1, can be reformulated as; [166]

$$R(k) = H(k)X(k) + W(k) \tag{5.1}$$

where $H(k)$ is the CTF of the time invariant multi-path dispersive channel. In order to estimate the time delays we need first to estimate the CTF, since both the transmitted and the received signals are known, we can estimate $H(k)$ by simply distinguishing

the received signal from the transmitted one as;

$$H(k) = \frac{R(k)}{X(k)} \tag{5.2}$$

The corresponding CIR can be calculated by taking IFFT of the CTF ($H(k)$) as

$$CIR(\tau) = \sum_{k=0}^{N-1} H(k)e^{j2\pi\tau k} \tag{5.3}$$

where τ represents the delays. By taking the first appearance of $CIR(\tau)$, we can get the first TOA, τ_0. This method is very effective in terms of noise since in many cases, the LOS signal is very weak and can not be distinguished well from the noise and the other parts. The CTF and the corresponding CIR for a sample of 200 carries, for our application, are shown in Fig. 5.1 and Fig. 5.2 respectively.
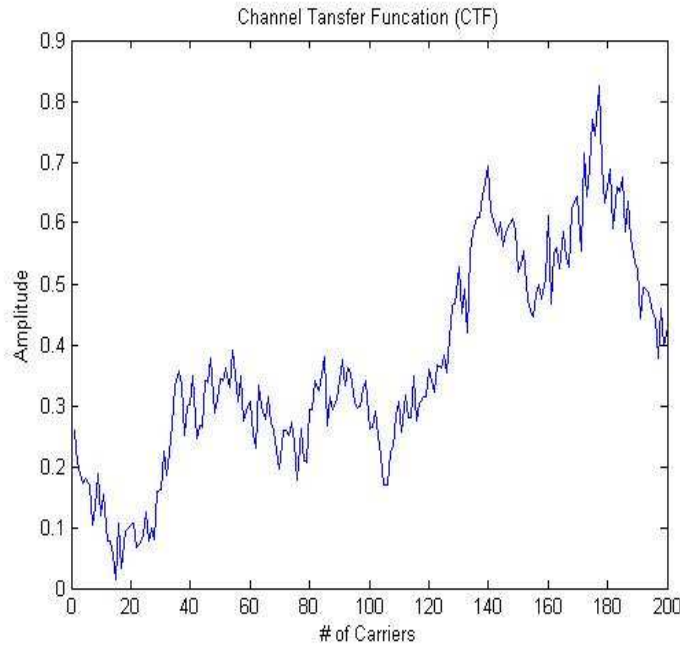
Figure 5.1: The Channel Transfer Function (CTF)

5.2.2 Cross-Correlation

The time delays can be calculated by taking the cross correlation between the received and the transmitted time domain signals, which can be written as

$$R_\tau = \sum_{n=-\infty}^{+\infty} y(n)x(n+\tau) \tag{5.4}$$
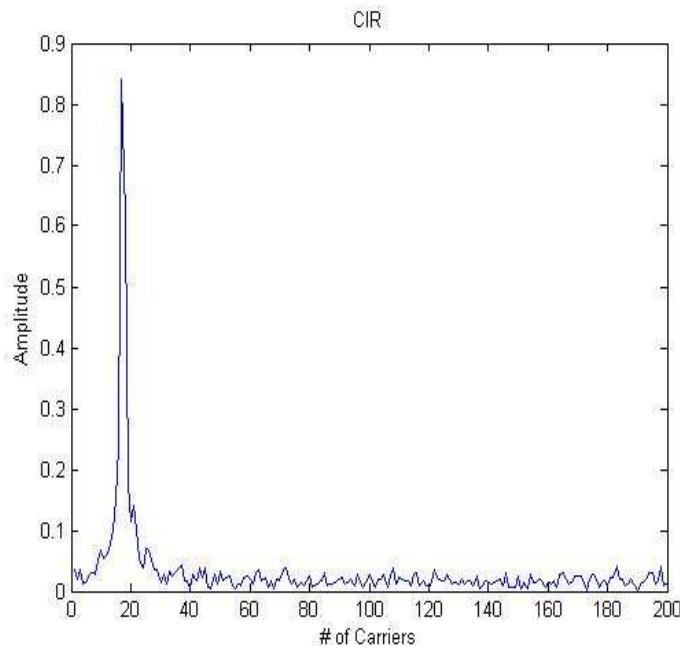
Figure 5.2: The Channel Impulse Response (CIR)

where n is the time index and y, x are the received and the transmitted time domain signals respectively. The y and x can be achieved by simply applying the IFFT operations on Y_n and X_n, the frequency domain counterparts of the earlier, respectively. The cross correlation R_τ for a sample of the current application is shown in Fig. 5.3. The maximum value of R_τ appears at the time delay of the received signal. The problem with this method is that, the first estimated delay is in fact the total delay of the received signal and may not correspond to the first path, which causes an error if the reflected parts are strong. An alternate expression for R_τ is R_{xy}, which can be written as $R_{xy} = E[X_n Y_n^\dagger]$ where $E[.]$ is the expectation operator and $\dagger$ is the Hermitian transpose.

5.2.3 Estimation of Signal Parameters via Rotational Invariance Technique (ESPRIT)

The ESPRIT is a subspace based algorithm for estimating parameters in a sinusoidal model [179] which is shown in Fig. 5.4. Unitary ESPRIT algorithm is an extended form of the ESPRIT algorithm. The ESPRIT algorithm can be summarized in the following steps [178];

1. Obtain an estimate of the signal subspaces for the two sub-arrays $\hat{\hat{E}} = \begin{pmatrix} \hat{E}_1 \\ \hat{E}_2 \end{pmatrix}$

2. Solve the over-determined system of equations $\hat{E}_1 \hat{\psi} \approx \hat{E}_2$
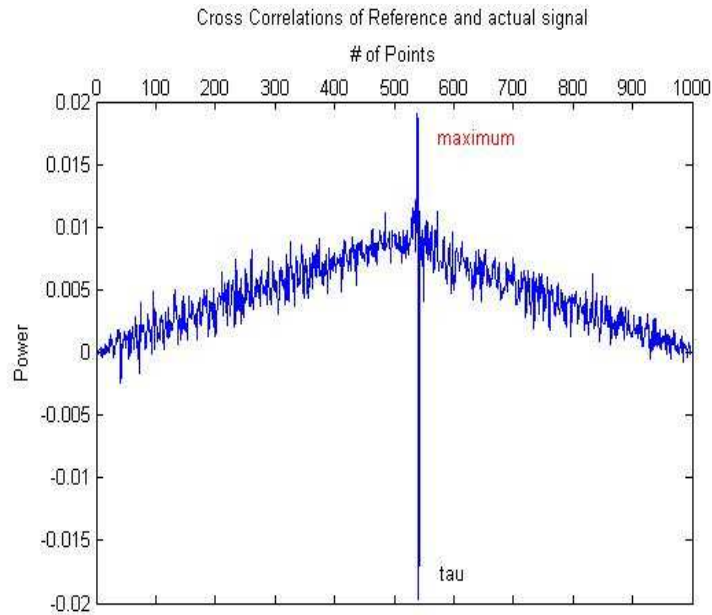
Figure 5.3: Correlation Function(R_τ)
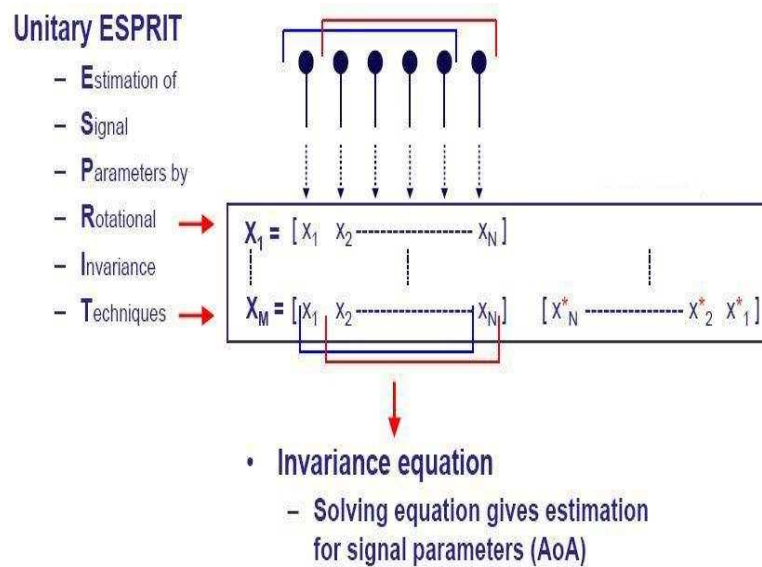
Figure 5.4: The ESPRIT Algorithm

3. Compute the signal poles by the EV decomposition $\hat{z}_i = \lambda_i(\hat{\psi})$

where;

- E_1, E_2 are the signal subspaces,

- z_i are the signal poles,

- $\lambda_i(\psi)$ denote the ith EVs of ψ,

- ψ is the unique non-singular matrix relating E_1 and E_2 and

- $\hat{[.]}$ operator denotes the estimation.

Once EVs, λ_i are computed using the above procedure, the time delays $\tau_0 > \tau_1, \ldots, > \tau_{L-1}$ are estimated based on the largest L peaks of $f(\tau)$ using eq. 5.8, given in section 5.2.4.

5.2.4 Root Multiple Signal Classification (Root-MUSIC)

The ROOT MUSIC is an algorithm which performs Eigen-space analysis of the channel correlation matrix in order to efficiently estimate the channel delay contents. It uses the estimated channel samples to estimate the delay [180]. Taking the correlation of the estimated CTF, we have

$$R_N = E[HH^\dagger] = A(\tau)R_d A^\dagger(\tau) + \sigma^2 I \tag{5.5}$$

where R_d is the covariance matrix of the channel amplitudes d, $A(\tau)$ is the $(N \times L)$ time delay matrix with columns $A(\tau)$, where eq. 5.6 presents $A(\tau)$.

$$A(\tau_i) = \left(\begin{pmatrix} 1 & 0 & 0 & \ldots & 0 \\ 0 & e^{\frac{j2\pi\tau_i}{N}} & 0 & \ldots & 0 \\ 0 & 0 & e^{\frac{2j2\pi\tau_i}{N}} & \ldots & 0 \\ \vdots & \vdots & \vdots & \ldots & \vdots \\ 0 & 0 & 0 & 0 & e^{\frac{(N-1)j2\pi\tau_i}{N}} \end{pmatrix} \begin{pmatrix} X_0 \\ X_1 \\ . \\ . \\ X_{N-1} \end{pmatrix} \right) \tag{5.6}$$

Solving the following Eigen-system

$$R_N E = E\Lambda \tag{5.7}$$

where;

- $\Lambda = diag(\lambda_0, \lambda_1, \ldots, \lambda_N)$ contains the EVs of R_N and

- E is a matrix that contains the corresponding Eigen-vectors E_k,

the number of paths is estimated from the fact that $\lambda_0 > \lambda_1, \ldots, > \lambda_L > \lambda_{\sigma_W^2}$, where $\lambda_{\sigma_W^2}$ is the noise variance. The time delays $\tau_0 > \tau_1, \ldots, > \tau_{L-1}$ are estimated by finding the largest L peaks of $f(\tau)$ where $f(\tau)$ can be calculated as following

$$f(\tau) = \frac{1}{A^\dagger(\tau)[\sum_{k=L}^{N-1} E_k E_k^\dagger] A(\tau)} \tag{5.8}$$

5.2.5 Matrix Pencil (MP1)

The MP, which is also termed as MP1 in WP2, is an efficient kind of super resolution algorithm. It utilizes a generalized pencil function used to obtain the exponents of a sum of complex exponentials. It is a variation of Eigen-structure approach and uses input MP instead of the correlation matrix. The signal components can be distinguished exactly by mapping the noise components to the null space. The MP is an accurate algorithm for calculating the time domain parameters of the network analyzer. It is used to obtain the poles of the system in one step.

The MP of a function can be defined as follows; If two functions $g(t)$ and $h(t)$ are combined on a common interval with scalar parameter ψ such that $f(t, \psi) = g(t) + \psi h(t)$ then, $f(t, \psi)$ is called the pencil of $g(t)$ and $h(t)$ parameterized by ψ. When $g(t)$, $f(t)$ and ψ are appropriately selected, the pencil of two functions contains very important features that are helpful in extracting information about the poles present in the particular functions [181]. MP1 is considered for multi-path parameters used for the channel modeling. The MP1 algorithm can be summarized as follows;

The parametric model for the discrete complex frequency domain channel response can be written as $H_n = H(f_n) = \sum_{l=0}^{L-1} h_l e^{-j2\pi f_n \tau_l}$, $n = 0, 1, \ldots, N - 1$ where L is the number of multi-path components, N is the number of measurement points, f_n is the frequency. The time domain sampled values can be written as $H_n = \sum_{l=0}^{L-1} \hat{h}_l z_l^n$ where

- $\hat{h}_l = h_l e^{-j2\pi f_o \tau_l}$,

- $z_l = e^{-j2\pi \Delta_f \tau_l}$,

- Δ_f is the frequency spacing between the adjacent channel samples and

- f_0 is the starting measurement frequency.

To apply MP1 for the measured frequency response the Linear Predictor (LP) is constructed [64] before calculating the pencil function in eq. 5.9

$$D_i = [H_i, H_{i+1}, \ldots, H_{i+N-P-1}]^T \tag{5.9}$$

where N is the number of measurement points and P is the pencil parameter chosen between $N/3$ to $2N/3$ to get good performance. The value of P should be greater than that of L, which is the number of paths. The next step is to construct $\overline{Y_1}$, $\overline{Y_2}$ and $\overline{Y}$ given by eq. 5.10, eq. 5.11 and eq. 5.13 respectively.

$$\overline{Y_1} = [D_0, D_1, \ldots, D_{P-1}] \tag{5.10}$$

$$\overline{Y_2} = [D_1, D_2, \ldots, D_P] \tag{5.11}$$

then the following MP is considered

$$\overline{Y_2} - \Lambda \overline{Y_1} = 0 \tag{5.12}$$

where Λ is same as defined under eq. 5.7 in section 5.2.4. To find the number of multi-path components L, a singular value decomposition of the matrix $\overline{Y}$ is carried out as

$$\overline{Y} = V \Delta U^\dagger \tag{5.13}$$

where

$$\overline{Y} = [D_0, D_1, \dots, D_P] \tag{5.14}$$

and V and U are unitary matrices and Δ is a diagonal matrix containing the EVs of $\overline{Y}$. The parameter L is chosen such that the singular values beyond L are set to zero. The time delays are estimated from the Λ_l as following;

$$\overline{\tau_l} = \frac{\ln(\Lambda)}{-j2\pi \Delta_f} \tag{5.15}$$

The amplitudes of h_l of the multi-path components can be calculated by solving the system $HX = \hat{h}$ using linear least squares as

$$\hat{h} = ([X]^\dagger [X])^{-1} [X]^\dagger H \tag{5.16}$$

where

$$X = [X(\tau_0), X(\tau_1), \dots, X(\tau_{L-1})] \tag{5.17}$$

$$X(\tau_k) = [1, e^{-j2\pi f_s \tau_k}, \dots, e^{-j2\pi(N-1)f_s \tau_k}]^T \tag{5.18}$$

and

$$\hat{h} = [\hat{h}_0, \hat{h}_1, \dots, \hat{h}_{L-1}]^T \tag{5.19}$$

5.2.6 Minimum Descriptive Length (MDL) Criterion

The MDL is a criterion to calculate the minimum effective length of the channel. There is no need to find the autocorrelation matrix or its EVs in the MDL. This significantly reduces the computation complexity. The MDL [93] is defined as

$$MDL(k) = L(\theta) + f(k, N_p) \tag{5.20}$$

where $f(k, Np)$ and $L(\theta)$ are the penalty function and the log-likelihood function, given by the eqs. 5.21 and 5.22 respectively.

$$f(k, N) = \frac{1}{2} k(2N - k) \log(M_B) \tag{5.21}$$

$$L(\theta) = -N \log(\det(R_{HH})) - tr(R_{HH})^{-1} R_{HH} \tag{5.22}$$

where tr represents the trace of the matrix. The close expression of the MLL function can be obtained as

$$L(\theta^{(k)}) = -(N - k)M_B \log(\frac{G(\lambda_{K+1}, \ldots, \lambda_N)}{A(\lambda_{K+1}, \ldots, \lambda_N)}) \tag{5.23}$$

where the functions G and A are the geometric and the arithmetic means of their arguments respectively. The value of M_B needs to be selected such that it provides a balance between the resolution and stability of the criteria. The CIR length L is taken to be the value of $k \in 0, 1, \ldots, N - 1$ for which the $MDL(k)$ is minimum.

5.3 Variants of the MP Algorithm

As stated earlier that our focus in WP2 is to improve the efficiency and the accuracy of the MP algorithm estimation. Three different variants of MP are implemented improving MP algorithm in different steps. Before explaining these steps it is necessary to introduce the terms that are used to name and represent different estimation algorithm variants and techniques. We have implemented different variants of the MP algorithm, which we refer in this text as MP1 [64], MP2 [182] and MP3 [84]. MP1 algorithm is used in the WP1 [95]. The MP2 variant of the MP algorithm uses forward-backward averaging in order to nullify the progressing noise and MP3 variant of that uses the Hankel matrix for de-noising the corrupted signal.

5.3.1 Forward Backward Averaging Method (MP2)

In this method MP1 is modified by applying forward backward averaging on the LP of eqs. 5.10 and 5.11 as following

$$FB_{av} = \frac{\overline{Y_i}inv(\overline{Y_i}) + J(\overline{Y_i}inv(\overline{Y_i}))^*}{2m} \tag{5.24}$$

where m is the length of each D_n in Y_i and J is the change matrix shown by eq. 5.25

$$J = \begin{bmatrix} 0 & 0 & \ldots & \ldots & 1 \\ 0 & \vdots & \vdots & 1 & \vdots \\ \vdots & \vdots & 1 & \vdots & \vdots \\ \vdots & 1 & \vdots & \vdots & 0 \\ 1 & \ldots & \vdots & 0 & 0 \end{bmatrix} \tag{5.25}$$

5.3.2 The Hankel Matrix Method (MP3)

This method uses the Hankel matrix instead of LP to modify the MP1. The generalized Hankel matrix is shown in appendix D. The Hankel matrix of the CTF is

calculated before the Single Value Decomposition (SVD). The Hankel matix of the CTF can be derived as

$$
J =
\begin{bmatrix}
H_1 & H_2 & H_3 & \dots & H_{N+P-1} \\
H_2 & H_3 & \vdots & H_{N+P-1} & H_{N+P} \\
H_3 & \vdots & H_{N+P-1} & H_{N+P} & \vdots \\
\vdots & H_{N+P-1} & H_{N+P} & \vdots & \vdots \\
H_{N+P-1} & H_{N+P} & \dots & \vdots & H_{N+P+M}
\end{bmatrix}
\tag{5.26}
$$

where M is the length of each D_n in Y_i and P is the predictor difference between Y_1 and Y_2. The SVD of the Hankel matrix provides a means of computing the matrices which define the state-space realization.

5.3.3 Variant Model Order Criteria

In practical implementation the noise EVs are all different and to distinguish the signal EVs from the noise EVs is a difficult task. The information theoretic criteria for the model order selection is normally applied to resolve this problem. We have combined a variety of information theoretic criteria with different variants of the MP algorithm which are MDL, EIG, Modified MDL (MDX) and AIC. For checking the performance of different combinations of the MP algorithms with different model order criteria, we have utilized all possible combinations. In the end we modified the MP algorithm to estimate the optimal model order with out use of any model order criterion. The corresponding variants of the three MP algorithms have MA1, MA2, and MA3 notions, where suffix **A** indicates the automatic selection. Table 5.1 summarizes the legends for MP variants and the model order variants with combination of each.

5.4 Analysis for the WP1

5.4.1 Averaging the Estimation Results

The conventional and the super resolution algorithms described in section 5.2 have been applied on the data sets of WP1 for estimating the distance directly from the CIR. The number of effective paths is estimated from the EVs of the correlation matrix according to a predefined threshold, which is related in fact to the noise variance. For distance estimation, only the first tap is required. For the IFFT and cross-correlation, the distance estimation accuracy is limited by the sampling rate, since one sample causes distance shift of 3 m (1/100E6 *c), that means even for very clean signal, an error of 3/2=1.5 m is normal. The circuit delay, shown in table 4.4,

for the different distances is subtracted from the estimated distance in order to get the proper distance. Fig. 5.5 shows the first arrival of path with the CIR. In order to get the accurate estimation, we have taken the median and the mean of the measured distances from 21 files of each data set. Since the measurements taken for most of the files of a package almost have a constant offset except one or two files, therefore, the right averaging for an accurate estimate is the median instead of the mean. The median searches for the highly repeated values and averages them to avoid the outlier values, whereas in the case of mean, a bad-recorded file can shift its value strongly.
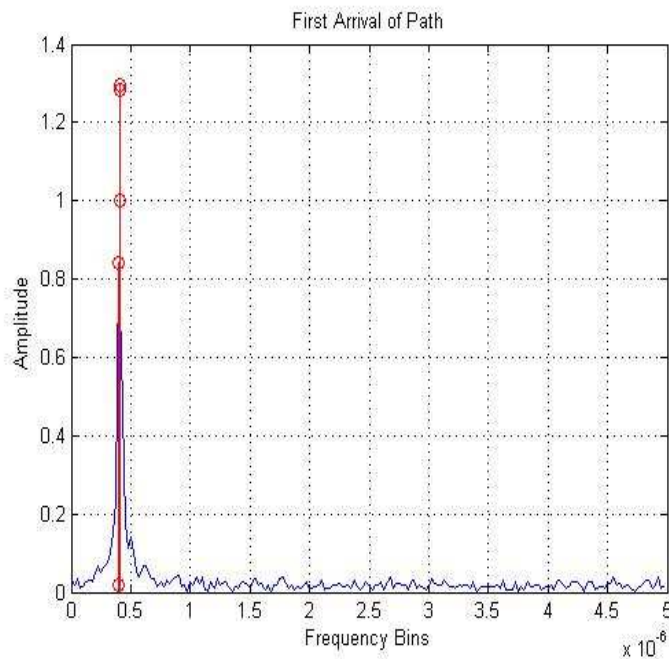
Figure 5.5: First Arrival of Path

5.4.2 Calibration, Accuracy of Estimation and Synchronization Issues

Regarding the accuracy of the super resolution algorithms, we have applied a known virtual channel with some paths to the transmitted signal by simple delay shifting and summation. The algorithms give very accurate distance estimation. For good estimation, the calibration of the circuit delay is necessary. This parameter is important to calculate the correct circuit delays on the basis of which, the estimation is calculated. A wrong circuit delay may result in totally incorrect estimation. Another issue is the estimation of the number of paths that may cause the variations in the estimation that we encountered for different packages. We have applied the MDL criteria, discussed in section 5.2.6, to resolve this problem.

Since the channel is static, it is expected that the two CIRs do not change between file to file, but as it is noticed, they change for the different delays, for each file. As long as the CIRs change each time, we cannot assume that they provide the right estimate of the difference delays. The validity of the right estimated difference totally depends upon the proper synchronization between the transmitters and the receiver.

5.4.3 Single Antenna TOA-System Results Analysis

Fig. 5.6 shows the comparison performance of the distance estimation. It consists of the results for all the algorithms for every possible file in a data set of single antenna case. It is clear from the figure that MP1 algorithm gives the optimal results. Correlation and IFFT have the deviations from $4m$ to $8m$ from the original distance, ESPRIT has up to $3m$ while Root-MUSIC and MP1 have deviations within $2m$ and $1m$ range respectively. Fig. 5.7 shows the averages and Fig. 5.8 shows the mean, median and
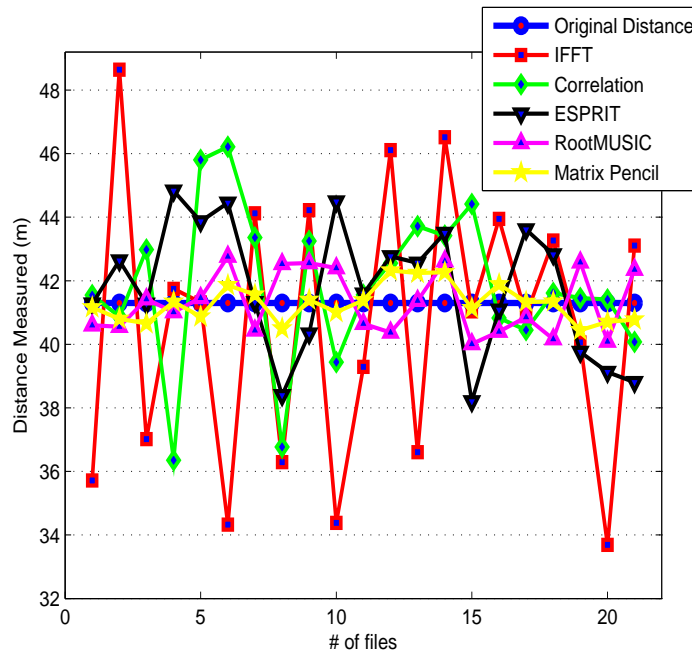
Figure 5.6: Estimates of distances for single antenna case

standard deviation values of the distances estimation for the conventional and the super resolution algorithms. The optimal estimation results are achieved by the ES-PRIT and MP1 algorithms. Figures 5.9, 5.10 and 5.11 show the distance estimation, their averages and the standard deviation comparisons for the signal generated from measured data received through channel 2 when a reference cable is applied. It can be seen clearly that in this case the ESPRIT and MP1 algorithms perform better than the other.

Table 5.1: MP Algorithm Variants with Model Order Combinations

Legend	Description
Algorithm Variants	
MP1	Matrix Pencil algorithm using generalized Matrix Pencil Function
MP2	Matrix Pencil algorithm using Forward-Backward averaging Method
MP3	Matrix Pencil algorithm using Hankel Matrix de-noising Method
Model Order Variants	
AIC	Akaike Information Criteria
EIG	Eigenvalue Criteria
MDL	Minimum Descriptive Length Criteria
MDX	Modified Minimum Descriptive Length Criteria
Combination of Algorithm and Model order used	
MP1-AIC	MP1 with AIC
MP1-EIG	MP1 with EIG
MP1-MDL	MP1 with MDL
MP1-MDX	MP1 with MDX
MP2-AIC	MP2 with AIC
MP2-EIG	MP2 with EIG
MP2-MDL	MP2 with MDL
MP2-MDX	MP2 with MDX
MP3-AIC	MP3 with AIC
MP3-EIG	MP3 with EIG
MP3-MDL	MP3 with MDL
MP3-MDX	MP3 with MDX
MA1	MP1 with with automatic model order selection
MA2	MP2 with with automatic model order selection
MA3	MP3 with with automatic model order selection

Figure 5.7: Mean, Median and Standard Deviation for single antenna case
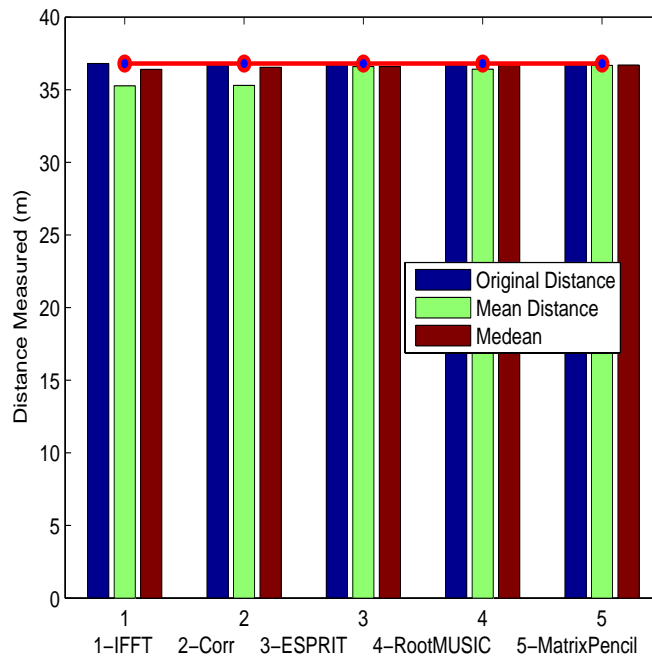
Figure 5.8: Averages of the estimated distances for single antenna case
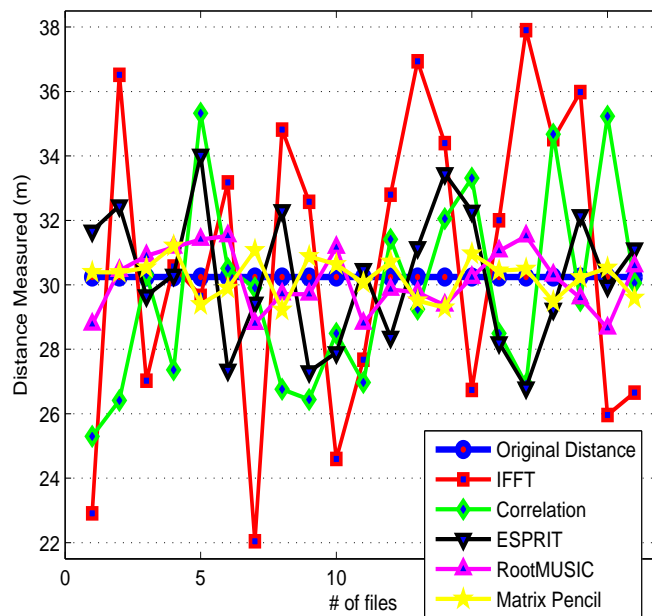
Figure 5.9: Estimates of distances with a reference cable
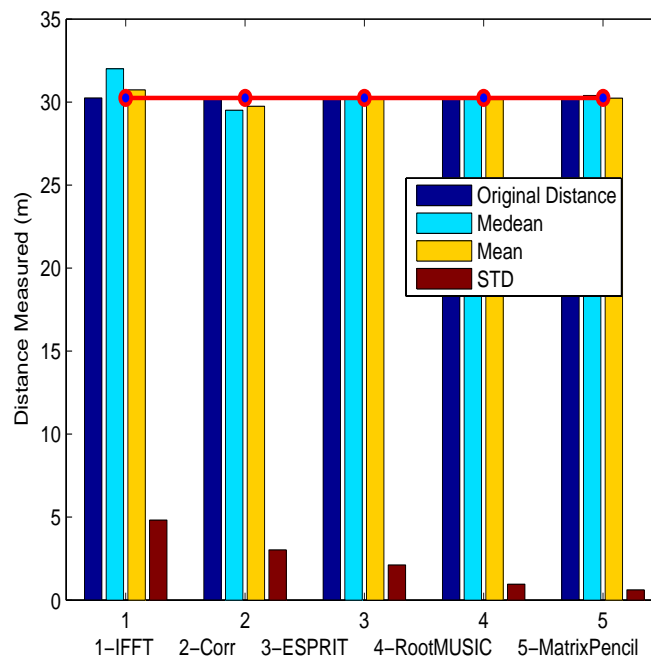
Figure 5.10: Mean, Median and Standard Deviation with a reference cable
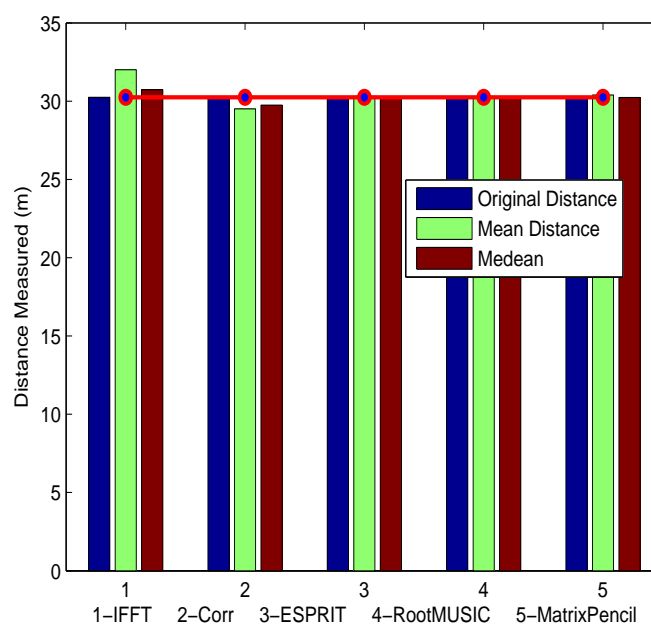
Figure 5.11: Averages of the estimated distances with a reference cable

Figures 5.12, 5.13 and 5.14 show similar results for another data set with the reference cable. We can see that the performance of the ESPRIT is slightly worse than the other super resolution algorithms. It achieves $3m$ to $4m$ deviations from the original distance while the other two algorithms achieve $1m$ to $2m$ deviations. Thus MP1 again achieved the optimal results as expected.
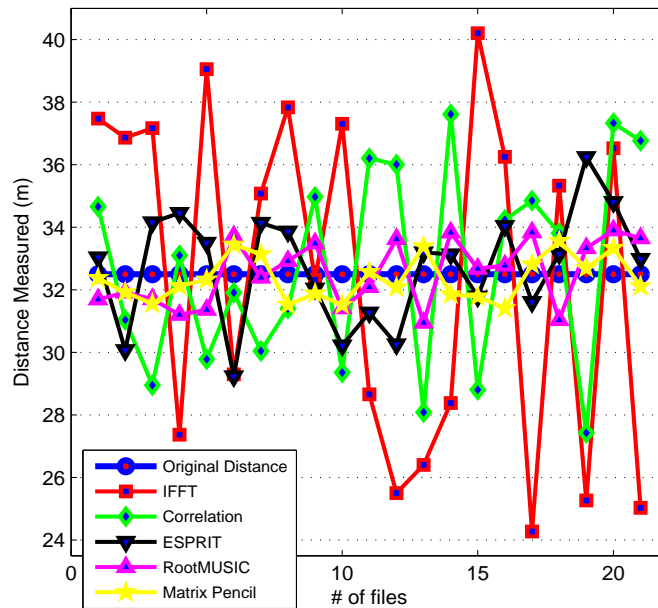
Figure 5.12: Estimates of distances with a reference cable (example 2)

5.4.4 Two Antenna TDOA-System Results Analysis

For the two antennas case we have the Figs. 5.15, 5.16 and 5.17 with similar results. It can be clearly noticed from these figures that the performance of the ESPRIT algorithm is the worst amongst all, in this case. It achieves a deviation of up to $5m$ while both the Root-MUSIC and MP1 have deviations up to $1.5m$ from the original range. Both the Root-MUSIC and MP1 again supersede the traditional algorithms along with the ESPRIT algorithm. However, we do not get the optimal estimations in the case of two antennas transmission.

5.5 Analysis for the Proposed Scheme

In order to improve the estimation results, we have introduced the scheme proposed in section 4.4.3. In this section we discuss the analysis of the simulation results for the said scheme implementations. Simple experiments for estimating DME, time
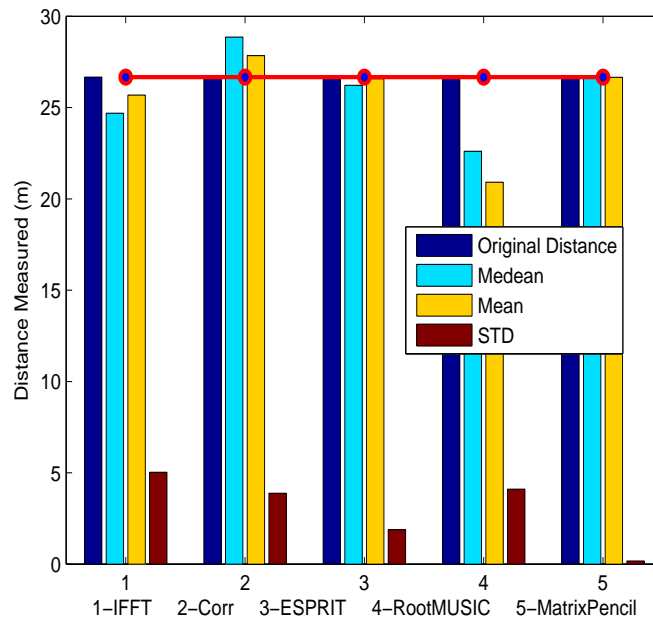
Figure 5.13: Mean, Median and Standard Deviation with a reference cable (example 2)
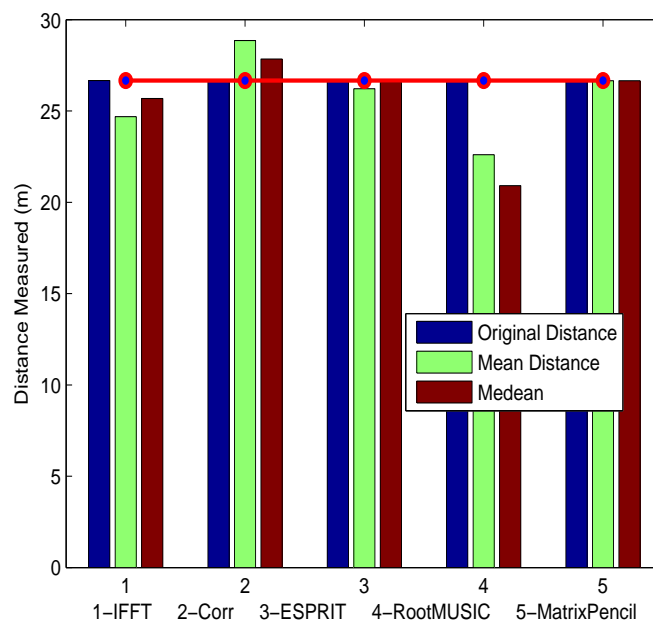
Figure 5.14: Averages of the estimated distances with a reference cable (example 2)
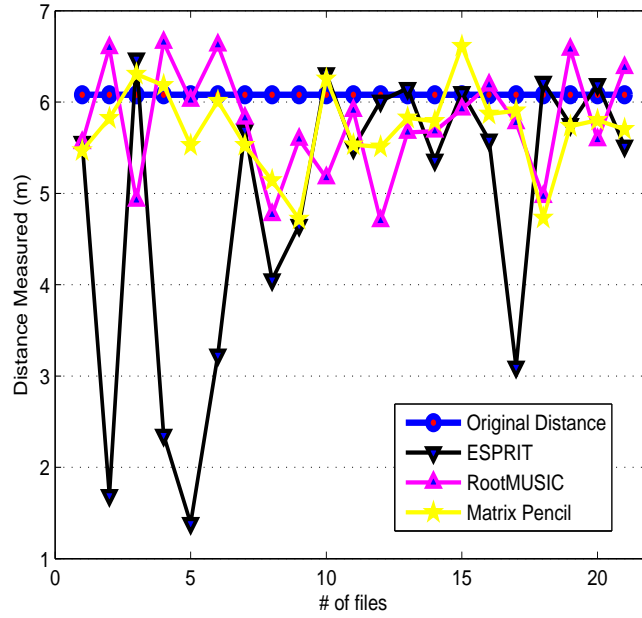
Figure 5.15: Estimates of distances for two antennas case
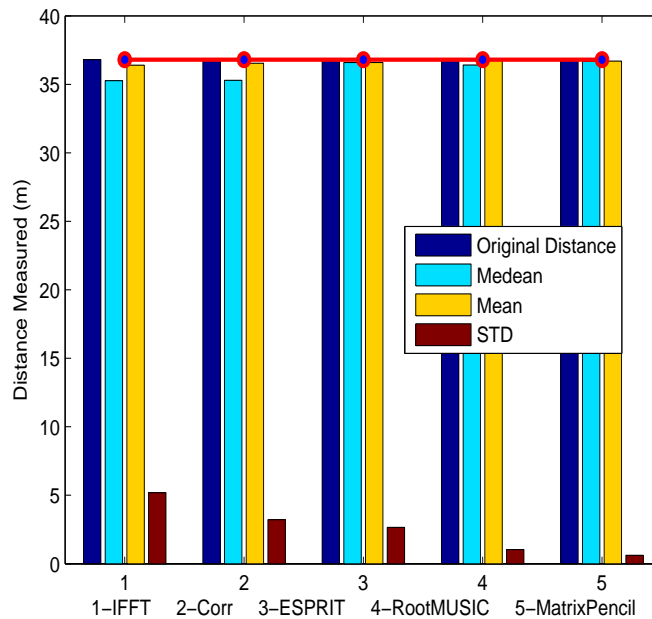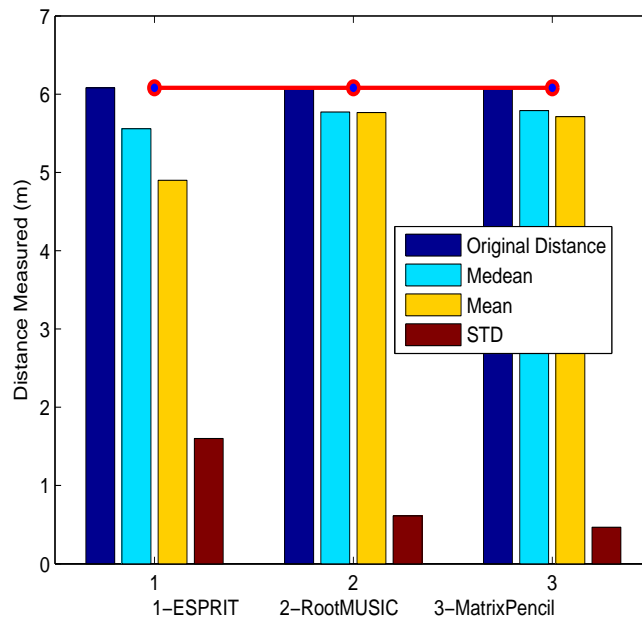

Figure 5.16: Mean, Median and Standard Deviation for two antennas case
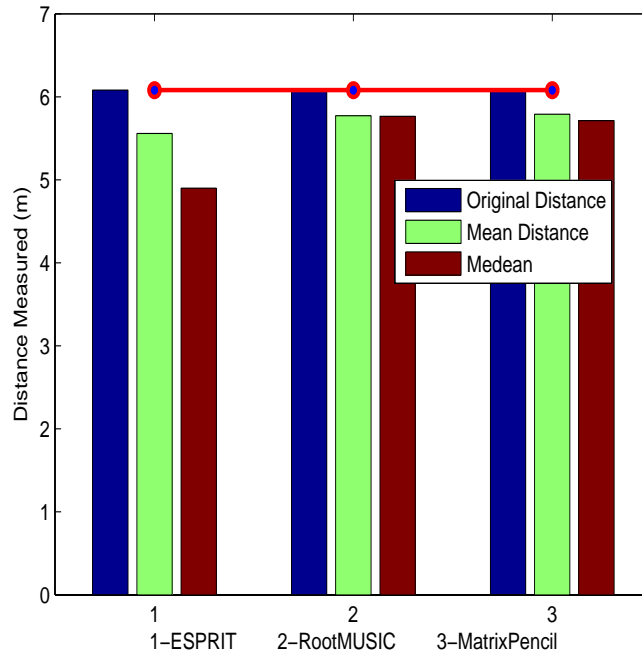
Figure 5.17: Averages of the estimated distances for two antennas case

resolution, number of carriers and SNR are performed using the super resolution algorithms. Fig. 5.18 shows the performance comparison of distance estimation for all the algorithms. A typical number of experiments are performed through our system described in section 4.4.3. It is clear from the Fig. 5.18 that the MP algorithm gives the optimal results. Correlation and IFFT have the deviations from $4m$ to $8m$ with respect to the original distance. ESPRIT has up to $3m$ while Root-MUSIC and MP have deviations within $2m$ and $1m$ respectively.

Fig. 5.19 shows the mean, median and standard deviation values of the distance estimations for the conventional and the super resolution algorithms. Having a reasonable number of experiments, it is concluded that optimal estimation results are achieved by the ESPRIT and MP1 algorithms and will be used for further analysis.

5.5.1 The Effects of the Bandwidth

As specified earlier that the time resolution affects the DME. The estimation can be improved by increasing the bandwidth of the system, in other words, by decreasing the time resolution. This can be analyzed by studying the results in Fig. 5.20 obtained by our simulations. The figure is divided in four different portions. The top portion shows the DME comparisons of the super resolution algorithms for higher (Ghz) bandwidth systems, the rest of the bottom three portions show similar results for the lower bandwidth systems subsequently. It can be clearly verified that the higher bandwidth systems (Ghz) dropped the DME in centimeters (cm) range from
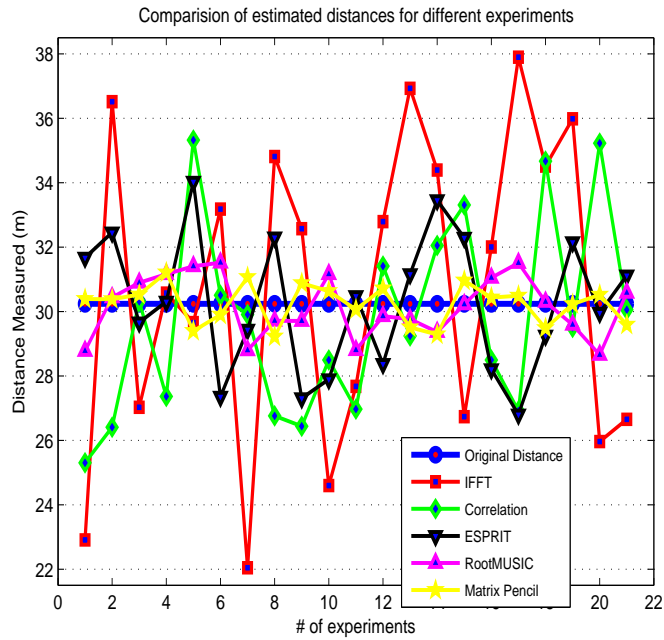
Figure 5.18: Performance for distance estimation experiments
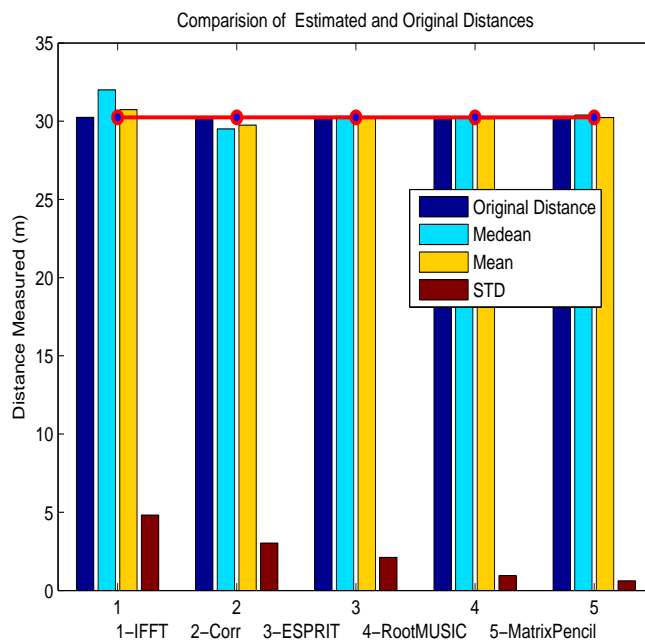
Figure 5.19: Mean, Median and Standard Deviation of the experiments

the tens of meters (m) of that, for the lower bandwidth systems (khz). Again it is worth to notice that the MP algorithm got most accurate estimates than the ESPRIT and Root-MUSIC in all the time resolutions. Fig. 5.21 shows that increasing the time resolution, increases the DME and the conventional algorithms fail to estimate the distance beyond 50 nsec. Above this level DME increases drastically, however, super resolution algorithms also got increment in DME but it is in the range of tens of meters, even in very high time resolution systems.
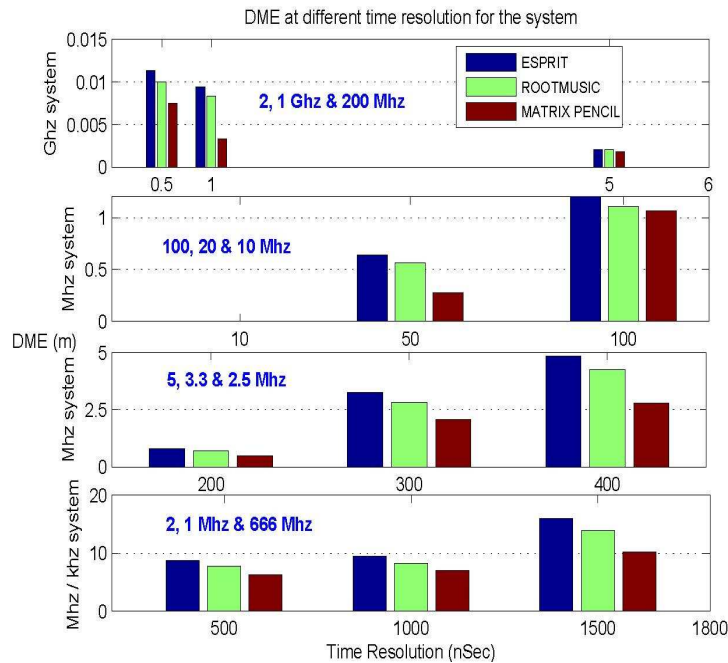
Figure 5.20: DME comparisons for different bandwidth of the systems

5.5.2 The Effects of Increasing the Number of Carriers

Analysis results for the effects of increasing the number of carriers on the OFDM/SC-DFE system are shown in Fig. 5.22. It can be noticed that the MP1 algorithm estimates the DME in the range of 0.8 m to 0.3 m for 32 to 64 carriers, while the other two counterparts get more reduced DME. However, when the number of carriers are increased to the higher order, the reduction in DME is increased by MP1 algorithm, which approaches to zero when we increase the number of carriers beyond 1024.

5.5.3 The Effects of Varying SNR

The SNR analysis is presented by Figs. 5.23 and 5.24 for two different resolution systems of 0 and 22.5 m separation respectively. By observing the Fig. 5.23, we can state that all algorithms, including the conventional ones, tend to reduce DME from
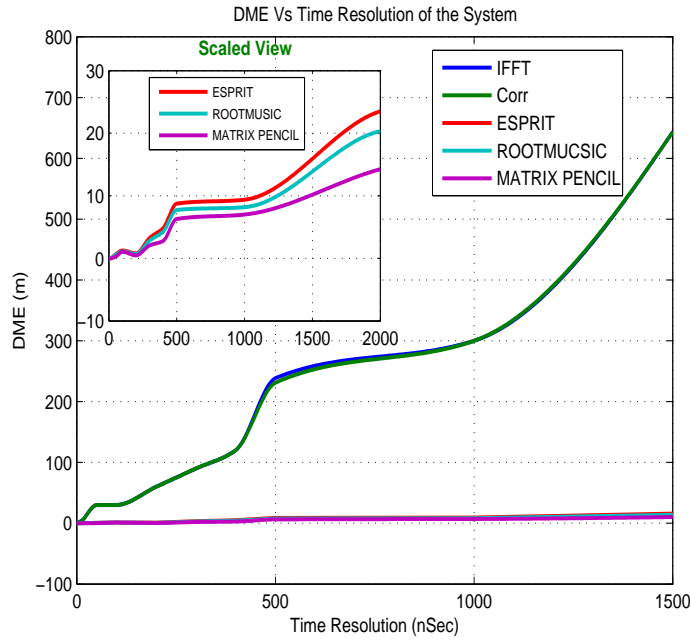
Figure 5.21: Time resolution analysis for super resolution algorithms
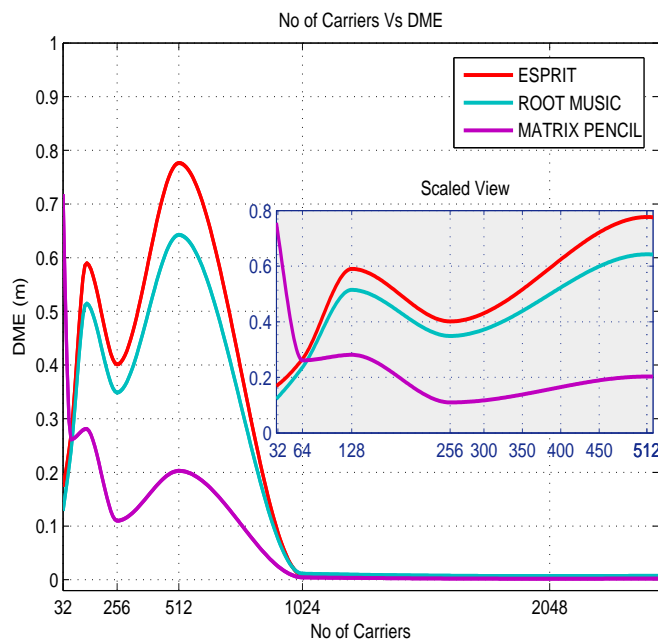
Figure 5.22: Effects of increasing number of carrierson DME

1 m to 0.2 m, as we approach the higher SNR values. Furthermore, we can say that the MP1 algorithm minimizes the DME at the optimal level amongst all. A similar trend can be observed from Fig. 5.24 with the DME reduction upto 0.001 m for all the super resolution algorithms. In order to compare these results with the conventional algorithms, we notice that in both situations the conventional algorithms got DME of 22m and 17m respectively, which is unacceptable for the indoor positioning systems. Thereby super resolution algorithms perform incredibly well by estimating the accurate distances in this situation.
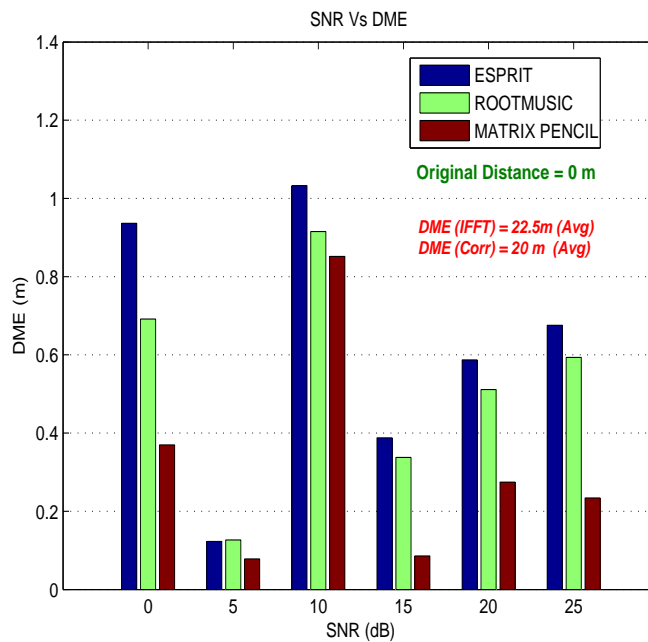
Figure 5.23: SNR analysis for DME for non delayed signal

5.6 Analysis for the WP2

In WP2 all the data sets were analyzed in order to improve the efficiency and accuracy of the previously used algorithms. Two initial estimation results using MP1 algorithm are shown in Fig. 5.25. The first result in Fig. 5.25 shows that the initial estimation using MP1 algorithm is quite oscillating and the position estimates are deviated by few meters while the second one estimates the results with a better precision after improving the MP1 algorithm.

5.6.1 Estimation and Gradual MP Algorithm Improvements

It is noticed that the MP1 algorithm performed better by implementing EIG criteria however the results oscillate to occur from the actual positions, on the other hand
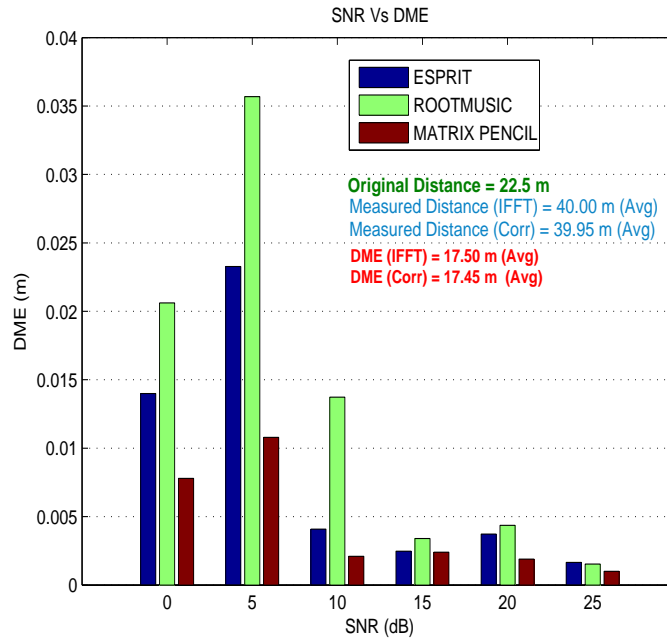
Figure 5.24: SNR analysis for DME for the delayed signal

MDL criteria got more accurate estimation. The use of Matlab Executable (MEX) files merely enables the algorithm to be implemented in positioning devices with less processing resources and less time hungry processes. In order to increase the efficiency, the algorithms is first compiled to the MEX file format and then to the p-code format. The adjusted algorithms got execution efficiency of 21235.27 mSec in case of the MDL and 1339.045 mSec in case of the EIG than their respective counterparts. Later on a large error in TDOA delay is introduced due to noisy recordings, but the MP1 algorithm was still able to estimate the position of the receiver with little deviation in the XY coordinates. In order to resolve this large error we have applied different strategies which initially could not resolve the problem. However, the later strategies reduced the error in estimation to a reasonable range. Each step helped us improve the MP1 algorithm in order to reduce the error to the optimal level. The gradual steps taken to improve the MP1 algorithm along with the results of those steps and their analysis for the further steps are summarized in table 5.2. The analysis steps are applied to update the MP1 algorithm using the data sets listed in table 4.6. Table 5.5 summarizes the analysis results of these packages. It also specifies the purpose of recording each data set, the algorithm applied on that, the findings from the results achieved by the algorithm and the further steps taken after analysis of these results in order to update the accuracy and/or efficiency of the MP1 algorithm. We can regard table 5.5 as a bird's eye view of the work carried out under WP2.
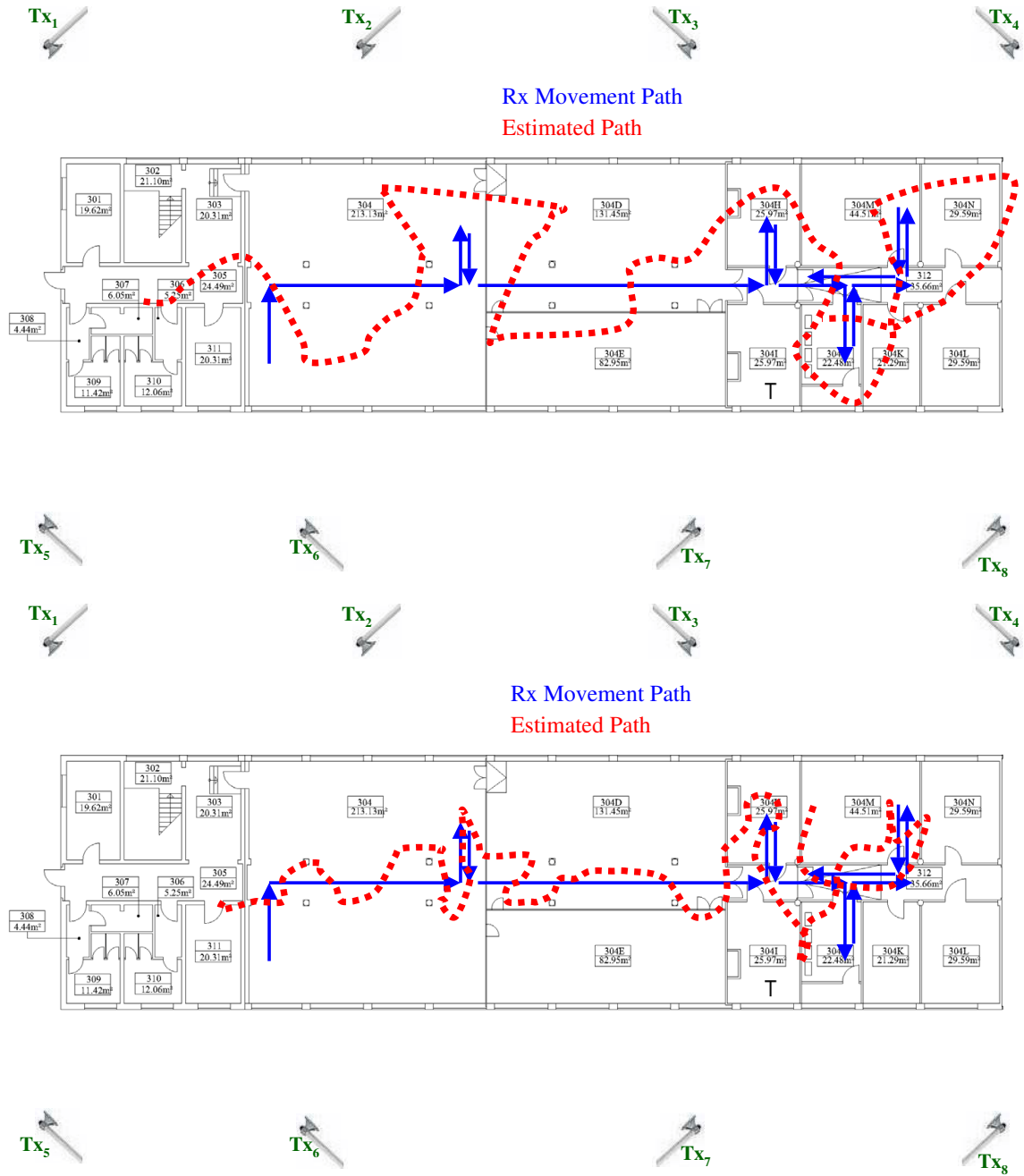
Figure 5.25: Two early estimations of the moving object

In the next section we present the results for each of the data packages listed in table 4.6 along with the analysis of each result and further steps taken for improvement of the MP1 algorithm.

Table 5.2: Strategies Used to Resolve the Unexpected Large Error

Strategy	Result	Analysis/Comments
Taking the absolute of the estimated coefficient	Some Large errors reduced but more errors introduced at other points or enhanced	Not acceptable solution
Changing the window size of moving average	Increasing upto 1/4th of the total points increased the accuracy	Acceptable with limitation
Putting limit on the maximum no of paths	Most errors were reduced	Seems good solution but may include unnecessary paths
Introducing variants of the MP algorithm	Some variants got noticeable reduction in the estimation error	MP3-MDL and MP3-EIG got most accurate estimation
Applying automatic estimation in all the MP variants	Some variants got good results for typical data estimation error	MA1 & MA3 got similar improvements as was achieved by MP1-MDL and MP3-MDL

5.6.2 S41

For the package S41, MP1-MDL is found to be the best estimation algorithm. It achieved the optimal values in order to estimate the position of a particular static receiver point using 4 transmit antennas. Table 5.3 shows the sample values of the MP1 algorithm applied to estimate the position of a point whose coordinates are $X = -10.854$ and $X = 11.784$. Mean and median values of the estimated positions are also shown in table 5.3. It is very evident that error is $e_X = 0.206m$, $e_Y = 0.534m$.

5.6.3 S81

The package S81 is recorded using 8 transmit antennas, Fig. 5.26 shows the difference between actual and estimated positions for five points in a typical noisy region. We have applied the moving average algorithm to reduce the error in the estimation. The window size of 20 is chosen to average the estimated values. Fig. 5.28 shows the estimated path in red and the receiver points in green. The left half of the figure shows the results achieved by the MP1-MDL and the right one by the MP1-EIG algorithm. By a close examination of the figure, one can resolve that the MP1-MDL acquired

Table 5.3: Estimation results for a single receiver point position

	X	Y		Diff-12	Diff-13	Diff-14	Diff-23	Diff-24	Diff-34
	-11.19	11.31		-2.63	3.74	11.1	6.37	13.73	7.36
	-11.12	11.26		-2.34	3.67	11.14	6.01	13.47	7.46
	-11.06	11.27		-2.32	3.58	11.07	5.9	13.39	7.49
	-11.06	11.17		-2.24	3.75	11.06	5.99	13.29	7.31
	-11.1	11.31		-2.38	3.56	11.11	5.94	13.49	7.55
	-11.01	11.19		-2.3	3.69	10.94	5.99	13.24	7.25
	-11.08	11.17		-2.23	3.78	11.09	6	13.32	7.32
	-11.1	11.21		-2.27	3.73	11.11	6	13.38	7.38
	-11.08	11.21		-2.24	3.7	11.11	5.94	13.35	7.41
	-11.05	11.23		-2.24	3.63	11.06	5.87	13.3	7.43
	-11.02	11.25		-2.25	3.55	11.04	5.8	13.29	7.49
	-11.02	11.25		-2.26	3.57	11.03	5.83	13.29	7.46
	-11.05	11.29		-2.29	3.52	11.08	5.82	13.38	7.56
	-11.05	11.31		-2.31	3.48	11.08	5.8	13.39	7.6
	-11.05	11.27		-2.27	3.56	11.07	5.84	13.35	7.51
	-11.05	11.28		-2.29	3.54	11.07	5.83	13.36	7.53
	-11.05	11.26		-2.26	3.57	11.08	5.83	13.34	7.51
	-11.03	11.26		-2.29	3.56	11.03	5.85	13.32	7.46
	-11.03	11.28		-2.28	3.53	11.05	5.81	13.33	7.52
	-11.03	11.26		-2.28	3.55	11.03	5.83	13.31	7.48
	-11.03	11.24		-2.25	3.59	11.05	5.83	13.29	7.46
MEAN	-11.06	11.25		-2.3	3.61	11.07	5.91	13.36	7.45
MEDIAN	-11.05	11.26		-2.28	3.57	11.07	5.85	13.34	7.46

closer estimates than the MP-EIG. However, the execution time for the MP1-EIG is faster than than that of the MP1-MDL. Therefore, both algorithms are utilized for further estimation.
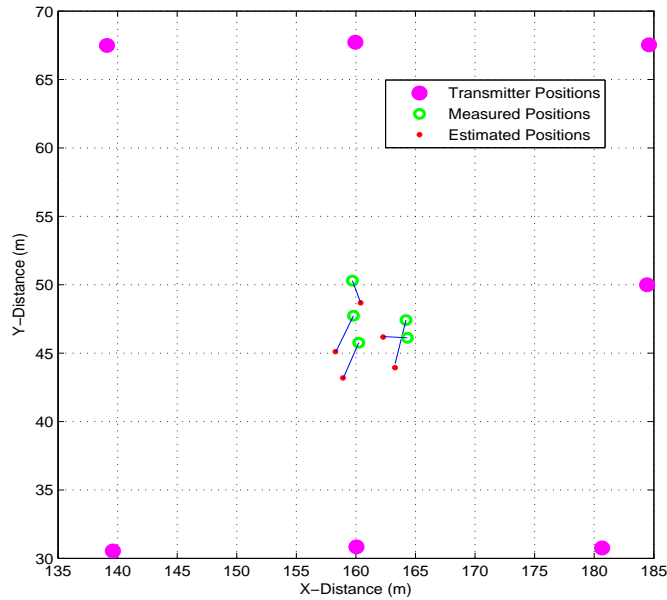
Figure 5.26: The actual and measured distance for 5 static points in noisy region

5.6.4 S82

The package S82 is used to improve the efficiency of MP1 algorithms. In order to increase efficiency, the algorithms are optimized in different levels which are enlisted as following;

- **Optimized1**   Some redundant statements removed from the code

- **Optimized2**   Sub functions like MDL, EIG are compiled separately

- **MEX**   Algorithms are converted to MEX format

- **PCODE**   PCode executable generated for the algorithms

Using conventions described above, table 5.4 compares the results of different levels of the optimizations. MP1-EIG achieved noticeable supremacy over the MP1-MDL algorithm in execution time.
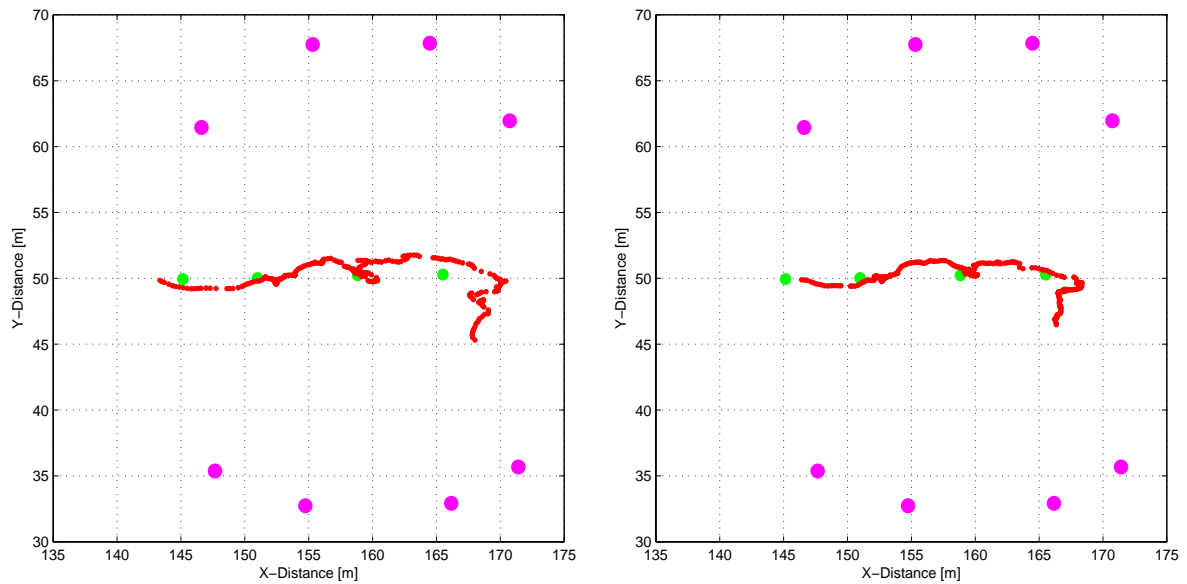
Figure 5.27: The S81 results for a.) MP1-MDL(left) and b.) MP1-EIG(right)

Table 5.4: Optimization of the MP Algorithms

Algorithm	No of files processed	Processing Time (sec)				
		Un-optimized	Optimzed1	Optimzed2	MEX	Pcode
MP1-MDL	100	67.32301	56.826	42.9074	26.1359	13.67
MP1-EIG	100	64.8535	52.456	38.567	21.3301	9.58

5.6.5   S83

The package S83 is used to improve model order of the MP1 algorithm, after achieving efficiency in the algorithm. The modified approach termed as (MDX) is used as a model order. The purpose of applying MDX is to estimate the actual number of paths, separating the noise values from actual signal contributions. The MDX helped in reducing the error caused by the MP1-MDL and MP1-EIG algorithms at the cost of drawback in the efficiency. It can be shown by Fig. 5.28 that the estimation errors are increased in locating the path of the receiver positions. In Fig. 5.28 the left half of the figure shows the estimation for the MP1-MDL and the right half of that for the MP1-EIG algorithm.
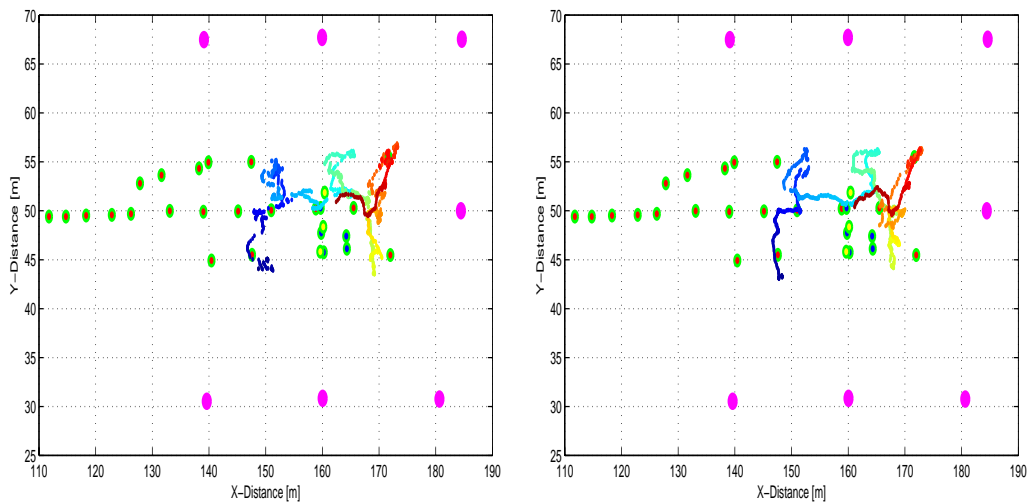
Figure 5.28: Deviated estimation in S83 a.) MP1-MDL(left) and b.) MP1-EIG(right)

5.7   Tracking the Moving Object Positions

The further analysis constitute the packages involving the dynamic recordings. The receiver object is moved dynamically to a locus of path and estimations of the moving object positions are computed. This provides analysis for tracking of the moving object positions.

5.7.1   Strategies to Improve the MP1 Algorithm Accuracy

The package D82-GF is reserved for the dynamic recordings of the data at the ground floor of the building. Initially all four variants of MP1 algorithm are applied i.e. MP1-AIC, MP1-EIG, MP1-MDL and MP1-MDX. Most of the estimation points are close to the actual positions but in some noisy recorded areas TDOA delta difference of the

typical antennas are enormously high. It is assumed that these errors are caused by
the recordings of the data near some metallic objects which deviated the coefficient
of path estimation largely. In order to resolve the large errors some strategies are
applied adaptively. At the initial stages the coefficients are considered to be small
enough such that the noise values are higher than the signal values, therefore the
absolute values of the coefficients are considered for the delay estimation. This re-
duced the large errors to a reasonable range but for some other points more errors are
increased. Another applied strategy is to change the window size of moving average
which also helped reducing the large errors but it is only considerable upto 1/4th of
the data. If it is increased further the errors increase again, therefore, this solution is
acceptable with the window size limited to 1/4th of the data . The next strategy is
to put the limit on maximum number of paths which also reduced most of the errors.
The drawback with this strategy is that it may include the unnecessary paths when
the limit is considerably increased. The last two effective strategies are to introduce
further variants of the MP1 algorithm and that of the model order criteria. Initially
two variants are developed as MP2 and MP3 which use forward-backward averag-
ing [182] and Hankel matrix method [84] for de-noising the corrupted signal. Later
on the automatic model order estimation is applied to MP1, MP2 and MP3 getting
the new variants as MA1, MA2 and MA3, where suffix A stands for an automatic es-
timation. Forward-backward averaging takes the enhanced noise progression through
consequent signal samples and gives poor estimation results with the MDL and EIG
criteria. The Hankel matrix method with MDL gives the most accurate estimation.
Table 5.2 summarizes these strategies. The further subsequent sections discuss the
results for the dynamic data for tracking the positions of the moving object.

5.7.2   D82-GF

D82-GF is the data set recorded for tracking the dynamic movement of the receiver
at ground floor of the building under study, detailed in chapter 5. The path of
the movement is shown in Figs. 4.17 and 4.18. Fig. 5.29 shows the estimation
results. The figure is divided in 9 portions. The top three portion of the figure show
the estimation results for the MDL, EIG and Automatic (MA) variants of the MP1
algorithm respectively. The middle and bottom six portions of the figure show the
estimation results for the MP2 and MP3 versions of the algorithm. It can be noticed
that the accurate estimation is achieved by the MP1-EIG and MP3-EIG while MP2-
EIG and MP2-MDL are giving more deviated results, which shows that the MP2
algorithm prone to noise with MDL and EIG criteria, however, it works fine with
the automatic estimation (MA2). MDL versions of MP1 & MP3 also estimate the
position with a minor deviations.
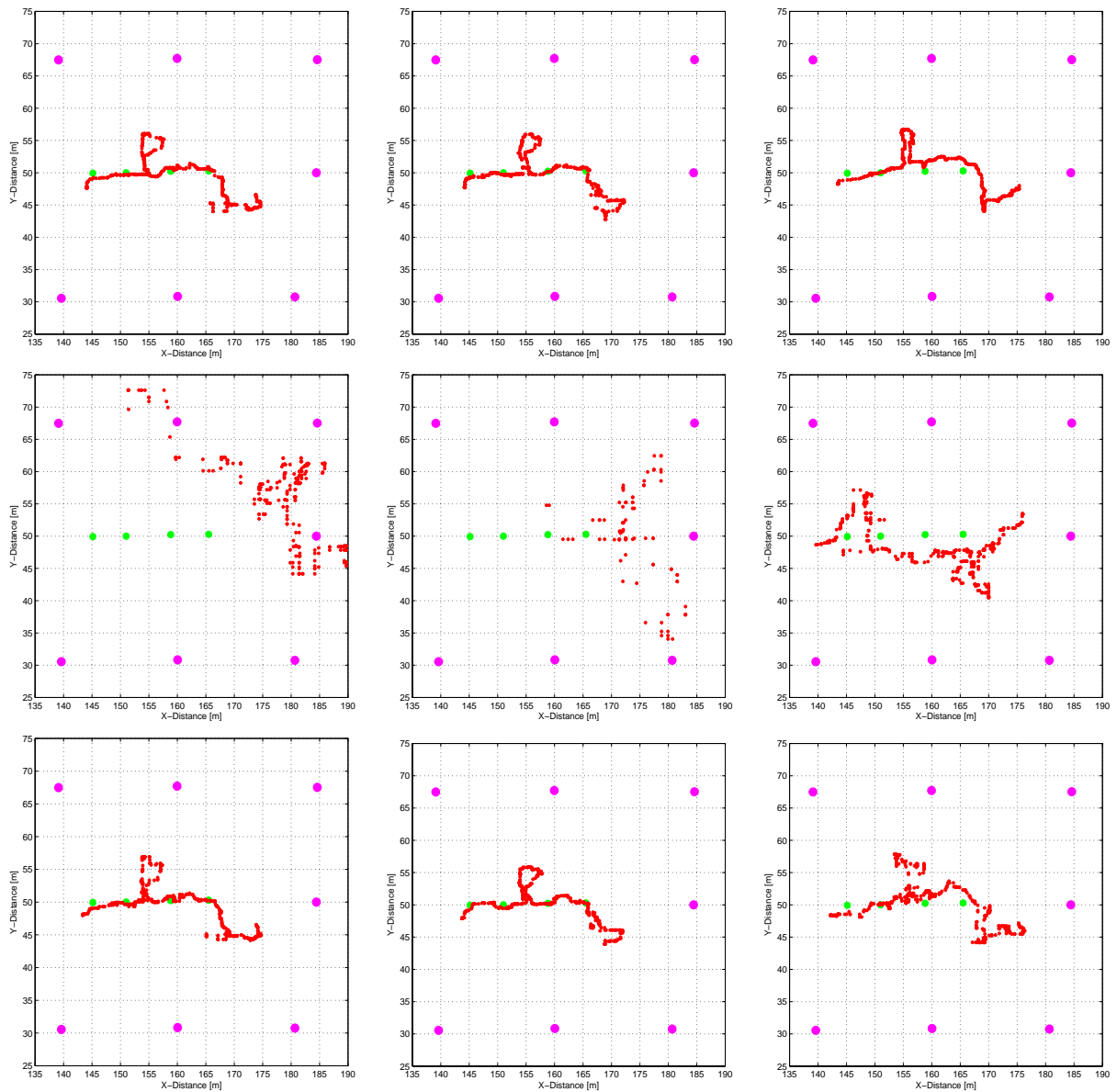
Figure 5.29: The D82-GF results for a.) MP1-MDL(top-left), b.) MP1-EIG(top-center) c.) MA1(top-right), d.) MP2-MDL(mid-left), e.) MP2-EIG(mid-center) f. MA2(mid-right), g.) MP3-MDL(bottom-left), h.) MP3-EIG(bottom-center) and i.) MA3(bottom-right)

5.7.3   D83-1F and D83-GF2

D83-1F and D83-GF2 are the dynamic data recordings for tracking the positions of the moving receiver. D83-1F data set is recorded at first floor of the building and D83-GF2 is recorded at the ground floor of the building. Fig. 5.30 shows the results obtained by all five model order variants (AIC, EIG, MDL, MDL and MA) of the MP1 algorithm. Similar results are shown in Figs. 5.31 and 5.32 for the MP2 and MP3 variants of the algorithm. Each figure contains five sub-figures related to AIC, EIG, MDL, MDX and MA variants of the algorithm respectively. Similar trends are shown in all these figures as we noticed for the last package. The data package D83-FG2 is for the repeated recordings on the ground floor. It has the same estimation results but with some errors in the estimation. It seems that the direction of movement is changed in this package and some more metallic objects lie in the path of the recordings. Figs. 5.33, 5.34 and 5.35 contain the estimation results for the package D83-GF2 using MP1, MP2 and MP3 variants. To summarize the estimation results of packages D83-1F and D83-GF2, we can state that MA1-EIG & MA3-EIG are found to be the efficient ones and MP1-MDL & MP3-MDL are accurate enough to locate the receiver positions, while MP2 variants are only feasible with the automatic estimation criteria.

5.8   Chapter Summary

We have simulated super resolution algorithms along with the conventional ones in order to estimate the distance and TOA/TDOA for the indoor positioning applications. Two different scenarios are tested . For each scenario multiple sets of data are recorded, each with 21 different recordings. For the single antenna scenario the super resolution algorithms like ESPRIT and MP1 the give optimal performance compared to the conventional algorithms. In most of the cases MP1 archived the estimation distance equal to the original distance, however ESPRIT got $1m$ to $3m$ deviation which is increased further by $1m$ to $2m$ with the Root-MUSIC algorithm. In two antennas scenario the Root-MUSIC and the MP1 algorithm performed better than the other algorithms for distance estimation. However, accuracies of all the algorithms are bad as compared to the single antenna scenario, because we have reference channel available in the single antenna case. In all cases MP1 is concluded as the best estimation technique.

In order to estimate distance and TDOA for the indoor positioning applications we have used OFDM/SC-DFE transceiver in our simulations. Optimal reduction in DME is achieved. Three super resolution algorithms i.e. ESPRIT, Root-MUSIC and MP are compared for the DME estimations. The MDL criteria is applied for these
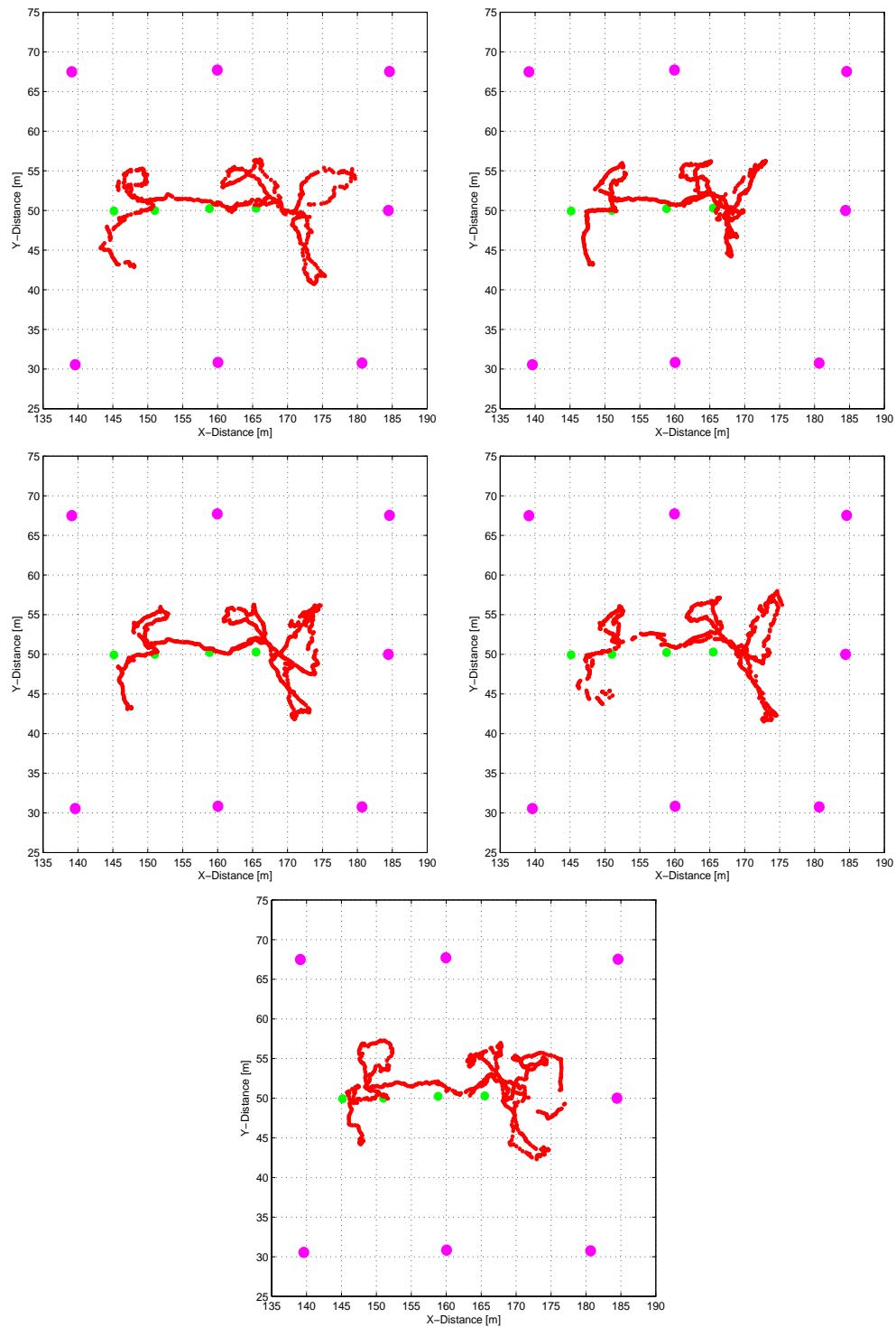
Figure 5.30: The D83-1F results for a.) MP1-AIC(top-left), b.) MP1-EIG(top-right), c.) MP1-MDL(mid-left), d.) MP1-MDX(mid-right), e.) MA1(bottom)
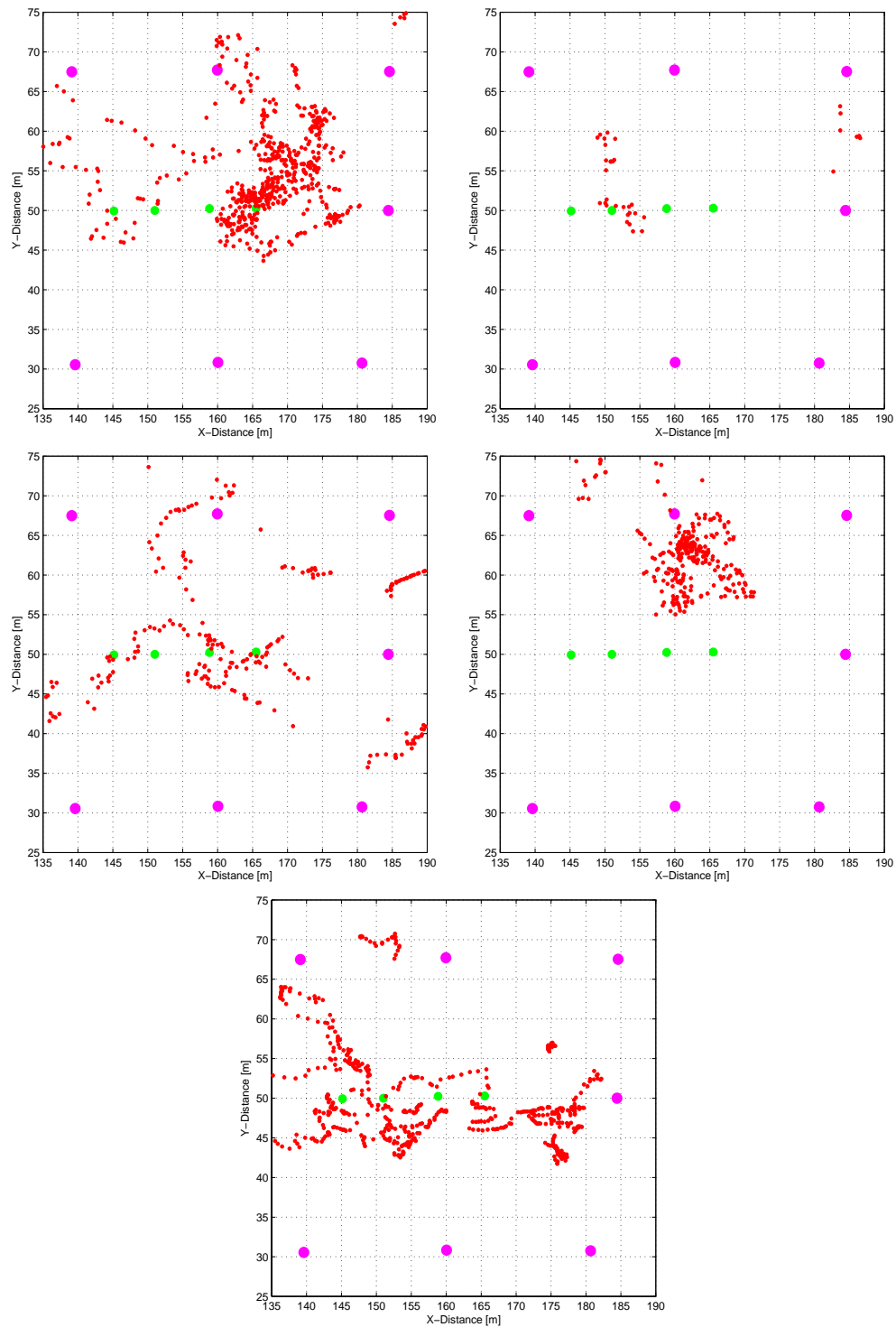
Figure 5.31: The D83-1F results for a.) MP2-AIC(top-left), b.) MP2-EIG(top-right), c.) MP2-MDL(mid-left), d.) MP2-MDX(mid-right) and e.) MA2(bottom)
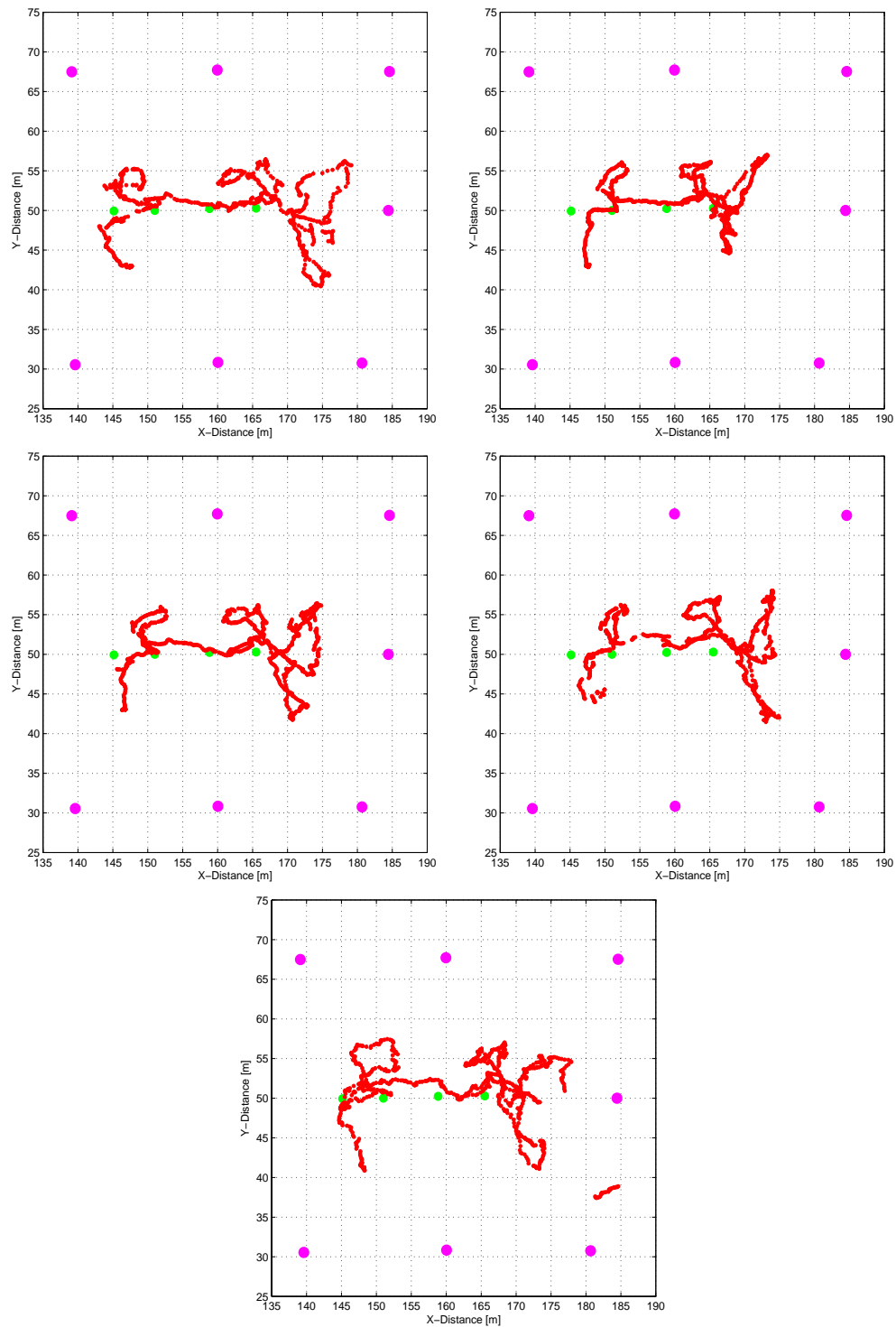
Figure 5.32: The D83-1F results for a.) MP3-AIC(top-left), b.) MP3-EIG(top-right), c.) MP3-MDL(mid-left), d.) MP3-MDX(mid-right) and e.) MA3(bottom)
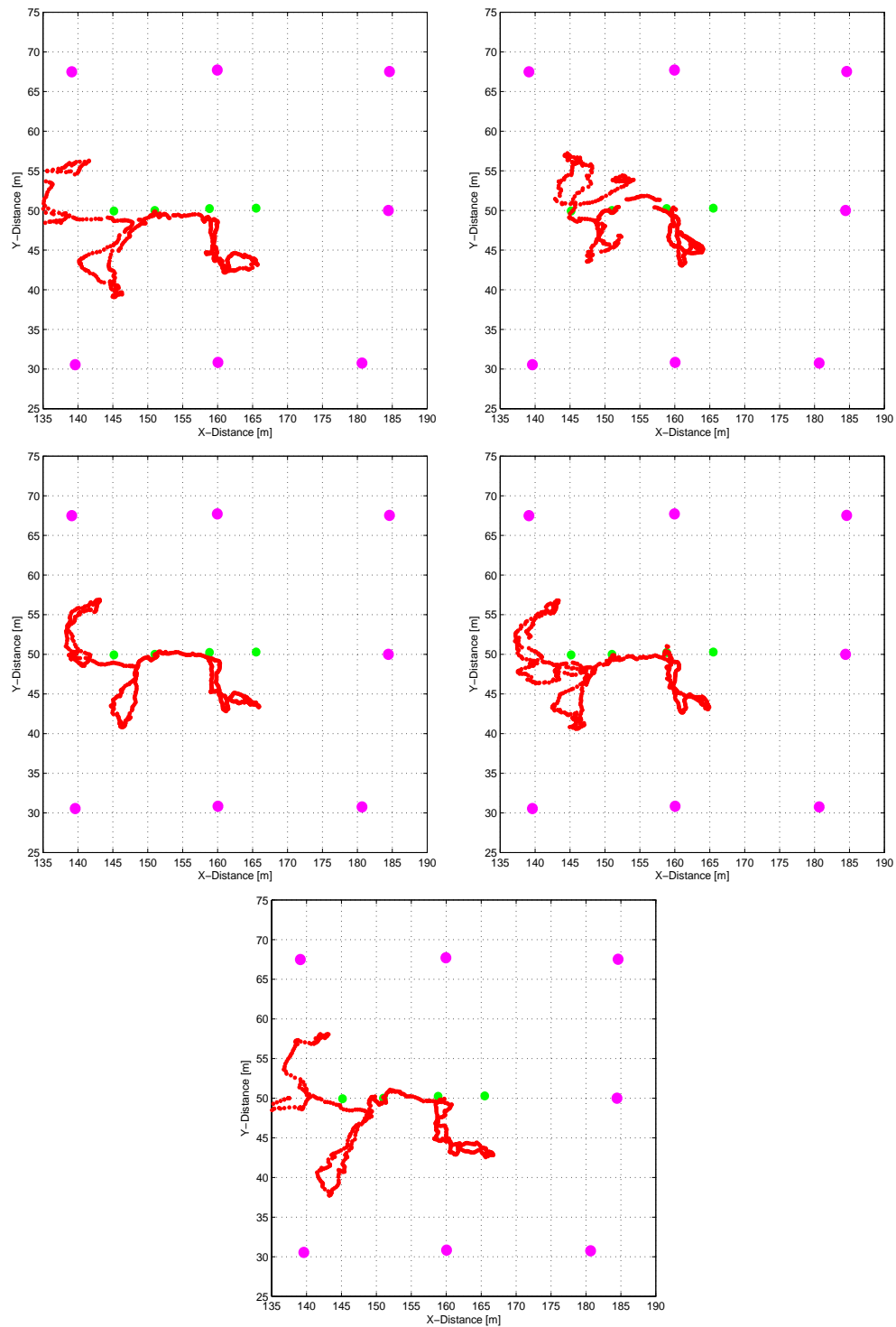
Figure 5.33: The D83-GF2 results for a.) MP1-AIC(top-left), b.) MP1-EIG(top-right), c.) MP1-MDL(mid-left), d.) MP1-MDX(mid-right) and e.) MA1(bottom)
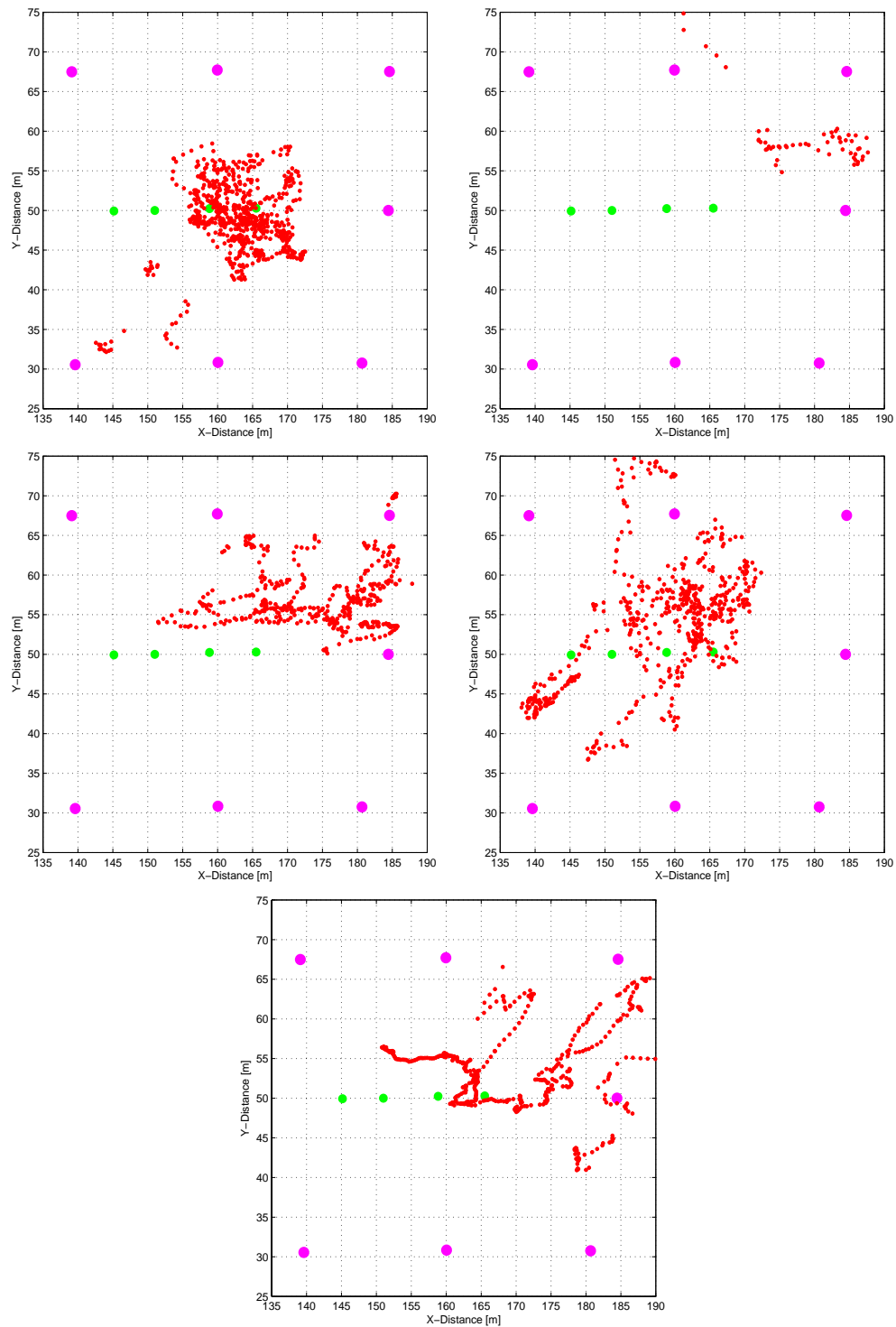
Figure 5.34: The D83-GF2 results for a.) MP2-AIC(top-left), b.) MP2-EIG(top-right), c.) MP2-MDL(mid-left), d.) MP2-MDX(mid-right) and e.) MA2(bottom)
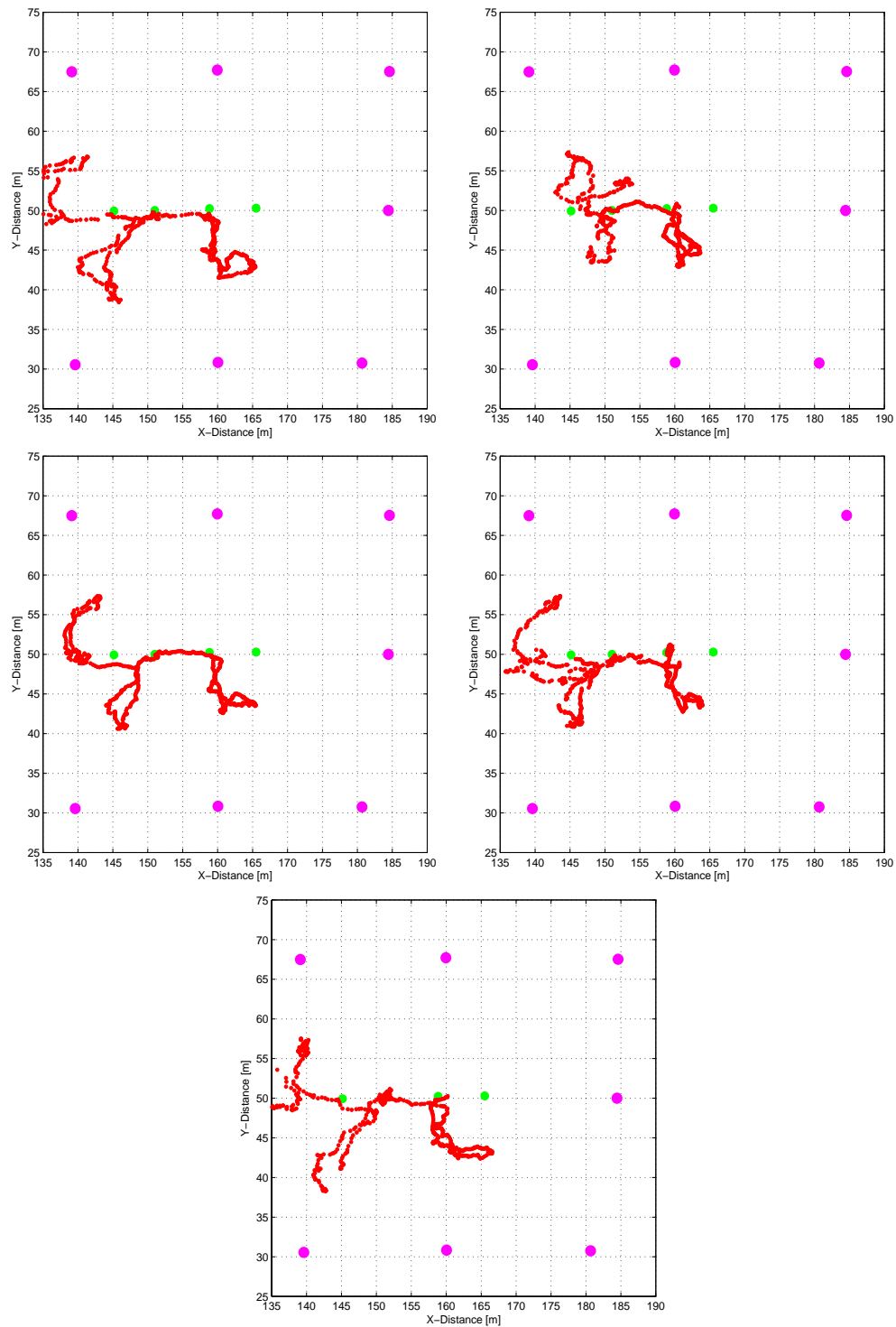
Figure 5.35: The D83-GF2 results for a.) MP3-AIC(top-left), b.) MP3-EIG(top-right), c.) MP3-MDL(mid-left), d.) MP3-MDX(mid-right) and e.) MA3(bottom)

algorithms to optimize the performance. An analysis of the DME is presented for varying SNR, variable time resolutions and multiple number of carriers. The DME reduction approaching to zero is achieved by the MP algorithm using our scheme.

The conventional algorithms fail to estimate the distance beyond 50 nsec and above this level DME increases drastically, which is unacceptable for indoor positioning applications. However, the super resolution algorithms also got increment in DME with increasing time resolution, but it is in the range of tens of meters, even in very high time resolution systems. The MP algorithm estimates DME in range of 0.8 m to 0.3 m for 32 to 64 number of carriers, while the other two counterparts show more reduced DME. However, when the number of carriers are increased to the higher order reduction in DME is more improved by the MP, which approaches to zero, when we increase the number of carriers beyond 1024. For the higher SNR values DME ranges from 1 m to 0.2 m. For the delayed signal DME reduction is achieved upto 0.001 m for all the super resolution algorithms. In all cases the MP is concluded as the optimal estimation algorithm.

Furthermore, different MP algorithm variants are used in order to reduce the error in estimation and to obtain accurate position of the receiver points. The complete estimation result analysis is summarized in table 5.5.

The generalized MP function in MP1, forward-backward averaging in MP2 and Hankel matrix method in MP3, are used to nullify progressing noise from the corrupted signal. AIC, EIG, MDL and MDX, are used as the model order criteria to separate the signal and the noise subspaces and then an automatic estimation criteria is introduced. The combination of all three MP variants with five model order criteria are used to compare the performance in different scenarios. It is observed that the accurate estimation is achieved by MP1-EIG and MP3-EIG while MP2-EIG and MP2-MDL achieved more deviated results, which shows that the MP2 algorithm is prone to noise with MDL and EIG criteria, however, it works fine with automatic estimation MA2. The MDL versions of MP1 & MP3 also estimate the position with a minor deviation. Some optimization steps are also applied to increase the efficiency of the MP algorithm variants and it is found that the EIG variants of the MP algorithms produced the fastest estimation results. Forward-backward averaging enhances the noise progression through consequent signal samples and gives poor estimation results with MDL and EIG criteria, the automatic estimation improves its performance.

Table 5.5: Summary of the Estimation Results Analysis in WP2

Package Name	Purpose	Algorithms Applied	Result	Comments Additional Information
S41	Validating antenna estimation and finding optimal algorithms	MP1-EIG, MP1-MDL, ESP,MUS	MP1-EIG and MP1-MDL are found to be optimal algorithms.	MP1-EIG & MP1-MDL emphasized for further estimation.
S81	Checking performance with moving average of window size =25 points	MP-EIG& MP1-MDL	Averaging helped in improving estimation accuracy.	Moving Average algorithm is utilized in further estimations.
S81	Validating 8 Tx estimation in stairs and different floors	MP1-EIG& MP1-MDL	Static measurement provided good agreement of measurement with estimation.	Efficiency is increased by few seconds for different optimization. Compiled algorithms script increased the efficiency of the MP1-EIG & MP1-MDL algorithms.
S82	Validating 8 Tx estimation in stairs and different floors	MP1-EIG& MP1-MDL	Static measurement provided good agreement of measurement with estimation. Optimization techniques are applied to reduce the execution time.	Efficiency is increased by few seconds for different optimization. Compiled algorithms script increased the efficiency of the MP1-EIG & MP1-MDL algorithms.
S81	Testing new model order Criteria	MP1-MDL MP1-MDX	Both criterion gave improvements in previous results at the cost of efficiency	In order to get efficient results MDL and EIG criteria sre carried out in parallel.
D82	Estimation for ground floor	MP1-MDL MP1-AIC MP1-EIG & MP1-MDX	Some Big Errors occurred in TDOA estimation. (Details in **table 5.2**)	1. Abs values applied, solution applied initially. 2. Improved techniques are applied in MP algorithm which helped in reducing the error. See **table 5.2**
D83-1F	Validating the MP2 & P3 algorithms	MA1, MA2 & MA3 variants are introduced for the preceding MP algorithms.	Some errors are high for MP2 but overcomed by MA variants	On having errors for MP2 variants the automatic estimation is applied to MP algorithms.
D83-GF2	Validating the MP2 & MP3 algorithms	All MP variants	Optimized results are obtained.	MA1-EIG &MA3-EIG are the efficient ones and MP1-MDL &MP3-MDL are the accurate ones.

Chapter 6

Conclusion and Future Work

6.1 Conclusion

The field of indoor positioning applications using concrete signal design for the forth-coming wireless communication systems is of great interest for research. Despite considerable amount of research being carried out in this field, precise indoor positioning and tracking still remains a challenge. Multi-path fading, progressive noise, design and bandwidth considerations of the signal, unavailability of the direct path conditions and the Doppler's effect for the moving object are major issues associated with the positioning application.

We presented a detailed review of the existing positioning techniques. The multi-path channel models and their parameters are explored at initial levels in order to consider them while designing the signal transmission parameters for the indoor positioning system. The real channel measurements are taken from the data sets for the transmitted and the received signals at the typical indoor areas.

In order to compare and select the multi-carrier signal design for the positioning application, a survey of the previous comparisons in this domain is presented. For two alternative signal structures of OFDM and SCT, their structure design, coding effects, and the transceiver design are considered for the indoor positioning application. To use these signal structures a combined OFDM/SCT transceiver is designed. The block iterative DFE is implemented for SCT and is combined with CP and ZP techniques. Both variants of this SC-DFE are compared with SC-LE and with the similar variants of OFDM. The new block DFE structure iteratively improves itself and performs better as the number of iterations is increased. Comparison results for BER simulations, for both variants of the OFDM and the SCT with LE and DFE, verified the analytical transceiver model. The transceiver implementation has also been modified and tested by the coding block, which improved performance of the system.

Moreover, we have investigated distance estimation methods and considered the TDOA method to estimate the distance in a real indoor environment due to its accuracy amongst all counterpart methods. The estimation algorithms are applied at the CMWCE, University of Magdeburg. It is divided into two stages WP1 and WP2. In WP1, the traditional and the super resolution algorithms like ESPRIT Root-MUSIC and MP are implemented using the real data sets to distinguish and verify the performance of these algorithms. The best performance is achieved by the MP algorithm, which reduced the DME to less than 1 meter. The system consisted of two antennas only. The MDL and AIC are utilized as model order, to estimate the minimum points containing the signal components separating the noise components. In WP2, three variants of MP algorithm are tested and compared under different conditions. These variants used generalized pencil function in MP1, forward backward averaging method in MP2 and Hankel matrix method in MP3. The system is extended from four to seven antennas in WP2. In order to estimate the precise results three more model order criteria are used in WP2, which are EIG, MDX and Automatic model order selection.

A new scheme is also proposed which is based on two different antennas used to transmit the OFDM/SCT symbols, mapped to multiple carriers using WLAN system. Two multi-path faded signals corrupted by AWGN are received through the OFDM/SCT receiver and are added together. The scheme increased the accuracy of the distance estimation. An analysis for the effects of the varying Signal to Noise Ratio (SNR), bandwidth and the number of carriers on the DME estimation is also conducted. DME reduction approaching zero is achieved by the MP algorithm using our scheme. The conventional algorithms failed to estimate the distance beyond 50 nsec. The DME increased drastically above this level, which is unacceptable for the indoor positioning applications. However, the super resolution algorithms also increase DME with increasing the time resolution, but only in the range of tens of meters, even in very high time resolution systems. The MP algorithm estimated the DME in range of 0.8 m to 0.3 m for 32 to 64 carriers, while the other two counterparts get more reduced DME. However, when the number of carriers is increased, the reduction in the DME is more improved by the MP. This reduction approaches to zero, when we increased the number of carriers beyond 1024. For the higher SNR values DME ranged from 1 m to 0.2 m. For the delayed signal the DME reduction is achieved upto 0.001 m for all the super resolution algorithms. In all the cases MP is found to be the optimal estimation algorithm.

Furthermore, different MP algorithm variants are used in order to reduce the

errors in estimation and to obtain the accurate position of the receiver objects. The tracking of the moving object positions is also considered in the WP2. To have a quick look at the complete estimation result analysis of WP2, we reproduce table 5.5 as table 6.1, that summarizes the different analysis steps.

Table 6.1: **Summary of the Estimation Results Analysis** (reproduced table 5.5)

Package Name	Purpose	Algorithms Applied	Result	Comments Additional Information
S41	Validating antenna estimation and finding optimal algorithms	MP1-EIG, MP1-MDL, ESP,MUS	MP1-EIG and MP1-MDL are found to be optimal algorithms.	MP1-EIG & MP1-MDL emphasized for further estimation.
S81	Checking performance with moving average of window size =25 points	MP-EIG& MP1-MDL	Averaging helped in improving estimation accuracy.	Moving Average algorithm is utilized in further estimations.
S81	Validating 8 Tx estimation in stairs and different floors	MP1-EIG& MP1-MDL	Static measurement provided good agreement of measurement with estimation.	Efficiency is increased by few seconds for different optimization. Compiled algorithms script increased the efficiency of the MP1-EIG & MP1-MDL algorithms.
S82	Validating 8 Tx estimation in stairs and different floors	MP1-EIG& MP1-MDL	Static measurement provided good agreement of measurement with estimation. Optimization techniques are applied to reduce the execution time.	Efficiency is increased by few seconds for different optimization. Compiled algorithms script increased the efficiency of the MP1-EIG & MP1-MDL algorithms.
S81	Testing new model order Criteria	MP1-MDL MP1-MDX	Both criterion gave improvements in previous results at the cost of efficiency	In order to get efficient results MDL and EIG criteria are carried out in parallel.
D82	Estimation for ground floor	MP1-MDL MP1-AIC MP1-EIG & MP1-MDX	Some Big Errors occurred in TDOA estimation. (Details in **table 5.2**)	1. Abs values applied solution applied initially. 2. Improved techniques are applied in MP algorithm which helped in reducing the error. See **table 5.2**
D83-1F	Validating the MP2 & P3 algorithms	MA1, MA2 & MA3 variants are introduced for the preceding MP algorithms.	Some errors are high for MP2 but overcomed by MA variants	On having errors for MP2 variants the automatic estimation is applied to MP algorithms.
D83-GF2	Validating the MP2 & MP3 algorithms	All MP variants	Optimized results are obtained.	MA1-EIG &MA3-EIG are the efficient ones and MP1-MDL &MP3-MDL are the accurate ones.

The MP1, MP2 and MP3 algorithms are used to nullify progressing noise from the corrupted signal in WP2. AIC, EIG, MDL and MDX are used as model order criteria to separate signal and noise subspaces and then an automatic estimation criteria is introduced. The combination of all three MP variants with five model order criteria are used to compare the performance in different scenarios. It is observed that accurate estimation is achieved by MP1-EIG and MP3-EIG while MP2-EIG and MP2-MDL

are giving more deviated results, which shows that MP2 algorithm is prone to noise with MDL and EIG criteria. However, it works fine with the automatic estimation MA2. MDL versions of MP1 and MP3 also estimate the position with a minor deviation. Some optimization steps are also applied to increase the efficiency of variants of the MP algorithm. It is found that EIG variants of MP algorithms produced the fastest estimation results. Forward-backward averaging enhanced noise progression through consequent signal samples and gave poor estimation results with MDL and EIG criteria, but the automatic estimation improved its performance.

Our algorithms MP1-EIG and MP3-EIG achieved the closest estimation and capable of tracking the position of moving objects with efficiency and accuracy, hence are able to be embedded in any wireless positioning device.

6.2 Future Work

As stated earlier that the indoor positioning is a growing area having multiple research aspects. The major investigations can be diversified in the channel measurement and modeling, design of the location sensing techniques and positioning algorithms. These research aspects become challenging and interesting. Our current research work can be extended in many directions. One possible direction to extend this work is to use multi-carrier signal design with MIMO systems. Another extension of this work can be the utilization of different signal formats in order to improve the performance.

Studying and developing the DME models for different type of environments can also be another dimension of research. On the other hand better detection algorithms that decrease the overall DME can be used. Tracking and positioning multiple objects is another extension of this work that needs to be investigated. The design of neural network algorithms, which can be trained using different signal parameters to improve the positioning accuracy, is another dimension of the future research. The development of algorithms using non-direct path to estimate the distance and position in absence of the direct path can be another future research aspect. Three dimensional positioning can also be investigated in order to extend our tracking and positioning algorithms. Algorithms that reduce errors adaptively by dynamic tracking application need to be developed.

Appendix A

Positioning (2×1) System Solution using 2D-TDOA Metric

With reference to Fig. 4.2 the two intersecting circles with centers at the base stations and radii equal to distances from the target can be modeled by simple geometry as [73]

$$d_1^2 = x^2 + y^2 \tag{A.1}$$

$$d_2^2 = (x - x_2)^2 + y^2 \tag{A.2}$$

These solutions for the coordinates x and y of the mobile station target can be explicitly found as

$$x = \frac{(d_1^2 - d_2^2 + x_2^2)}{2 \cdot x_2} \tag{A.3}$$

and

$$y = \pm\sqrt{d_1^2 - x^2} \tag{A.4}$$

In the above equation, y has two possible solutions. This employs that the TOA method gives the correct location of the target in two dimensions without ambiguity if at least three fixed base stations are used in the measurement.

Appendix B

Positioning (4×1) System Solution using 2D-TDOA Metric

Improved location finding can be performed using four fixed terminals labeled as P1, P2, P3, and P4, with known coordinates, and a target terminal P0 whose location is to be determined as shown in Fig. B.1.
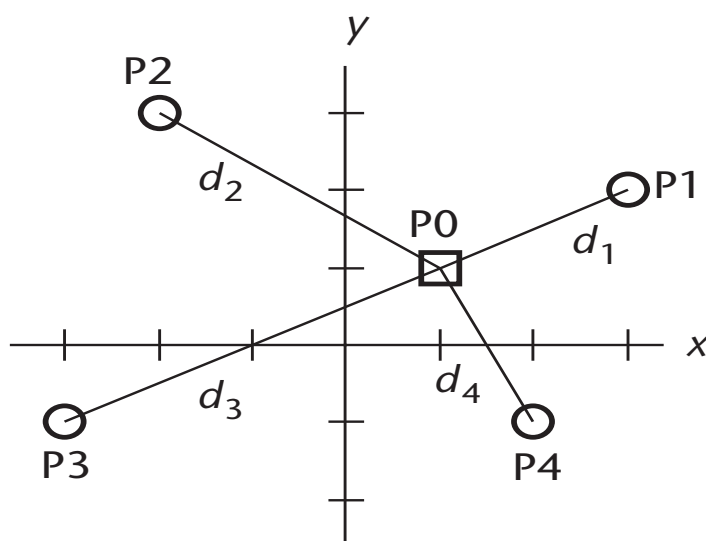
Figure B.1: Improved location finding using 4 terminals

If the true distances d_1 through d_4 could be measured exactly, the coordinates of P0 would be at the point of intersection of the circles formed with the fixed stations at the centers and the radii equal to the distances to the target [73]. However, the actual distance measurements, designated as D_1, D_2, D_3, and D_4, are not exact. The circles do not cross at one point, and it is necessary to define a criterion for deciding on the estimated location coordinates. The equations of the four circles defined by base station positions $P1(x_1, y_1)$ through $P4(x_4, y_4)$ and measured distances to target

$P0$, D_1 through D_4, are

$$(x_1 - x)^2 + (y_1 - y)^2 = D_1^2 \tag{B.1}$$

$$(x_2 - x)^2 + (y_2 - y)^2 = D_2^2 \tag{B.2}$$

$$(x_3 - x)^2 + (y_3 - y)^2 = D_3^2 \tag{B.3}$$

$$(x_4 - x)^2 + (y_4 - y)^2 = D_4^2 \tag{B.4}$$

Appendix C

The Least Squares Algorithm and its Alternative

The position of P0 can be estimated using a Least Squares (LS) error criterion. The position estimate has coordinates x_e , y_e that minimize the function F:

$$F = \sum_{i=1}^{M}(\sqrt{(x_i - x_e)^2 + (y_i - y_e)^2} - D_1)^2 \tag{C.1}$$

where $M = 4$ for the current case.

Coordinates x_e , y_e that minimize the nonlinear expression C.1, can be found by an iterative algorithm based on a Taylor series expansion or gradient descent [53, 11].

C.1   Alternative Method

LS may be time consuming and inconvenient to implement for many applications. An alternative approach, described below, gives a closed form solution to the estimation problem. It is described as follows.

Expand the factors on the left side of the equations of B.1-B.4 and subtract equations B.2, B.3, and B.4 from B.1, to give the following new set of M - 1 (3 in the current case), equations:

$$(x_1 - x_2)x + (y_1 - y_2)y_e = \frac{1}{2}(x_1^2 - x_2^2 + y_1^2 - y_2^2 + D_2^2 - D_1^2) \tag{C.2}$$

$$(x_1 - x_3)x + (y_1 - y_3)y_e = \frac{1}{2}(x_1^2 - x_3^2 + y_1^2 - y_3^2 + D_3^2 - D_1^2) \tag{C.3}$$

$$(x_1 - x_4)x + (y_1 - y_4)y_e = \frac{1}{2}(x_1^2 - x_4^2 + y_1^2 - y_4^2 + D_4^2 - D_1^2) \tag{C.4}$$

Equations C.2-C.4 are the overdetermined set of linear equations in x, y. It can be expressed in matrix form as

$$A \cdot P_e = b \tag{C.5}$$

$$A = \begin{bmatrix} x_1 - x_2 & y_1 - y_2 \\ x_1 - x_3 & y_1 - y_3 \\ x_1 - x_4 & y_1 - y_4 \end{bmatrix} \tag{C.6}$$

$$b = \frac{1}{2} \cdot \begin{bmatrix} x_1^2 - x_2^2 + y_1^2 - y_2^2 + D_2^2 - D_1 \\ x_1^2 - x_3^2 + y_1^2 - y_3^2 + D_3^2 - D_1 \\ x_1^2 - x_4^2 + y_1^2 - y_4^2 + D_4^2 - D_1 \end{bmatrix} \tag{C.7}$$

$$P_e = \begin{bmatrix} x_e \\ y_e \end{bmatrix} \tag{C.8}$$

The closed form LS solution to C.2-C.4 is [73, 18]:

$$P_e = \begin{bmatrix} x_e \\ y_e \end{bmatrix} = (A^T \cdot A)^T \cdot A^T \cdot b \tag{C.9}$$

While this development uses four base stations, it can be extended logically to a larger number and also to three dimensions, when the number of base stations, M, must be equal to four or more.

Appendix D

Formulation of the Hankel Matrix

The Hankel matrix, is a square matrix with constant (positive sloping) skew-diagonals. The Hankel matrix is closely related to the Toeplitz matrix. It is an upside-down Toeplitz matrix. The structure of the 5×5 matrix is given by D.1

$$J = \begin{bmatrix} a & b & c & d & e \\ b & c & d & e & f \\ c & d & e & f & g \\ d & e & f & g & h \\ e & f & g & h & i \end{bmatrix} \tag{D.1}$$

The generalized form of the Hankel matrix elements can formulated by eq. D.2

$$a_{i,j} = a_{i-1,j+1} \qquad \forall i,j \in \mathbb{Z} \tag{D.2}$$

Bibliography

[1] J. Bingham. *ADSL, VDSL and Multi Carrier Modulation*. New York: Wiley Interscience, 2000.

[2] C. Smith and J. Meyer. 3G wireless with 802.16 and 802.11. Etsi en 301 958 v1.1.1, (2002-03), Aug 2004.

[3] H. G. Myung et al. Single carrier FDMA for uplink wireless transmission. *IEEE Vehic. Tech. Mag.*, 1(3), Sep 2006.

[4] Nayef Alsindi. *Indoor Cooperative Localization for Ultra Wideband Wireless Sensor Networks*. PhD thesis, Electrical and Computer Engineering, Worcester Polytechnic Institute, April 2008.

[5] A. Kupper. *Location-Based Services: Fundamentals and Operation*. Wiley Interscience, New York, 2005.

[6] M. Kanaan, F.O. Akgul, B. Alavi, and K. Pahlavan. A study of the effects of reference point density on TOA-based UWBindoor positioning systems. In *IEEE 17th International Symposium on Personal, Indoor and Mobile Radio Communications*, pages 1 − 5, Helsinki, Sep 2006.

[7] K. Pahlavan and P. Krishnamurthy. *Principles of Wireless Networks A Unified Approach*. Prentice Hall, 2002.

[8] X. Li and K. Pahlavan. Super resolution TOA estimation with diversity for indoor geolocation. *IEEE Trans. Wireless Comm.*, 3(1):224–234, Jan 2004.

[9] R. Richard Badeau, G. David, and B. Ecole Nat. Adaptive ESPRIT algorithm based on the PAST subspace tracker. In *IEEE Int. Conf. on Acoustics, Speech, and Signal Processing, ICASSP '03*, volume 6, pages 229–232, Hong Kong, 6-10 April 2003.

[10] E. D. Kaplan. *Understanding GPS: Principles and Applications*. Artech House, 1996.

[11] J. Caffery and G. Stuber. Subscriber location in cdma cellular networks. *IEEE Trans. VT*, 47(2):406–416, May 1998.

[12] Glonass summary. Technical report, Space and Tech, Dec 2007.

[13] Satoshi KOGURE. Presentation at the 47th meeting of the civil global positioning system service interface committee (cgsic). Technical report, Bureau des Longitudes, 23, Quai Conti ,75006 Paris FRANCE, Sep 25 2002.

[14] ISRO Space. SATNAV industry meet 2006. ISRO Space India Newsletter, Apr - Sep 2006.

[15] G. Gibbons. China GNSS 101. Compass in the rearview mirror, Jan - Feb 2008.

[16] G.Gibbons. DORIS analysis working group meeting (AWG) of the international DORIS service, March 13-14 2008.

[17] B. Bandemer, H. Denks, A. Hornbostel, and A. Konovaltsev. Performance of acquisition methods for galileo SW receivers. *European journal of Navigation*, 4(3):17–29, Jul 2006.

[18] A. H. Sayed and N. R. Yousef. *'Wireless Location,"in Wiley Encyclopedia of Telecommunications.* John Wiley Sons, New York, 2003.

[19] L. D. Mech and S. M. Barber. A critique of wildlife radio-tracking and its use in national parks. Technical report, A Report to the U.S. National Park Service, Feb 2002.

[20] K. Pahlavan, P. Krishnamurthy, and J. Beneat. Wideband radio propagation modeling for indoor geolocation applications. *IEEE Commun. Mag.*, 36:60–65, Apr 1998.

[21] K. Pahlavan, X. Li, and J. Makela. Indoor geolocation science and technology. *IEEE Commun. Mag.*, 40:112–118, Feb 2002.

[22] L. Dumont, M. Fattouche, and G. Morrison. Super resolution of multipath channels in a spread spectrum location system. *Electron. Lett.*, 30:1583–1584, Sep 1994.

[23] P. C Chen. A non-line-of-sight error mitigation algorithm in location estimation. In *IEEE Wireless Communications and Networking Conference (WCNC 99)*, pages 316–320, New Orleans, LA, USA, Sep 1999.

[24] N. Alsindi, M. Heidari, and K. Pahlavan. Blockage identification in indoor UWB TOA-based ranging using multi band OFDM signals. In *IEEE Wireless Communications and Networking Conference*, Las Vegas, NV, Apr 2008.

[25] K. Pahlavan, F.O. Akgul, M. Heidari, A. Hatami, J.M. Elwell, and R.D. Tingley. Indoor geolocation in the absence of the direct path. *IEEE Wireless Communications Magazine*, 13(6):50–58, Dec 2006.

[26] R. J. Fontana and S. J Gunderson. Ultra-wideband precision asset location system. In *IEEE Conference on UWB Systems and Technolgies (UWBST)*, pages 147–150, Baltimore, MD, 2002.

[27] J. Y. Lee and S. Yoo. Large error performance of UWB ranging in multipath and multiuser environments. *IEEE Trans. on Microwave Theory and Techniques*, 54(4):1887–1895, Apr 2006.

[28] B. Alavi and K. Pahlavan. Bandwidth effect on distance error modeling for indoor geolocation. In *IEEE Proceeding on Personal, Indoor and Mobile Communications*, volume 3, pages 2198–2202, Sept 2003.

[29] N. Patwari, A.O. Hero, M. Perkins, N.S. Correal, and R.J. ODea. Relative location estimation in wireless sensor networks. *IEEE Trans. Signal Processing*, 51(8):2137–2148, Aug 2003.

[30] B. Denis and N. Daniele. NLOS ranging error mitigation in a distributed positioning algorithm for indoor UWB ad-hoc networks. In *3rd IEEE International Workshop on Wireless Ad-hoc Networks (IWWAN)*, pages 356–360, Oulu, Finland, Jun 2004.

[31] B. Alavi and K. Pahlavan. Analysis of undetected direct path in time of arrival based UWB indoor geolocation. In *IEEE Vehicular Technology Conference*, volume 4, pages 2627–2631, Dallas, TX, USA, Sep 2005.

[32] Z.N. Low, J.H. Cheong, C.L. Law, W.T. Ng, and Y.J. Lee. Pulse detection algorithm for line-of-sight (LOS) UWB ranging applications. *IEEE Antennas and Wireless Propagation Letters*, 4:63–67, 2005.

[33] Z. Tarique, W.Q. Malik, and D.J. Edwards. Bandwidth requirements for accurate detection of direct path in multipath environment. *IEE Electronic Letters*, 42(2):100–102, Jan 2006.

[34] Bardia Alavi. *Distance Measurement Error Modeling for Time-of-Arrival Based Indoor Geolocation*. PhD thesis, Department of Electrical and Communications Engineering,Worcester Polytechnic Institute, Apr 2006.

[35] C. Falsi, D. Dardari, L. Mucchi, and M.Z. Win. Time of arrival estimation for UWB localizers in realistic environments. *EURASIP journal on Applied Signal Processing*, 2006:1–13, 2006.

[36] Ahmad Hatami. *Application of Channel Modeling for Indoor Localization Using TOA and RSS*. PhD thesis, Worcester Polytechnic Institute, 2006.

[37] K. Hatami, A.; Pahlavan. Comparative statistical analysis of indoor positioning using empirical data and indoor radio channel models. In *3rd IEEE Consumer Communications and Networking Conference, CCNC 2006*, volume 2, pages 1018 – 1022, Helsinki, 8-10 Jan 2006.

[38] A. Hatami and K. Pahlavan. In-building intruder detection for wlan access. In *Position Location and Navigation Symposium, PLANS 2004*, 2004.

[39] Ahmad Hatami, Bardia Alavi, Kaveh Pahlavan, and Muzaffer Kanaan. A comparative performance evaluation of indoor geolocation technologies. *Interdisciplinary Information Sciences*, 12(2):133–146, 2006.

[40] A. Hatami and K. Pahlavan. Hybrid TOA-RSS based localization using neural networks. In *IEEE Global Telecommunications Conference, GLOBECOM '06*, pages 1–5, Dec 2006.

[41] E.G. Larsson. Cramer-rao bound analysis of distributed positioning in 144 sensor networks. *IEEE Signal Processing Letters*, 11(3):334–337, Mar 2004.

[42] C. Chang and A. Sahai. Cramer-rao-type bounds for localization. *EURASIP journal on Applied Signal Processing*, pages 1–13, 2006.

[43] N. Alsindi and K. Pahlavan. *Node Localization, Wireless Sensor Networks: A Networking Perspective.* Wiley Interscience - IEEE Press, 2008.

[44] N. Alsindi, B. Alavi, and K. Pahlavan. Empirical pathloss model for indoor geolocation using UWB measurements. *IEE Electronic Letters*, 43(7):370–372, March 2007.

[45] N.Alsindi, B.Alavi, and K.Pahlavan. Spatial characteristics of UWB TOA based ranging in indoor multipath environments. In *IEEE International Symposium on Personal Indoor and Mobile Radio Communications (PIMRC) 07*, pages 1 – 6, Athens, Greece, Sep 2007.

[46] N. Alsindi and K. Pahlavan. Cooperative localization bounds for indoor ultra wideband sensor networks. *EURASIP ASP special issue on Cooperative Localization in Wireless Ad Hoc and Sensor Networks*, pages 1–13, Apr 2008.

[47] D.B.Jourdan, D.Dardari, and M.Z.Win. Position error bound for UWB localization in dense cluttered environments. In *IEEE Intl Conf. on Commun. (ICC) 06*, volume 8, pages 3705–3710, Istanbul, Turkey, Jun 2006.

[48] D.B. Jourdan, D. Dardari, and M.Z. Win. Position error bound and localization accuracy outage in dense cluttered environments. In *IEEE International Conference on Ultra-Wideband*, pages 519–524, Boston, MA, USA, Sep 2006.

[49] N. Alsindi, K. Pahlavan, B. Alavi, and X. Li. A novel cooperative localization algorithm for indoor sensor networks. In *International Symposium on Personal Indoor and Mobile Radio Communications (PIMRC 06)*, pages 1 – 6, Helsinki, Finland, Sep 2006.

[50] N. Alsindi, K. Pahlavan, and B. Alavi. An error propagation aware algorithm for precise cooperative indoor localization. In *IEEE Military Communications Conference (MILCOM)*, pages 1 – 7, Washington D.C., Oct 2006.

[51] S. R. Saunders. *Antennas and propagation for wireless communication systems.* John Wiley and Sons, New York, 1999.

[52] R. Steele. *Mobile Radio Communications.* John Wiley and Sons, New York, 1992.

[53] H. Hashemi. The indoor radio propagation channel. *Proc. IEEE*, 81(4):941–968, 1993.

[54] G. Morrison and M. Fattouche. Super resolution modeling of the indoor radio propagation channel. *IEEE Trans. Veh. Technol.*, 47:649–657, May 1998.

[55] R. van Nee and R. Prasad. *OFDM for Wireless Multimedia Communications.* Artech House, 2000.

[56] J. G. Proakis. *Digital Communications.* McGraw Hill, New York, 1995.

[57] Lajos Hanzo, M. Mnster, B.J. Choi, and Thomas Keller. *OFDM and MCCDMA for Broadband Multi-User Communications, WLANs and Broadcasting.* Artech House, Sep 2003.

[58] C. Sgraja and J. Linder. Estimation of rapid time-variant channels for OFDM using wiener filtering. In *IEEE International Conference on Communications (ICC)*, volume 4, pages 2390–2395, Anchorage (AK),US, May 2003.

[59] B. Muquet, M. de Courville, and P. Duhame. Subspace based blind and semi blind channel estimation for OFDM systems. *IEEE Trans. Signal Process*, 50(7):3065–3073, Jul 2002.

[60] Jr. L.J. Cimini. Analysis and simulation of a digital mobile channel using orthogonal frequency division multiplexing. *IEEE Trans. Commun.*, 33(7):665–675, Jul 1985.

[61] S. B. Weinstein and P. M. Ebert. Data transmission by frequency division multiplexing using the discrete fourier transform. In *IEEE Trans. Comm. Tech.*, volume 19, pages 628–634, Oct 1971.

[62] A. R. Ali, A. Aassie-Ali, and A. S. Omar. A multistage channel estimation and ICI reduction method for OFDM systems in double dispersive channels. In *IEEE Radio and Wireless Symposium (RWS-2006)*, San Diego,USA, 2006.

[63] M.X. Chang and Y. T. Su. Blind and semiblind detections of OFDM signals in fading channels. *IEEE Trans. Communications*, 52(5):744–754, May 2004.

[64] A. Aassie-Ali and A.S. Omar. Super resolution matrix pencil algorithm for future fading prediction of mobile radio channels. In *Proc. 8th IEEE International Symposium on Signal Processing and its Application, ISSAP2005*, volume 1, pages 295– 298, Sydney,Austerlia, 2005.

[65] H. Sari, G. Karam, and I. Jeanclaude. Channel equalization and carrier synchronization in OFDM systems. In *Audio and Video Digital Radio Broadcasting Systems and Techniques*, pages 191–202, Amsterdam, Netherlands, Sept 1993. Elsevier Science publishers.

[66] D. Falconer, S.L.Ariyavisitakul, A. Benyamin-Seeyar, and B. Eidson. Frequency domain equalization for single carrier broadband wireless systems. *IEEE Commun. Mag.*, 40(4):58–66, Apr 2002.

[67] J.T.E. McDonnell and T.A. Wilkinson. Comparison of computational complexity of adaptive equalization and OFDM for indoor wireless networks. In *Proc. PIMRC 96*, pages 1088–1090, Taipei, 24th/25th Sep 2003.

[68] H. Sari, G. Karam, and I. Jeanclaude. Frequency domain equalization of mobile radio and terrestrial broadcast channels. In *Proc. IEEE Global Telecommun. Conf.*, volume 1, pages 1–5, Nov 1994.

[69] S.U.H. Qureshi. Adaptive equalization. In *Proc. IEEE*, volume 73, pages 1349–1387, Sep 1985.

[70] V. Aue, G.P. Fettweis, and R. Valenzuela. A comparison of the performance of linearly equalized single carrier and coded OFDM over frequency selective fading channels using the random coding technique. In *Proc. ICC 98 IEEE International Conference on Communications*, volume 2, pages 753–757, June 1998.

[71] Tariq J. S. Khanzada, Ali Ramadan Ali, A. Q. K. Rajput, and Abbas S. Omar. A design and chronological survey of decision feedback equalizer for single carrier transmission compared with OFDM. *Springer Journal for Wireless Networks, Information Processing and Systems*, 20:378–390, Jan 2009.

[72] H. Sari, G. Karam, and I. Jeanclaude. Transmission techniques for digital terrestrial TV broadcasting. 33:100–109, Feb 1995.

[73] Alan Bensky. *Wireless Positioning Technologies and Applications.* Artech House, Inc., 2008.

[74] T. J. S. Khanzada, A. R. Ali, and A. S. Omar. An analytical model for SLTDM to reduce the PAPR and ICI in OFDM systems for fast varying channels. In *Proc. 10th IEEE INMIC06*, pages 57–61, Islamabad, Pakistan, Dec 2006.

[75] T.J.S. Khanzada, A.R. Ali, and A.S. Omar. Study of variable channel length for single carrier transmission with decision feedback equalizer. In *IEEE Radio and Wireless Symposium 2008*, pages 267–270, Orlando, FL, USA, 22-24 Jan 2008.

[76] T. J. S. Khanzada, A. R. Ali, and A. S. Omar. The effect of coding on OFDM and single carrier transmission with decision feedback equalizer. In *CNSR 2008, the Sixth Annual Conference on Communication Networks and Services Research*, Halifax, NS, Canada, 05-08 May 2008.

[77] J. J. Caffery. *Wireless Location in CDMA Cellular Radio Systems.* Kluwer Academic publishers, 2000.

[78] Eurescom GmbH. WINNER project, IST-2003-507581, `https://www.ist-winner.org`, germany, 2003.

[79] WINNER Deliverable D4.8.1. Winner ii intramode and intermode cooperation schemes definition. Technical Report IST-2003-507581, Jun 2006.

[80] Y. T. Chan and K. C. Ho. A simple and efficient estimator for hyperbolic location. *IEEE Transactions on Signal Processing*, 42(8), Aug 1994.

[81] F. Gustafsson and F. Gunnarsson. Positioning using time-difference of arrival measurements. In *IEEE Int. Conf. on Acoustics, Speech, and Signal Processing, ICASSP '03*, Hong Kong, 2003.

[82] W. Beyene. Improving time-domain measurements with a network analyzer using a robust rational interpolation technique. *IEEE*.

[83] H. Saarnisaari. TLS-ESPRIT in a time delay estimation. In *IEEE 47th VTC*, pages 1619–1623, 1997.

[84] T. K. Sarkar and O. Pereira. Using the matrix pencil method to estimate the parameters by a sum of complex exponentials. *IEEE Antennas Propagation Magazine*, 37(1):48–55, Feb. 1995.

[85] W. Beyene. Improving time-domain measurements with a network analyzer using a robust rational interpolation technique. *IEEE Trans. Microwave Theory Tech*, 49:500–508, Mar 2001.

[86] H. Yamada, M. Ohmiya, Y. Ogawa, and K. Itoh. Super resolution techniques for time domain measurements with a network analyzer. *IEEE Trans. Antennas Propagat*, 39:177–183, Feb 1991.

[87] T. Lo, J. Litva, and H. Leung. A new approach for estimating indoor radio propagation characteristics. *IEEE Trans. Antennas Propagat.*, 42(3):1369–1376, Oct 1994.

[88] H.K. Parikh and W.R. Michaelis. Error mechanisms in an rf-based indoor positioning system. In *ICASSP 08, IEEE Int. Conf. on Acoustics, Speech and Signal Processing*, volume 3, pages 5320–5323, Las Vegas, NV, 31 March- 4 April 2008.

[89] W. H. Cantrell and W. A. Davis. The research and geometric analysis of indoor positioning using multiple pseudolites signals. In *Congress on Image and Signal Processing, CISP '08*, volume 5, pages 203 – 207, 27-30 May 2008.

[90] Tariq J. S. Khanzada, Ali Ramadan Ali, and Abbas S. Omar. Time difference of arrival estimation using super resolution algorithms to minimize distance measurement error for indoor positioning systems. In *12th Intl. IEEE Multitopic Conference, INMIC '08.*, Karachi, Pakistan, 23-24 Dec 2008.

[91] A. P. Liavas and P. A. Regalia. On the behavior of information theoretic criteria for model order selection. *IEEE Trans. Signal Processing*, 49(8):1689–1695, August 2001.

[92] M. Wax and T. Kailath. Detection of signals by information theoretic criteria. *IEEE Trans. Acoust. Speech Signal Process.*, 33(2):387–392, Apr 1985.

[93] A.A. Ali, V.D. Nguyen, K. Kyamakya, and A.S. Omar. Estimation of the channel-impulse-response length for adaptive ofdm systems based on information theoretic criteria. In *Vehicular Technology Conf. VTC-06*, volume 4, pages 1888–1892, May 2006.

[94] Hirotugu Akaike. A new look at the statistical model identification. *IEEE Transactions on Automatic Control*, pages 716–723, 1974.

[95] Tariq J. S. Khanzada and Ali Ramadan Ali. Super resolution techniques for range estimation time delay of arrival - a report for the TOA estimation. Technical Report IESK-HF-CMWCE/0508, Chair of Microwave and Communication Engineering (CMWCE) University of Magdeburg, Magdeburg, May 2008.

[96] Tariq J. S. Khanzada and Ali Ramadan Ali. Variations of matrix pencil algorithm implemented for range estimation using time difference of arrival method - A report for the working package 2 for IESK-HF-CMWCE. Technical Report

IESK-HF-CMWCE/1008, Chair of Microwave and Communication Engineering (CMWCE), University of Magdeburg, Magdeburg, Oct 2008.

[97] W. C. Jakes. *Microwave Mobile Communications*. Wiley Interscience − IEEE Press, 1994.

[98] J. Hwang and J. Winters. Sinusoidal modeling and prediction of fast fading processes. In *IEEE GLOBECOM*, pages 892–897, Nov 1998.

[99] Theodore S. Rappaport. *Wireless Communications: Principles and Practice*. Prentice Hall, 1996.

[100] A. Hatami, K. Pahlavan, M. Heidari, and F. Akgul. On RSS and TOA based indoor geolocation - A comparative performance evaluation. In *IEEE Wireless Communications and Networking Conference (WCNC 2006)*, volume 4, pages 2267–2272, Las Vegas, USA, Apr 3-6 2006.

[101] Erceg V. et al. TGn channel models. Technical report, IEEE 802.11 document 03/940r4, May 2004.

[102] J. Medbo and P. Schramm. Channel models for HIPERLAN/2, ETSI/BRAN document no. 3ERI085B, 1998.

[103] Zoran A. Maricevic, Sarkar Tapan K., Yingbo Hua, and Antonije R. Djordjevic. Time-domain measurements with the hewlett-packard network analyzer hp 8510 using the matrix pencil method. *IEEE Transactions on Microwave Theory and Techniques*, 39(3):538–547, March 1991.

[104] S. V. Vaseghi. *Advanced digital signal processing and noise reduction*. LTD, John Wiley & Sons, New York, USA, 2 edition, 2000.

[105] M. A. Hasan, M. R. Azimi-Sadjadi, and G. J. Dobeck. Separation of multiple time delays using new spectral estimationschemes. *IEEE Transactions on Signal Processing*, 46(3):1580–1590, Jun 1998.

[106] R.O. Schmidt. Multiple emitter location and signal parameter estimation. *IEEE Trans. Antenn. Propagat.*, 34:276–280, March 1986.

[107] Bhaskar D. Rao and K. V. S. Hari. Performance analysis of root-music. *IEEE Transactions on Acoustics, Speech and Signal Processing*, 43(12):1939–1949, 1989.

[108] R. Roy and T. Kailath. ESPRIT estimation of signal parameters via rotational invariance techniques. *IEEE Trans. Acoust., Speech, Signal Processing*, 37(7):984–995, July 1989.

[109] Y. Hua and T. Sarkar. On svd for estimating generalized eigenvalues of singular matrix pencil in noise. *IEEE Transactions on Signal Processing*, 39(4):892–900, April 1991.

[110] A. Swindlehurst and T. Kailath. A performance analysis of subspace-based methods in the presence of model errors, pt. i: The music algorithm. *IEEE Transactions on Acoustics, Speech, Signal Processing*, 40(7):1758–1774, 1992.

[111] S. M. Kay. *Modern Spectral Estimation: Theory and Application.* Prentice-Hall, Englewood-Cliffs,NJ, 1988.

[112] Z. Wang and G. B. Giannakis. Wireless multicarrier communications: Where fourier meets shannon. *IEEE Signal Process. Mag.*, 17(3):29–48, 2000.

[113] T. Walzman and M. Schwartz. Automatic equalization using the discrete frequency domain. *IEEE Trans. Commun.*, IT-19(1):59–68, Jan 1973.

[114] Jr. E.R. Ferrara. *Frequency-Domain Adaptive Filtering.* Prentice-Hall, 1985.

[115] H. Sari, G. Karam, and I. Jeanclaude. An analysis of Orthogonal Frequency Division Multiplexing for mobile radio applications. pages 1–5, June 1994.

[116] K. Berberidis and J. Palicot. A frequency domain decision feedback equalizer for multipath echo cancellation. In *Proc. Globecom95 Conf.*, pages 98–102, Dec 1995.

[117] S. Ariyavisitakul and L.J. Greenstein. Reduced-complexity equalization techniques for broadband wirelesschannels. In *5th IEEE International Conference on Universal Personal Communications, 1996*, volume 1, pages 125–130, Sep 1996.

[118] S. Hara, T. Matsuda, K. Ishikura, and N. Morinaga. Co-existence problem of TDMA and DS-CDMA systems-application of complexmultirate filter bank. In *GLOBECOM 96: Proceedings of IEEE Global Telecommunications Conference*, volume 2, pages 1281–1285, London, UK, Nov 1996.

[119] Karsten Brninghaus and Hermann Rohling. On the duality of multi-carrier spread spectrum and single-carrier transmission. pages 187–194, 1997.

[120] A. Czylwik. Comparison between adaptive OFDM and single carrier modulation with frequency domain equalization. In *Proc. IEEE Veh.Technol. Conf.*, volume 2, pages 865–869, May 1997.

[121] M. V. Clark. Adaptive frequency-domain equalization and diversity combining for broadband wireless communications. *IEEE J. Sel. Areas Commun.*, 16(8):1385–1395, Oct 1998.

[122] A. Gusmao, R. Dinis, J. Conceio, and N. Esteves. Comparison of two modulation choices for broadband wireless communications. In *Proc. IEEE Vehicular Technology Conf.*, volume 2, pages 1300–1305, May 2000.

[123] N. Al-Dhahir. Single-carrier frequency-domain equalization for space– time block-coded transmission over frequency-selective fading channels. *IEEE Commun. Lett.*, 5(7):304–306, Jul 2001.

[124] J. Tubbax, B. Come, L. Van der Perre, L. Deneire, S. Donnay, and M. Engels. OFDM versus single carrier with cyclic prefix: a system-based comparison. *Vehicular Technology Conference*, 2:1115–1119, 2001.

[125] Ender Ayanoglu, V.K. Jones, Gregory G. Raleigh, James Gardner, Derek Gerlach, and Karim Toussi. VOFDM broadband wireless transmission and its advantages over single carrier modulation, November 2001.

[126] J. Alhava and M. Renfors. Adaptive sine-modulated/cosinemodulated filter bank equalizer for transmultiplexers. In *ECCTD 01: Proc. European Conf. on Circuit Theory and Design*, pages 337–340, Espoo, Finland, August 2001.

[127] D. Falconer and S. L. Ariyavisitakul. Broadband wireless using single carrier and frequency domain equalization. In *5th International Symposium on Wireless Personal Multimedia Communications*, volume 1, pages 27–36, 27-30 Oct 2002.

[128] N. Benvenuto and S. Tomasin. On the comparison between OFDM and single carrier modulation with a DFE using a frequency-domain feedforward filter. *IEEE Trans. Commun.*, 50(6):947–955, 2002.

[129] N.Benvenuto and S.Tomasin. Block iterative DFE for single carrier modulation. *Electron. Lett.*, 38(19):1144–1145, 12 Sep 2002.

[130] F. Petre, G. Leus, L. Deneire, and M. Moonen. Downlink frequency domain chip equalization for single-carrier block transmission DSCDMA with known symbol padding. In *IEEE Global Telecommunications Conference*, volume 1, pages 453–457. IEEE Commun. Society, November 2002.

[131] Zhou Shengli and G. B. Giannakis. Single-carrier space-time block-coded transmissions over frequency-selective fading channels. *IEEE Transactions on Information Theory, one*, 49(1):164–179, Jan 2003.

[132] F. Petre, G. Leus, L. Deneire, M. Engels, M. Moonen, and H. De Man. Space-time block coding for single-carrier block transmission DSCDMA downlink. *IEEE J. Select. Areas Commun.*, 21(3):350–361, Apr 2003.

[133] J. Alhava, A. Viholainen, and M. Renfors. Efficient implementation of complex exponentially-modulated filter banks. In *Proc. IEEE Symp. on Circuits and Systems*, volume 4, pages 157–160, Bangkok, Thailand, May 2004.

[134] A. Gusmao, R. Dinis, and N. Esteves. On frequency-domain equalization and diversity combining for broadband wireless communications. *IEEE Trans. Commun.*, 51(7):1029–1033, Jul 2003.

[135] A. Gusmo R. Dinis and N. Esteves. On broadband block transmission over strongly frequency-selective fading channels. In *Wireless confernece 2003*, pages 261–269, Calgary, Canada, July 2003.

[136] P. Schniter and L. Hong. Iterative equalization for single-carrier cyclic-prefix in doubly-dispersive channels. In *37th Asilomar Conference on Signals, Systems and Computers*, volume 1, pages 502–506, 9–12 Nov 2003.

[137] Zhengdao Wang, Xiaoli Ma, and Georgios B. Giannakis. OFDM or single-carrier block transmissions? *IEEE Trans. Commun.*, 52(3):380–394, Mar 2004.

[138] T. A. Tran, T. X. Lai, and A. B. Sesay. Single-carrier concatenated space-time block coded transmissions over selective-fading channels. *Canadian Conference on Electrical and Computer Engineering*, 3:1577–1580, 2-5 May 2004.

[139] M. Oltean, A. Vesa, and E. Marza. Performance evaluation of single-carrier broadband transmission with frequency domain equalization. *IEEE Trans. Electronics and Commun.*, 49, 2004.

[140] Fumiyuki Adachi Hiromichi Tomeba, Kazuaki Takeda. Performance evaluation for single-user transmission with frequency-domain pre-equalization in DS-CDMA mobile radio. IEICE Technical Report RCS2004-195 399, IEICE , Tohoku Univ., The Institute of Electronics, Information and Communication Engineers (IEICE),Tohoku Univ. Sendai Japan, Oct 2004.

[141] Hiromichi Tomeba, Kazuaki Takeda, and Fumiyuki Adachi. Pre-equalization for single carrier transmission. IEICE Technical Report RCS2004-214 439, IEICE , Tohoku Univ., The Institute of Electronics, Information and Communication Engineers (IEICE),Tohoku Univ. Sendai Japan, Nov 2004.

[142] Qing Zhang and Tho Le-Ngoc. Channel-estimate-based frequency-domain equalization (ce-fde) for broadband single-carrier transmission. *Wireless Commun. and Mobile Computing*, 4(4):449–461, Jun 2004.

[143] R. Dinis, R. Kalbasi, D. Falconer, and A. H. Banihashemi. Iterative layered space-time receivers for single-carrier transmission over severe time-dispersive channels. *IEEE Communications Letters*, 8(9):579–581, Sep 2004.

[144] P. Schniter and H. Liu. Iterative frequency-domain equalization for single-carrier systems in doubly-dispersive channels. In *38th Asilomar Conference on Signals, Systems,and Computers*, volume 1, pages 667–671, Nov 2004.

[145] T. Hidalgo Stitz and M. Renfors. Filter-bank-based narrowband interference detection and suppression in spread spectrum systems. *EURASIP J. on Applied Signal Processing*, 2004(8):11631176, 2004.

[146] Y. Yang, T. Ihalainen, and M. Renfors. Filter bank based frequency domain equalizer in single carrier modulation. In *14th IST Mobile and Wireless Communications Summit 04*, pages 865–869, Dresden, Germany, Jun 2005.

[147] F. Adachi, K. Takeda, and H. Tomeba. Multi-antenna pre-equalization for single-carrier/TDD system. In *IEEE 61st Vehicular Technology Conference, VTC 2005-Spring*, volume 1, pages 452–456, Stockholm, Sweden, Jun 2005.

[148] J. Coon, S. Armour, M. Beach, and J. McGeehan. Adaptive frequency-domain equalization for single-carrier multiple-input multiple-output wireless transmissions. *IEEE Trans. Signal Process.*, 53(8):3247–3256, August 2005.

[149] F. S. Agathe and H. Sari. Single-carrier transmission with iterative frequency-domain decision-feedback equalization. In *13th european Signal processing conference*, Antalya,Turkey, September 2005.

[150] Jin-Ho Jang Hui-Chul Won Gi-Hong Im. Cyclic prefixed single carrier transmission with SFBC over mobile wireless channels. *IEEE Signal Processing Letters*, 13(5):261–264, May 2006.

[151] A. Gusmao, P. Torres, R.Dinis, and N. Esteves. On SC/FDE block transmission with reduced cyclic prefix assistance. In *ICC '06. IEEE International Conference on Communications*, volume 11, pages 5058–5063, Istanbul, Jun 2006.

[152] T. W. Yune, C.H. Choi, and G. H. Im. Single carrier frequency-domain equalization with transmit diversity over mobile multipath channels. *IEEE Trans. Commun.*, E89B(7), July 2006.

[153] A. Viholainen, J. Alhava, and M. Renfors. Efficient implementation of complex modulated filter banks using cosine and sine modulated filter banks. *URASIP J. on Applied Signal Process.*, 2006(ID:58-5645), 2006.

[154] A. Viholainen, J. Alhava, and M. Renfors. Efficient implementation of 2x over-sampled exponentially modulated filter banks. *IEEE Trans. on Circuits and Systems II*, 53:1138–1142, 2006.

[155] Y. Yang, T. Hidalgo Stitz, M. Rinne, and M. Renfors. Mitigation of narrowband interference in single carrier transmission with filter bank equalization. In *Proc. IEEE Asia Pacific Conference on Circuits and Systems*, pages 749–752, Singapore, Dec 2006.

[156] R. K. Martin, K. Vanbleu, G. Ysebaert, and A. G. Klein. Bit error rate minimizing channel shortening equalizers for multicarrier systems. In *IEEE 7th Workshop on Signal Processing Advances in Wireless Communications, SPAWC '06.*, 10.1109/SPAWC.2006.346351, pages 1–5, Cannes, France, July 2006.

[157] F. S. Agathe and H. Sari. New results in iterative frequency-domain decision-feedback equalization. In *Proc. 14th European Conference on Signal Processing (EUSIPCO 2006)*, Florence, Italy, Sep 2006.

[158] Luciano Sarperi, Xu Zhu, and Asoke K. Nandi. Semi-blind space time equalization for single carrier MIMO systems with block transmittion. In *Proc. 14th European Conference on Signal Processing (EUSIPCO 2006)*, Florence, Italy, Sep 2006.

[159] Fumiyuki Adachi Hiromichi Tomeba, Kazuaki Takeda. BER performance of single-carrier transmission in a channel having fractionally spaced time delays. IEICE RCS2005-146 559, The Institute of Electronics, Information and Communication Engineers (IEICE), Tohoku Univ. Sendai Japan, Jan 2006.

[160] Fumiyuki Adachi Kazuki Takeda, Hiromichi Tomeba. Single carrier transmission with frequency-domain equalization using tomlinson-harashima precoding. IEICE RCS2006-41 119, The Institute of Electronics, Information and Communication Engineers (IEICE), Tohoku Univ. Sendai Japan, June 2006.

[161] Kazuki Takeda, Hiromichi Tomeba, and Fumiyuki Adachi. BER performance of turbo coded single-carrier transmission with joint tomlinson-harashima precoding and frequency-domain equalization. IEICE RCS2006-269 555, The Institute of Electronics, Information and Communication Engineers (IEICE), Japan, March 2007.

[162] Y. Yang, T. Ihalainen, M. Rinne, and M. Renfors. Frequency-domain equalization in single-carrier transmission: Filter bank approach. (ID:10438), 2007.

[163] Z. Tang and G. Leus. Receiver design for single-carrier transmission over time-varying channels. In *International Conference on Acoustics, Speech and Signal Processing, 2007. ICASSP 2007. IEEE*, volume 3, pages III–129–III–132, Honolulu, HI, USA, April 2007.

[164] G. Ysebaert R. Martin, K. Vanbleu. Bit error rate minimizing channel shortening equalizers for single carrier cyclic prefixed systems. In *International Confrence on Acoustics , Speech and Signal Processing ICASSP 07*, Hawaii,USA, April 2007.

[165] R. K. Martin, G. Ysebaert, and K. Vanbleu. Bit error rate minimizing channel shortening equalizers for cyclic prefixed systems. In *IEEE Transactions on Signal Processing*, volume 55, pages 2605–2616, Hawaii,USA, June 2007.

[166] Ramjee Prasad. *OFDM for Wireless Communications Systems.* Artech House, 2004.

[167] J. Hightower and G. Borriello. Location systems for ubiquitous computing. *IEEE Computer*, 34(8):57–66, August 2001.

[168] Federal Communications Commission Tech. Rep. Revision of the commissions rules to insure compatibility with enhanced 911 emergency calling systems. Technical Report FCC Docket No. 94-102. RM-8143, Jul 1996.

[169] Ali H. Sayed, Alireza Tarighat, and Nima Khajehnouri. Network-based wireless location. *IEEE Signal Processing Mag.*, 2005.

[170] P. Krishnamurthy and Kaveh Pahlavan. Distribution of range error and radio channel modeling for indoor geolocation applications. In *PIMRC*, Kyoto, Japan, Sept 1999.

[171] A.Hatami and K.Pahlavan. Performance comparison of RSS and TOA indoor geolocation based on UWB measurement of channel characteristics. In *17th IEEE nternational Symposium on Personal, Indoor and Mobile Radio Communications PIMRC'2006*, pages 1–6, Helsinki, Finland, 11-14 Sept 2006.

[172] W. Wei, X. J. Yu, and Z. Z. Liang. A new NLOS error mitigation algorithm in location estimation. *IEEE Trans. on Vehicular Technology*, 54(6):2048–2053, Nov 2005.

[173] Satoshi Kogure. Loran-C user handbook. Technical report, Commandant Publication P16562.5, U.S. Coast Guard, 1980.

[174] Agilent Technologies. N5182A MXG RF Vector Signal Generator- product brochure, 2009.

[175] Agilent Technologies. N9010A EXA Vector Signal Analyzer- product brochure, 2009.

[176] Anritsu GmbH. MS2690A Series Signal Analyzer and Signal Generator- product brochure, 2009.

[177] N. Yuen and B. Friedlander. Asymptotic performance analysis of three ESPRIT algorithms. In *29th Asilomar Conference on Signals, Systems and Computers (2-Volume Set)*, Apr 1997.

[178] Schmidt Mikkel N. Seiersen Jens Brosted. Perceptual unitary ESPRIT algorithm. Project group: 03gr1048, Department of Communication Technology, Aalborg University, Denmark, Jun 2003.

[179] N. Lemma Aweke, Jan van der Veen Alle, and F. Deprettere Ed. Multiresolution ESPRIT algorithm. *IEEE Transactions on Signal Process.*, 47(6):1722–1726, Jun 1999.

[180] Pesavento, M. Gershman, and M. A.B. Haardt. A theoretical and experimental performance study of a root-MUSIC algorithm based on a real-valued eigendecomposition. In *IEEE Int. Conf. on Acoustics, Speech, and Signal Processing, ICASSP '00*, volume 5, pages 3049–3052, Istanbul, Turkey, 6-10 April 2000.

[181] Darren H. Haddad and Andrew J. Noga. The matrix pencil and its applications to speech processing. Technical Report ADA–466668, Air Force Research Lab, Rome NY Inofrmation Directorate, Dec 2006.

[182] Yingbo Hua and Tapan K.Sarkar. Matrix pencil method for estimating parameters of exponentially damped/undamped sinusoids in noise. *IEEE Trans. Acoust., Speech, Signal Processing*, ASSP-38:814–824, May 1990.

Curriculum Vitae

Name:	Tariq Jamil Saifullah Khanzada
Date of Birth:	August 13, 1973 at TandoAllahYar, Pakistan
Nationality:	Pakistani
Status:	Married, 3 Children
Address:	Germany: Walther Rathenau Str. 56/302,
	39104 Magdeburg, Germany
	Ph-49-176-45307582
	Pakistan: B-100 Mir Fazal Twon, Latifabad 9,
	Hyderabad, Sind, Pakistan
	Ph 92-22-3866276
E-mail:	Khanzada@ovgu.de;Khanzada@ieee.org

Education

Since 06.2005 Working towards Ph.D. degree at the Institute for Electronics, Signal Processing, and Communication, University of Magdeburg, Germany
Thesis Title: Wireless Communication Techniques for Indoor Positioning and Tracking Applications
Supervisor: Prof. Dr. Ing.- A.S. Omar

12.2003 M.E. in Communications Systems & Networking
Mehran University of Engineering and Technology (MUET), Pakistan
Thesis Title: Use of Data Mining Strategies in Mobile Communication Techniques
Supervisor: Prof. Dr. A.Q.K Rajput

06.1999 B.E. in Computer Systems Engineering from
MUET, Pakistan

09.1992 Diploma in Computer Science
PETROMAN Hyderabad, Pakistan

04.1991 Higher Secondary School Certificate (Pre- Engineering)
Govt. Model High School Hyderabad, Pakistan

Work Experience

07.2005– till now   Research Assistant for a Communication research group,
at the Chair of Microwave and Communication Engineering,
Institute for High Frequency and Communications Technology
Otto-von-Guericke University of Magdeburg Germany

with the following tasks:

Research: Signal Proc. Techs. for Wireless Comm. Sys.
Positioning and Tracking Applications
Tutor: Conducts Lectures and Exercises

06.2004– 06.2005	Assistant Professor at CS & SE Dept.	MUET Pakistan
03.2001– 06.2004	Lecturer in CS & SE Dept.	MUET Pakistan
08.2000– 02.2001	Senior Lecturer in Muhammad Inst. of Sc. & Tech.	Mirpur Khas, Pakistan
01.2000– 07.2000	Instructor (E-1) at Pertroman Training Inst.	Hyderabad, Pakistan
07.1999– 01.2000	Network Administrator at Softech Inc.	Hyderabad, Pakistan
02.1999– 07.2000	Instructor(NE-V) Pertroman Training Inst.	Hyderabad, Pakistan

Professional Trainings

2003	Microstrategy	NCR Islamabad, Pakistan
2003	Pakistan Developer Conference	Microsoft, Pakistan
2003	RIMS Training Course (Lab Windows)	RIMS Karachi, Pakistan
2002	Teradata Factory Course	NCR Karachi, Pakistan
2002	Data Warehousing Course	NCR Karachi, Pakistan
1998	ISO-9000 Course Certificate	Q & A Inspection Services , Pakistan

Publication List

Journal Publications

1. Ali Ramadan Ali, Tariq J. S. Khanzada and Abbas S. Omar, "Frequency Offset Compensation for OFDM Systems Using A Combined Autocorrelation and Wiener Filtering Scheme", *Journal of Telecommunications and Information Technology JTIT* Vol. 1. pp. 40-47, 2010.

2. Ali Ramadan Ali, Tariq J. S. Khanzada and Abbas S. Omar, " ICI Cancellation for OFDM Systems in Rapidly Time-Variant Channels", *IEICE Trans. Comm.* Vol.E92-B, No.4, pp. 1388-1391, Apr. 2009.

3. Tariq J. S. Khanzada, Ali Ramadan Ali and Abbas S. Omar, "A Design and Chronological Survey of Decision Feedback Equalizer for Single Carrier Transmission Compared with OFDM " , *Computer Science Series for Wireless Networks, Information Processing and Systems*, Springer Berlin Heidelberg, Volume 20, 2009 pp. 378-390 ISSN 1865-0929 (Print) 1865-0937 (online), Revised Selected Papers 2009.

4. Tariq J. S. Khanzada, N. A. Jaffri and A. Q. K. Rajput, "A Design of PC Based Administrator Via Parallel Port Interfacing", published at *Mehran University Research Journal of Engineering and Technology, Jamshoro, Pakistan*, Jan 2005.

5. A. Q. K. Rajput, A. A. Araian and Tariq J. S. Khanzada, "Computer System Workshop", A Practical Workbook, printed for *B.E. Curriculum Text book*, published in 2004.

6. A. Q. K. Rajput, M. Z. Shaikh and Tariq J. S. Khanzada, "Use of Holographic Environment in Business and Educational Applications" , published at *Mehran University Research Journal of Engineering and Technology, Jamshoro, Pakistan* , pp. 261-268, Vol. 22, No 4, October 2003.

Technical Reports / Book Chapters

1. Tariq J. S. Khanzada and Michael Anis, "Development of an Evaluation Scenarios for Analysis and Visualization of Radio-Based Technologies" A technical report for the sub project 2 (TAP 2.3) of *Virtual and Augmented Reality for Security and Reliability of Embedded Systems -ViERforES*, `http://vierfores.de/`, no:IESK-HF-CMWCE-ViERforES/1209, University of Magdeburg, Dec. 2009.

2. Tariq J. S. Khanzada and Michael Anis, "Reliability Analysis of TAP-Radio-Based Identification for Tracking and Communication System" A technical report for the sub project 2 (TAP 2.2) of *Virtual and Augmented Reality for Security and Reliability of Embedded Systems -ViERforES*, `http://vierfores.de/`, no:IESK-HF-CMWCE-ViERforES/0909, University of Magdeburg, Aug. 2009.

3. Tariq J. S. Khanzada and Michael Anis, "WLAN Security Recommendations for DHL - Leipzig Hub / Schkeuditz" An initial technical report for the sub project 2 (TAP 2.1) of *Virtual and Augmented Reality for Security and Reliability of Embedded Systems -ViERforES*, `http://vierfores.de/`, no:IESK-HF-CMWCE-ViERforES/0409, University of Magdeburg, Apr. 2009.

4. Tariq J. S. Khanzada and Ali Ramadan Ali, "Super Resolution Techniques for Range Estimation Time Delay of Arrival- A Report for the TOA Estimation", no:IESK-HF-CMWCE/0508, Chair of Microwave and Communication Engineering (CMWCE), *University of Magdeburg*, Magdeburg, May 2008.

5. Tariq J. S. Khanzada and Ali Ramadan Ali, "Variations of Matrix Pencil Algorithm Implemented for Range Estimation using Time Difference of Arrival Method - A Report for the Working Package 2 for (IESK-HF-CMWCE)", no:IESK-HF-CMWCE/1008, Chair of Microwave and Communication Engineering (CMWCE), *University of Magdeburg*, Magdeburg, Oct 2008.

Conference / Workshop Publications

1. Tariq J. S. Khanzada, Ali Ramadan Ali, Sameh Napoleon and Abbas Omar, "Use of Super Resolution Algorithms for Indoor Positioning Keeping Novel Designed WLAN Signal Structure", *1st International Workshop on Digital Engineering (IWDE 2010)* to be held in *Magdeburg, Germany*, 14-15 Jun. 2010.

2. Tariq J. S. Khanzada, Ali Ramadan Ali and Abbas Omar, "Application of the Super Resolution Algorithms to the Indoor Positioning and Tracking System", in *German Microwave Conference GeMic2010, Berlin*, 15-17 Mar. 2010.

3. Ali Ramadan Ali, Ali Alsaih, Tariq J. S. Khanzada, Jan Machac and Abbas Omar, "Adaptive Symbol Length for OFDM Systems in Doubly Selective Channels", in *APMC2009, Singapore*, Dec. 2009.

4. Ali Ramadan Ali, Tariq J. S. Khanzada and Abbas S. Omar, "Adaptive Time Interpolator for OFDM Systems in Time-Variant Channels", in Proc. *IEEE Radio and Wireless Symposium*, RWS-2009, San Diego, CA, USA, Jan. 2009.

5. Tariq J. S. Khanzada, Ali Ramadan Ali and Abbas S. Omar, "Time Difference of Arrival Estimation using Super Resolution Algorithms to Minimize Distance Measurement Error for Indoor Positioning Systems", In proc. *IEEE Multitopic Conference, INMIC '08, Karachi, Pakistan*, 23-24 Dec. 2008.

6. Ahmed Boutejdar, Michael Senst, Tariq J. S. Khanzada and Abbas Omar, "A New Compact 2.4GHz Bandpass Filter Using Direct Coupled Defected Ground Structure (DGS) Hairpin Resonators", in Proc. *8th Mediterranean Microwave Symposium – MMS'2008, Damascus, Syria* 14-16 Oct. 2008.

7. Ali Ramadan Ali, Atallah Balalem, Tariq J. S. Khanzada, Jan Machac and Abbas S. Omar, "Adaptive Pilot Distribution for OFDM Systems in Time-Variant Channels", in Proc. *APMC 2008, Hong Kong*, Dec. 2008.

8. Ali Ramadan Ali, Tariq J. S. Khanzada and Abbas S. Omar "Channel Estimation for OFDM Systems in Rapidly Time-Variant Channels Using High Degree Channel Approximation," *WIMOB 2008, Avingon, France*, Oct. 2008.

9. Ali Ramadan Ali, Tariq J. S. Khanzada and Abbas S. Omar "Adaptive Guard Interval length for OFDM-Based WLAN Systems in Frequency Selective Channels," *European Microwave conference EUMW 2008, Amsterdam, Netherland*, Oct. 2008.

10. Ali Ramadan Ali, Tariq J. S. Khanzada and Abbas S. Omar "ICI Cancellation for OFDM Systems Using Lagrange Polynomial Approximation," *13th OFDM workshop, Hamburg, Germany*, Aug. 2008.

11. Ali Ramadan Ali, Atallah Balalem, Tariq J. S. Khanzada, Jan Machac and Abbas S. Omar "Doppler Spread Estimation for OFDM Systems Using Newton Polynomials," in proc. of *Radioelektronika 2008, Prague, Czech Republic*, Jun. 2008.

12. Tariq J. S. Khanzada, Ali Ramadan Ali and Abbas S. Omar, "The Effect of Coding on OFDM and Single Carrier Transmission with Decision Feedback Equalizer " , *CNSR 2008 Conference , Halifax, Nova Scotia, Canada* May 2008.

13. Tariq J. S. Khanzada, Ali Ramadan Ali and Abbas S. Omar, "A Design and Chronological Survey of Decision Feedback Equalizer for Single Carrier Transmission Compared with OFDM ", *IMTIC 2008, Pakistan* 11-12 Apr. 2008.

14. Tariq J. S. Khanzada, Ali Ramadan Ali and Abbas S. Omar, "A Study of Variable Channel Length for Single Carrier Transmission with Decision Feedback Equalizer" ,in Proc. *IEEE Radio and Wireless Symposium, 2008, Orlando, Fl, USA*, page(s): 267-270, Jan. 2008.

15. Ali Ramadan Ali, Tariq J. S. Khanzada and Abbas S. Omar, "Adaptive Pilot Distribution for OFDM-Based WLANSystems in Doubly Dispersive Channels", *Wireless Rural and Emergency Communications Conference WRECOM, Rome, Italy* October 2007.

16. Tariq J. S. Khanzada, Ali Ramadan Ali and Abbas S. Omar, "SLTDM: An Analytical Model for Reduction of PAPR and ICI in OFDM Systems for Fast Varying Channels " , in Proc. *IEEE Multitopic Conference, 2006. INMIC '06, Pakistan*, Page(s):56 - 61, 23-24 Dec. 2006.

Related Publications

The presented thesis is based on the following international reviewed journal and conferences papers:

List of Publications

Journal Publications

1. Ali Ramadan Ali, Tariq J. S. Khanzada, and Abbas S. Omar, "Frequency Offset Compensation for OFDM Systems Using A Combined Autocorrelation and Wiener Filtering Scheme", *Journal of Telecommunications and Information Technology JTIT* Vol. 1. pp. 40-47, 2010.

2. Ali Ramadan Ali, Tariq J. S. Khanzada, and Abbas S. Omar, " ICI Cancellation for OFDM Systems in Rapidly Time-Variant Channels", *IEICE Trans. Comm.* Vol.E92-B, No.4, pp. 1388-1391, Apr. 2009.

3. Tariq J. S. Khanzada, Ali Ramadan Ali, and Abbas S. Omar, "A Design and Chronological Survey of Decision Feedback Equalizer for Single Carrier Transmission Compared with OFDM " , *Computer Science Series for Wireless Networks, Information Processing and Systems*, , Springer Berlin Heidelberg, Volume 20, 2009 pp. 378-390 ISSN 1865-0929 (Print) 1865-0937 (online), Revised Selected Papers 2009.

Conference/Workshop Publications

1. Tariq Jamil Khanzada, Ali Ramadan Ali, Sameh Napoleon and Abbas Omar, "Use of Super Resolution Algorithms for Indoor Positioning Keeping Novel Designed WLAN Signal Structure", *1st International Workshop on Digital Engineering (IWDE 2010)* to be held in Magdeburg, Germany, 14-15 Jun. 2010.

2. Tariq Jamil Khanzada, Ali Ramadan Ali, and Abbas Omar, "Application of the Super Resolution Algorithms to the Indoor Positioning and Tracking System", in *German Microwave Conference GeMic2010*, 15-17 Mar. Berlin 2010.

3. Ali Ramadan Ali, Ali Alsaih, Tariq Jamil Khanzada, Jan Machac, and Abbas Omar, "Adaptive Symbol Length for OFDM Systems in Doubly Selective Channels", in *APMC2009, Singapore*, Dec., 2009.

4. Ali Ramadan Ali, Tariq J. S. Khanzada, and Abbas S. Omar, "Adaptive Time Interpolator for OFDM Systems in Time-Variant Channels", in Proc. *IEEE Radio and Wireless Symposium*, RWS-2009, San Diego, CA, USA, Jan. 2009.

5. Tariq J. S. Khanzada, Ali Ramadan Ali, and Abbas S. Omar, "Time Difference of Arrival Estimation using Super Resolution Algorithms to Minimize Distance Measurement Error for Indoor Positioning Systems", In proc. *IEEE Multitopic Conference, INMIC '08, Karachi, Pakistan*, 23-24 Dec. 2008.

6. Ahmed Boutejdar, Michael Senst, Tariq J. Khanzada and Abbas Omar, "A New Compact 2.4GHz Bandpass Filter Using Direct Coupled Defected Ground Structure (DGS) Hairpin Resonators", in Proc. *8th Mediterranean Microwave Symposium – MMS'2008, Damascus, Syria* 14-16 October, 2008.

7. Ali Ramadan Ali, Atallah Balalem, Tariq J. S. Khanzada, Jan Machac, and Abbas S. Omar, "Adaptive Pilot Distribution for OFDM Systems in Time-Variant Channels", in Proc. *APMC 2008, Hong Kong*, Dec., 2008.

8. Ali Ramadan Ali, Tariq J. S. Khanzada and Abbas S. Omar "Channel Estimation for OFDM Systems in Rapidly Time-Variant Channels Using High Degree Channel Approximation," *WIMOB 2008, Avingon, France*, Oct. 2008.

9. Ali Ramadan Ali, Tariq J. S. Khanzada and Abbas S. Omar "Adaptive Guard Interval length for OFDM-Based WLAN Systems in Frequency Selective Channels," *European Microwave conference EUMW 2008, Amsterdam, Netherland*, Oct. 2008.

10. Ali Ramadan Ali, Tariq J. S. Khanzada and Abbas S. Omar "ICI Cancellation for OFDM Systems Using Lagrange Polynomial Approximation," *13th OFDM workshop, Hamburg, Germany*, Aug. 2008.

11. Ali Ramadan Ali, Atallah Balalem, Tariq J. S. Khanzada , Jan Machac, and Abbas S. Omar "Doppler Spread Estimation for OFDM Systems Using Newton Polynomials," in proc. of *Radioelektronika 2008, Prague, Czech Republic*, Jun. 2008.

12. Tariq J. S. Khanzada, Ali Ramadan Ali, and Abbas S. Omar, "The Effect of Coding on OFDM and Single Carrier Transmission with Decision Feedback Equalizer " , *CNSR 2008 Conference , Halifax, Nova Scotia, Canada* 2008.

13. Ali Ramadan Ali, Tariq J. S. Khanzada and Abbas S. Omar, "Adaptive Pilot Distribution for OFDM-Based WLANSystems in Doubly Dispersive Channels", *Wireless Rural and Emergency Communications Conference WRECOM, Rome, Italy* October 2007.

14. Tariq J. S. Khanzada, Ali Ramadan Ali, and Abbas S. Omar, "A Design and Chronological Survey of Decision Feedback Equalizer for Single Carrier Transmission Compared with OFDM " , *IMTIC 2008, Pakistan* 11-12 Apr. 2008.

15. Tariq J. S. Khanzada, Ali Ramadan Ali, and Abbas S. Omar, "A Study of Variable Channel Length for Single Carrier Transmission with Decision Feedback Equalizer" ,in Proc. *IEEE Radio and Wireless Symposium, 2008, Orlando, Fl, USA*, Jan 2008. page(s): 267-270.

16. Tariq J. S. Khanzada, Ali Ramadan Ali, and Abbas S. Omar, "SLTDM: An Analytical Model for Reduction of PAPR and ICI in OFDM Systems for Fast Varying Channels " , in Proc. *IEEE Multitopic Conference, 2006. INMIC '06, Pakistan*, 23-24 Dec. 2006 Page(s):56 - 61.